

1976

Szillard-Chalmers and thermal annealing processes in D-tris(ethylenediamine)cobalt(III) nitrate

John Lee Bonte
Iowa State University

Follow this and additional works at: <https://lib.dr.iastate.edu/rtd>

 Part of the [Inorganic Chemistry Commons](#)

Recommended Citation

Bonte, John Lee, "Szillard-Chalmers and thermal annealing processes in D-tris(ethylenediamine)cobalt(III) nitrate " (1976).
Retrospective Theses and Dissertations. 6258.
<https://lib.dr.iastate.edu/rtd/6258>

This Dissertation is brought to you for free and open access by the Iowa State University Capstones, Theses and Dissertations at Iowa State University Digital Repository. It has been accepted for inclusion in Retrospective Theses and Dissertations by an authorized administrator of Iowa State University Digital Repository. For more information, please contact digirep@iastate.edu.

INFORMATION TO USERS

This material was produced from a microfilm copy of the original document. While the most advanced technological means to photograph and reproduce this document have been used, the quality is heavily dependent upon the quality of the original submitted.

The following explanation of techniques is provided to help you understand markings or patterns which may appear on this reproduction.

1. The sign or "target" for pages apparently lacking from the document photographed is "Missing Page(s)". If it was possible to obtain the missing page(s) or section, they are spliced into the film along with adjacent pages. This may have necessitated cutting thru an image and duplicating adjacent pages to insure you complete continuity.
2. When an image on the film is obliterated with a large round black mark, it is an indication that the photographer suspected that the copy may have moved during exposure and thus cause a blurred image. You will find a good image of the page in the adjacent frame.
3. When a map, drawing or chart, etc., was part of the material being photographed the photographer followed a definite method in "sectioning" the material. It is customary to begin photoing at the upper left hand corner of a large sheet and to continue photoing from left to right in equal sections with a small overlap. If necessary, sectioning is continued again — beginning below the first row and continuing on until complete.
4. The majority of users indicate that the textual content is of greatest value, however, a somewhat higher quality reproduction could be made from "photographs" if essential to the understanding of the dissertation. Silver prints of "photographs" may be ordered at additional charge by writing the Order Department, giving the catalog number, title, author and specific pages you wish reproduced.
5. PLEASE NOTE: Some pages may have indistinct print. Filmed as received.

Xerox University Microfilms

300 North Zeeb Road
Ann Arbor, Michigan 48106

77-1013

BONTE, John Lee, 1946-
SZILARD-CHALMERS AND THERMAL ANNEALING PROCESSES
IN D-TRIS(ETHYLENEDIAMINE)COBALT(III) NITRATE.

Iowa State University, Ph.D., 1976
Chemistry, inorganic

Xerox University Microfilms, Ann Arbor, Michigan 48106

Szilard-Chalmers and thermal annealing processes in

D-tris(ethylenediamine)cobalt(III) nitrate

by

John Lee Bonte

A Dissertation Submitted to the
Graduate Faculty in Partial Fulfillment of

The Requirements for the Degree of

DOCTOR OF PHILOSOPHY

Department: Chemistry

Major: Inorganic Chemistry

Approved:

Signature was redacted for privacy.

In Charge of Major Work

Signature was redacted for privacy.

For the Major ~~Department~~

Signature was redacted for privacy.

For the Graduate College

Iowa State University
Ames, Iowa

1976

TABLE OF CONTENTS

	<u>Page</u>
I. INTRODUCTION	1
A. Szilard-Chalmers Processes and Neutron Capture and Recoil in Cobalt-59	1
B. Distribution of Products Obtained From Szilard-Chalmers Recoil in <u>tris</u> -(ethylenediamine)cobalt (III) Salts	18
C. Annealing of Products and Solid State Isotopic Exchange	26
II. EXPERIMENTAL	38
A. Materials	38
B. Equipment	39
C. Preparations	41
D. Analysis	44
E. Irradiation Conditions	47
F. Radiochemical Measurements	48
G. Separations	50
H. Thermal Annealing	63
I. Storage Conditions and Solution Aging	63
III. RESULTS AND DISCUSSION	66
A. Characterization of Radiochemical Species	66
B. Transient Species	77
C. Solid-State Thermal Annealing	85
D. Conclusions and Significance of Results for the Various Recoil and Thermal Annealing Models	106

	<u>Page</u>
IV. APPLICATION, IMPLICATION, AND SUGGESTION FOR FUTURE WORK	117
V. REFERENCES CITED	119
VI. ACKNOWLEDGMENTS	123

I. INTRODUCTION

A. Szilard-Chalmers Processes and
Neutron Capture and Recoil in Cobalt-59

The research described in this dissertation was undertaken to describe the distribution and identity of radiochemical species produced as a result of the $^{59}\text{Co}(n,\gamma)^{60}\text{Co}$ reaction in solid D-tris(ethylenediamine)-cobalt(III) nitrate after various treatments of the irradiated material.

If the nucleus of a ^{59}Co atom captures a thermal neutron, a compound nucleus [^{60}Co] is formed with about 7.49 MeV (1) excess energy relative to the ground state. To lose this excess energy, the compound nucleus emits one or more gamma rays. These gamma rays possess momentum, and by the law of conservation of momentum the nucleus must receive an opposite but equal momentum. In condensed media, the momentum of the nucleus is sufficient that chemical bonds are broken. In a solid, the nucleus leaves its primary coordination sphere and may recombine with other atoms or remain as an interstitial atom in the crystal lattice. Such reactions are called hot atom reactions. The "hot" recoil atom may lose its kinetic energy in moving through the lattice by breaking bonds, ionizing atoms, or transferring kinetic energy to other atoms. The environment of the activated atom after it comes to rest may be such that the atom may recombine further with atoms or radicals in the damaged lattice. A redistribution of radiochemical species may then result from thermal annealing of the irradiated crystals.

When a ^{59}Co nucleus captures a thermal neutron and emits one or more

gamma photons, either ^{60g}Co or ^{60m}Co is formed immediately. The ^{60m}Co formed is converted to ^{60g}Co by a 10.5 min decay (2). Within an hour or two following an irradiation, substantially all of the meta-stable species will have been converted to the ground state, or ^{60g}Co . In general, the net rate of production of a radionuclide is equal to the rate of neutron capture minus the decay rate (3).

$$dN/dt = P - \lambda N \quad (1)$$

In Equation (1) P is the rate of neutron capture, λ is the decay constant, and N is the number of radioactive atoms. Because of its long half-life, only a negligible fraction of the ^{60g}Co nuclei will have decayed during irradiation and prior to detection, which may occur a few days after production. The number of ^{60g}Co atoms present a few hours after irradiation will be given by the expression

$$N_g = (P_g + P_m)t \quad (2)$$

where t is the irradiation time. The capture rate is the product of the cross section (σ_g for the production of ^{60g}Co , σ_m for the production of ^{60m}Co), the thermal neutron flux, f , and the number of atoms available for activation. The total number of ^{60g}Co atoms produced can be calculated from Equation (3), where g is the mass in grams irradiated, N_a is Avogadro's number, and M_c is the molecular weight of the compound.

$$N = \frac{fgN_a(\sigma_g + \sigma_m)t}{M_c} \quad (3)$$

If 10.0 mg, $\text{D-}[\text{Co}(\text{en})_3](\text{NO}_3)_3$ is irradiated with a thermal neutron flux

of 1.0×10^{13} n/cm²-sec for 10.0 minutes, where $\sigma_g = 19.0 \times 10^{-24}$ cm² and $\sigma_m = 18.0 \times 10^{-24}$ cm² (2), 3.06×10^{12} ⁶⁰Co atoms will be produced. This number of atoms is far below the amount needed for detection by ordinary physical or chemical means. Therefore, the atoms can be detected only by the characteristic radiation they emit in decay. The decay rate or activity of the sample is proportional to the number of atoms and the decay constant. For the example cited above, the half life is 5.26 years. This corresponds to a decay constant of 1.52×10^{-6} sec⁻¹. The activity produced would be 1.27×10^4 d/sec or 0.345 μ Ci.

In general, the recoil of an atom in an (n, γ) process may occur by the emission of one γ photon or several photons in cascade to the ground state. For a one photon process the momentum of the nucleus, \vec{p}_r , is equal and opposite to the momentum of the emitted photon, \vec{p}_p ,

$$-\vec{p}_r = \vec{p}_p = E_\gamma/c \quad (4)$$

where c is the velocity of light, E_γ is the energy of the photon. The kinetic energy, E_r , can be calculated from the momentum:

$$E_r = \frac{1}{2} \vec{p}_r^2 / M = \frac{1}{2} E_\gamma^2 / c^2 M \quad (5)$$

where M is the mass of the nucleus. With E_r in eV, E_γ in MeV, and M in a.m.u.,

$$E_r = 537 E_\gamma^2 / M \quad (6)$$

The energy of a single gamma ray emitted in a transition from the highest energy excited state can be estimated from the difference in the masses

of the particles involved:

$$E = [M(^{59}\text{Co}) + M(\text{neutron}) - M(^{60}\text{Co})] c^2 . \quad (7)$$

The prompt gamma energy calculated from Equation (7) is 7.493 MeV. This value is in good agreement with that measured by Prestwich et al. (1) from prompt gamma determinations, 7.495 MeV.

The recoil kinetic energy imparted by such a photon is 502 eV or 8.04×10^{-10} ergs. The velocity of the atom is 4.01×10^6 cm/sec. From the kinetic theory of gases, the kinetic energy is related to the temperature.

$$E = \frac{3}{2} kT \quad (8)$$

The temperature of such a recoiling atom would be 3.89×10^6 K. This very high temperature is the reason why recoil reactions are sometimes termed "hot atom reactions."

Only 2.6% of the recoil atoms are produced as a result of a single photon de-excitation to the ground state (1). The remainder of the recoil atoms are produced by multi-photon cascade de-excitation processes. The highest excited state (7.495 MeV) is probably a 4^- state (1). In the case of decay to the 5^+ (2) ground state, the transition is an electric dipole E-1 type transition. Cascade type transitions involve de-excitation from the high energy state to a lower excited state due to an E-1 transition. The resultant state is either 5^+ or 3^+ . These lower energy excited nuclei may then decay by higher order processes to either the ground state, the metastable state, or another excited state. This

process continues until all the nuclei are either in the 5^+ ground state or the 2^+ metastable state. The 58 KeV metastable state decays with a half life of 10.5 min by a M-3 transition to the ground state (1,2). Little further momentum is imparted to the already displaced recoil atom. However, Auger excitation may cause a change in the oxidation state of the atom.

If the second or later transition occurs rapidly in succession, compared to the time of collision in the lattice, the momentum of the recoil atom is equal to the vector sum of the momenta of the emitted gamma rays.

$$-\vec{p}_r = \vec{p}_1 + \vec{p}_2 + \dots + \vec{p}_n \quad (9)$$

In Equation (9), n is the total number of cascade gamma rays involved. The energy of the recoil atom is proportional to the dot product of the recoil momentum on itself:

$$E_r = (\vec{p}_r \cdot \vec{p}_r) / 2M \quad (10)$$

For two photons (4):

$$E_r = [E_1^2 + E_2^2 + 2E_1E_2 \cos \theta] / 2Mc^2 \quad (11)$$

where θ is the angle between the two emitted photons. The minimum energy in eV is $536(E_1 - E_2)^2 / M$ where E_1 and E_2 are in MeV, M is in amu. The maximum energy is $536(E_1 + E_2)^2 / M$, the same recoil energy if the transition had occurred as a single photon process.

If it is assumed that the directions of emission of the two gamma

rays are unrelated, the emission is said to be isotropic. Libby (4) has shown that for such isotropic emission, the distribution of recoil energies is flat between the minimum and maximum values stated above with a spread of $4 \times 536(E_1 E_2/M)$ eV. The normalized probability of a given atom having a certain recoil energy can be calculated as:

$$N(E) = \frac{M}{E_1 E_2 \times 4 \times 536} \quad . \quad (12)$$

Prestwich et al. (1) have observed 15 processes in which de-excitation occurred as two photon cascades. The energies observed and transition probabilities based on gamma intensities for E_1 are shown in Table 1. The recoil energy distribution was calculated by summing the recoil probabilities, $N(E)$, listed in Table 1, for each energy. A plot of this distribution is shown in Figure 1. Figure 1 shows that the most probable recoil energies are in the high energy region and that 96% of the recoil atoms have energy in excess of 175 eV.

The "hot" recoil atom can lose its large amount of translational kinetic energy in a variety of ways by interaction with the crystal lattice. All the recoil energy is eventually absorbed in the crystal lattice in the form of heat, or in the form of a latent potential energy by virtue of the existence of crystal defects produced by the traumatic disruption of the lattice by the recoil atom. The eventual fate of the recoil atom in the crystal lattice will depend upon its energy of recoil and the nature of the crystal lattice itself. The fate of the recoil atoms can be investigated by dissolving solid material, performing chemical separations, and determining the fraction of radioactivity in

Table 1. Probability of ^{60}Co nuclei possessing certain recoil energy
calculated from correlated two photon energies^a

n	Energy of first gamma photon E_1 (MeV)	Energy of sec- ond gamma photons E_2 (MeV)	Minimum recoil energy E_{\min} (eV) ^{b,c}	Recoil energy spread E_s (eV) ^d	Intensity (Percent of probab- intensity ity of all gamma peaks)	Recoil probabil- ity $N(E)$ ^e $\times 10^3$
1	7.218	0.278	430.3	71.7	3.8	5.289
2	7.059	0.436	391.9	110.0	1.5	3.546
3	6.710	0.786	313.5	188.5	6.1	3.098
4	6.490	1.007	268.6	233.5	5.4	2.033
5	6.278	1.216	228.9	272.8	0.85	1.274
6	6.177	1.317	211.0	290.7	0.25	1.172
7	5.981	1.514	178.3	323.6	5.4	1.143
8	5.663	1.830	131.2	370.3	5.4	0.595
9	4.444	3.053	17.28	484.8	0.1	0.116
10	4.397	3.092	15.2	485.8	0.2	0.109
11	4.306	3.192	11.1	491.1	0.1	0.095
12	4.274	3.219	9.9	491.6	0.1	0.088
13	4.247	3.244	9.0	492.3	0.05	0.082
14	4.209	3.283	7.7	493.8	0.55	0.079
15	4.027	3.467	2.8	498.9	0.63	0.042

^aData from Reference (1).

$$^b E_{\min} = (E_1 - E_2)^2 \times 8.933.$$

^cThe maximum recoil energy in all cases is 501.8 eV.

$$^d E_s = E_{\max} - E_{\min}.$$

^e $N(E)$ is the probability of an atom receiving a recoil energy between E_r and $E_r + dE_r$.

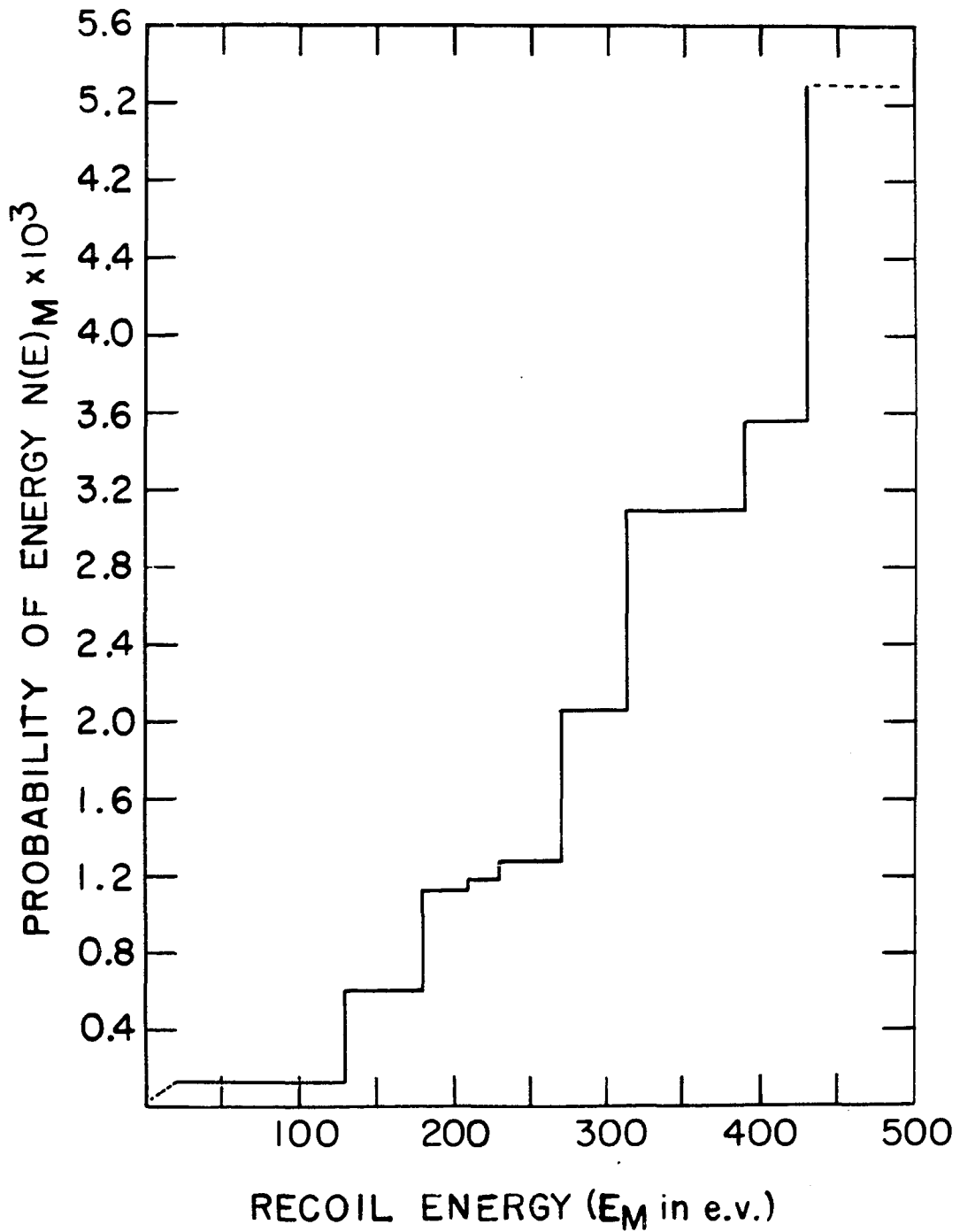


Figure 1. Calculated recoil energy distribution from two-photon cascade in the $^{59}\text{Co}(n,\gamma)^{60}\text{Co}$ reaction

each component obtained from the separation.

Szilard and Chalmers (5) first performed such a separation in 1934 when they bombarded ethyl iodide with neutrons from a radon-beryllium source. They found that radioactive "free" iodine, which they precipitated as silver iodide, was formed. As a result, the recoil species was separated from the bulk organic halide. Since that time, many workers have reported the separation of activity in a chemical form different from the bombarded material.

Several theories have been advanced to explain the Szilard-Chalmers separation phenomenon. Although many mechanisms have been proposed, the theory does not allow one to predict the nature of the interstitial recoil atoms and defects produced or the nature and percentages of radioactive recoil products observed finally. Harbottle and Sutin (6) and Harbottle (7) have reviewed the models which have been invoked to explain the interaction and slowing down of recoil atoms in a crystal lattice. These models can be used to explain the eventual fate of the recoil atom in the crystal lattice. The models proposed fall into five categories: 1) the elastic collision or billiard-ball model, 2) the elastic-inelastic collision model, 3) the epithermal reaction model, 4) the brush heap or random fragmentation model, and 5) the hot-zone model.

The first model proposed to explain recoil phenomena was the elastic collision or "billiard-ball" model of Libby (4). In this model, the recoil atom was assumed to produce no appreciable ionization, and the energy of the recoil atom was greatly in excess of that required to break chemical bonds. The recoil atom would cool or slow down by a series of

elastic collisions with other atoms. The energy loss in a given collision would depend on the mass M' of the atom collided into and the mass M of the recoil atom. Libby showed from such an analysis that the energy of the recoil atom after n collisions is an exponential function of the number of collisions.

$$E_n = E_0 e^{-Kn} \quad (13)$$

In Equation (13) E_0 is the initial recoil energy, E_n is the energy after n collisions, and K is defined by Equations (14) and (15).

$$K = \frac{1-(1-\gamma) [1-\ln(1-\gamma)]}{\gamma} \quad (14)$$

$$\gamma = 4M'M/(M+M')^2 \quad (15)$$

In this model the collision with atoms much lighter than the recoil atom (e.g. collision of a recoil atom of ^{60}Co with N, C, or O) will remove only a small fraction of the kinetic energy of the recoiling atom. Libby noted that this residual velocity will insure the escape of the radioactive atom from the vicinity of the collision and the molecular fragment produced so the chance of combination between the molecular fragment and the radioactive atom is nearly zero. However, head-on collisions between atoms of similar masses (e.g. ^{60}Co or ^{59}Co) could leave the recoil atom with considerably less energy than its initial energy. In fact, the energy of the recoil atom may be reduced to less than the bond energy, so that the recoil atom is trapped in the lattice cage and retained, bonded in place of the inactive atom displaced. Such a result would lead to

retention of the radioactivity in the target material.

Friedman and Libby (8) modified Libby's model in the elastic-inelastic collision model. In this model they still maintained that retention of activity in the parent compound was due to an elastic collision in which the inactive heavy atom was replaced by the recoiling atom. However, at lower energies after the recoil atom was moving with less velocity, it could undergo inelastic collisions with molecules or ions composed of lighter atoms. Such collisions could lead to C-H, C-C, C-N, N-O, etc. bond rupture. These processes would probably occur in the ten eV energy region and were termed "epithermal" reactions. Friedman and Libby (8) investigated the hot atom chemistry of n- and i-propyl bromides. They proposed that recoil bromine atoms were substituted for hydrogen atoms in an organic halide near the end of the range of the recoiling bromine atom. In this region the kinetic energy of the bromine atom was still somewhat larger than the chemical bond energy but was not a great deal larger. The energy was sufficient to cause bond rupture but was insufficient to warrant treatment of the collision as a process occurring essentially between free atoms. The process allowed the molecule as a whole to act in an inelastic manner to stop the radiobromine atom in the same solvent "cage" and to itself dissociate, for example, by losing a hydrogen atom. The whole process resulted in the replacement of hydrogen by bromine. Friedman and Libby observed that such a process dominated when the medium contained a very low concentration of heavy atoms. If there were no heavy atoms in solution, energy loss would occur entirely by collision with much lighter atoms so that every halogen atom would

move through the critical energy range in which inelastic collisions occurred. In every case, substitution of bromine for hydrogen would result. On the other hand, if an appreciable fraction of the cooling collisions occurred with atoms of equal mass, the chance of the atom jumping discontinuously through the critical energy interval is appreciable; and a considerable fraction of the atoms would have no opportunity to substitute for hydrogen. It should be noted, however, that reactions could occur after the recoil atom had slowed to thermal velocities. Free atoms, especially halogens studied by Friedman and Libby, are very reactive species which can combine with organic fragments in the medium. Impurity compounds which will react with the reactive halogen atoms pose special problems with regard to free radical type reactions which may lead to a misinterpretation of the experimental results.

Miller and Dodson (9), who studied the recoil reaction of chlorine from CCl_4 in SiCl_4 and hydrocarbon media, were unable to account for their results in terms of Libby's elastic collision model and proposed the epithermal reaction theory to explain their experiments. The retention of activity in CCl_4 decreased rapidly with the addition of cyclohexane or benzene. Substituted chlorocyclohexane or chlorobenzene were obtained as additional radiochemical products. The yield of radioactive target material, according to the elastic-inelastic or elastic collision theories, can be expressed as shown in Equation (16).

$$R = \int_0^{\infty} pN(E)W(E) dE \quad (16)$$

In Equation (16) p is the probability that a collision of an active

chlorine atom is a collision with a carbon tetrachloride molecule, $N(E)dE$ is the number of active chlorine atoms making collisions per unit time in an energy interval dE at E , and $W(E)$ is the probability that the exchange reaction occurs in a collision with a carbon tetrachloride molecule at energy E . Below a certain critical energy $W(E)$ will vanish. This energy is a type of activation energy for recoil recombination. Since high energy collision would not lead to stable chemical bonding, $W(E)$ should become quite small at higher energies. The billiard-ball model, in which no interaction of the heavy atoms displacing carbon atoms can give rise to recombination, predicted that with $SiCl_4$ diluent, the retention of activity as CCl_4 should be a linear function of CCl_4 concentration. Such a phenomenon was observed experimentally. However, the collision theories predicted that in hydrocarbon media there should not be a sharp decrease in retention, but rather a slow drop in retention with decreasing CCl_4 concentration. The retention of activity in CCl_4 decreased rapidly with the addition of hydrocarbon diluent. Due to the inability of the elastic collision theory to explain the experimental facts, Miller and Dodson invoked a new theory, the epithermal reaction theory, with which theoretical retention vs. mole fraction curves were calculated. These curves were calculated by assuming that: 1) every radioactive recoil atom formed an excited intermediate complex with the hydrocarbon diluent; 2) this complex could decompose by any of at least four reaction paths, each path characterized by a definite probability which is independent of the composition of the system. Products of these paths were, respectively, 1) chlorine substituted hydrocarbon,

2) the lower boiling active component found with CCl_4 , 3) free active chlorine atoms, and 4) an extractable compound of chlorine which did not exchange with CCl_4 (possibly HCl). Dodson and Miller asserted that the concept of elastic atom-atom collisions could be entirely relinquished in their "epithermal reaction model." The results of their calculations predicted the rapid decrease in retention with the addition of hydrocarbon diluent. In this model the distribution of products was determined by competing chemical reactions in the epithermal region.

Willard (10) objected to the billiard-ball model by showing that the billiard-ball hypothesis would predict that all of those recoil atoms which re-enter organic combination must do so as the parent compound. Such a conclusion was not viable in light of the experimental facts. Furthermore, modification of the theory, such as the epithermal reaction theory or the inelastic-elastic collision theory, did not give a consistent correlation to all the experimental facts. The random fragmentation or "brush heap" theory of Willard offered a broad base from which to rationalize the experimental evidence. In this theory, when a halogen (or heavy) atom in a molecule acquired several hundred eV of recoil energy, it started moving rapidly. Upon traveling less than a molecular diameter it encountered a solvent molecule. If this were an isolated molecule, the energetic atom would transfer momentum to it or to one of its atoms in an elastic collision and would continue on its way. In the liquid or solid state this could not happen because the struck molecule was backed by a close-packed and sometimes intertwined wall of other molecules. The result was that the energy was dissipated

by the breaking of bonds in a rather indiscriminate manner. This breaking of bonds occurred in the immediate vicinity of the energetic atom. When the energy of the atom had been reduced below bond breaking energies, the atom would find itself in, or adjacent to, a pocket of high local concentration of organic radicals and inorganic atoms. The atom may have combined with one of these radicals or atoms after it had been moderated to an energy where combination was possible but before it had an opportunity to diffuse in the system as a thermal atom. Alternatively, following diffusion it may have combined with an organic molecule in the medium and formed a stable compound by a thermal process. The relative yields of the recoil atom in different product species will depend on the types of organic and inorganic recoil products produced, on the chemical nature of the medium, on the density and crystal structure of the medium, and on the mass and energy of the recoil atom.

In objecting to the Willard theory, Harbottle and Sutin (11) conceded that the appearance of a wide variety of radioactive products formed in the alkyl halides (as well as in Co(III) complexes as will be pointed out later) lent support to the brush-heap model. However, the distribution of products observed was not the distribution expected from a random fragmentation of chemical bonds. Harbottle and Sutin (11) have proposed the hot-zone model for Szilard-Chalmers recoil reactions. The hot-zone model was based on the "displacement spike" concept of radiation damage in solids. Essentially, in this model the energy of the recoil atom was dissipated in producing displaced atoms and in heating a small region of the crystal (the displacement spike). The

recoil atom slowed to energies below the threshold for displacement in about 10^{-13} sec. Harbottle estimated that during the slowing down process about six displacements were produced in ionic crystals, and about sixteen displacements were produced in molecular crystals when the recoil energy was about 300 eV. The displaced atoms represented local hot spots and resided in a sphere with a radius of about $5 r_s$, where r_s is the atomic radius. These local hot spots merged within about 10^{-12} sec to produce a hot zone of relatively uniform and high temperature. The time required for a temperature of the hot zone to fall below the melting point of the crystal was about 10^{-11} sec, somewhat longer in molecular crystals. There was a good chance that the recoil atom would react with species in its immediate vicinity during the lifetime of the hot zone, even though such reactions require moderate activation energy. Since recoil atoms in solids could undergo recombination reactions during post-irradiation annealing, the reactions in the hot zone were quenched by cooling before their completion. The size of the hot zone was a consequence of the range of the recoil atom. Harbottle and Sutin estimated that the hot zone may have contained about 1000 atoms in an ionic crystal to about 4000 atoms in a molecular crystal. The range of the recoil atom was dependent on the recoil energy to a great extent. On the other hand, the billiard-ball model would predict a much smaller hot zone, independent of recoil energy. The random fragmentation model, on the other hand, was based on free radical recombination. The hot-zone predicted that there would be a very low concentration of free radicals available for recombination. Therefore, reaction with the parent species

must have played an important role in the recombination process.

The models described will play an important role in the interpretation of the experimental results concerning Szilard-Chalmers recoil in $D-[Co(en)_3](NO_3)_3$. It has become increasingly evident that experimental results of initial radiochemical yields of various species should be interpreted with caution. Thermal annealing reactions, annealing by ionizing radiation, and interfering reactions in the dissolution and separation processes can give rise to radiochemical yields which do not accurately reflect the fate of the recoil atom immediately following recoil. The problems involved with these effects and methods of minimizing or correcting for them will be discussed in a later section. In the meantime, it should be pointed out that the application of any model to the experimental facts should be done with caution. These interfering effects should be considered in any interpretation of experimental results.

In addition to gamma recoil, a fraction of the atoms may undergo internal conversion, causing the ejection of an electron from the atom. Such ejection may cause the ionization of the recoil atom. Since the conversion coefficients for the various de-excitation pathways are not known, it is impossible to determine the extent of ionization. Such ionization may give rise to effects not accounted for in the various models, and ion-molecule reactions may give rise to the possibility of reactions not predicted by the models discussed above.

B. Distribution of Products Obtained from Szilard-Chalmers Recoil in tris-(ethylenediamine)cobalt(III) Salts

Several reports of investigations of the Szilard-Chalmers process in $[\text{Co}(\text{en})_3]^{3+}$ compounds have appeared in the literature. The authors of these reports have assigned the ^{60}Co activity produced to two chemical forms, Co^{2+} and $[\text{Co}(\text{en})_3]^{3+}$. The word "retention" has sometimes been used to mean the percent activity recovered as $[\text{Co}(\text{en})_3]^{3+}$. However, "retention" has also been used to mean the percent activity not extracted as Co^{2+} . If $[\text{Co}(\text{en})_3]^{3+}$ and Co^{2+} were the only chemical forms of ^{60}Co produced, the percent activity recovered as $[\text{Co}(\text{en})_3]^{3+}$ would be equal to the percent activity not extracted as Co^{2+} . As a result of the research reported in this work, it has been found that radiochemical forms other than Co^{2+} or $[\text{Co}(\text{en})_3]^{3+}$ were produced, and that the percent activity as $[\text{Co}(\text{en})_3]^{3+}$ was not equal to the percent activity not extracted as Co^{2+} . The usage of "retention" has therefore been somewhat ambiguous. For the purpose of this work the word "retention" will mean the percent activity recovered in a form identical to the target material. The description, "total retention" will refer to the percent activity which was not extracted as Co^{2+} . "Total retention" will include activities of nonlabile cobalt complexes as well as the target ion.

Süe and Kayas (12) were the first to investigate the radiochemical products resulting from the neutron irradiation of $[\text{Co}(\text{en})_3] (\text{NO}_3)_3$ in the solid state. They found that 75% of the cobalt activity could be extracted from solution as precipitated $\text{Co}(\text{OH})_2$. Few experimental details were given except that their neutron source was the cyclotron at

the College of France. No attempt was made to recrystallize the target material or to separate and identify the radiochemical identity of the remaining 35% of activity.

In 1954, Zuber (13) reported the results of his experiments concerning the Szilard-Chalmers recoil phenomenon in both D,L-[Co(en)₃](NO₃)₃ and D-[Co(en)₃](NO₃)₃. Zuber found component yields for four different radiochemical forms. In the neutron irradiation of the D-complex, 4.6% of the activity was found to be associated with the D-[Co(en)₃]³⁺ ion (retention); 0.6% of the activity was associated with the L-[Co(en)₃]³⁺ ion; and 14.2% of the activity was in a chemical form which he could not identify. The remainder of the activity was extracted as Co²⁺ by precipitation with hydroxide ion as Co(OH)₂. Zuber labeled his compound [Co(en)₃](NO₃)₃·3H₂O. Since he gave no analysis for his compound, and since his preparative methods were similar to those used in this work, he was no doubt working with the anhydrous salt. Furthermore, Dimotakis and coworkers (14) noted that the trihydrate had not been reported elsewhere in the literature. Zuber's compound was irradiated for 24 hours at ambient temperatures with a low flux of 10⁹ neutrons/cm²·sec for 24 hours. The total tris-(ethylenediamine)cobalt(III) activity was determined by recrystallization as the bromide salt. The activity in the various isomers was determined by adding D-[Co(en)₃]Br₃ carrier. The less soluble D-isomer was separated from the racemate by precipitation. The remaining activity, which was unidentified, was determined from the difference of the total activity and the activity recovered as complex and Co²⁺. The unknown component was not identified, but he

speculated it might be of the form, $[\text{Co}(\text{en})_2(\text{NO}_3)_2]\text{NO}_3$, $[\text{Co}(\text{en})_2(\text{H}_2\text{O})_2](\text{NO}_3)_3$, $[\text{Co}(\text{en})_2(\text{NO}_2)_2]\text{NO}_3$, or $[\text{Co}(\text{en})_2(\text{NH}_3)_2](\text{NO}_3)_3$. The possibility of other products resulting from the ligation of other degradation procedures was also mentioned. It is important to note that Zuber found a small, but definite percent of the activity in the L form. Few authors have considered the possibility of optical isomerism in these systems. The change in optical isomeric form may give an important clue to the mechanisms of recoil and annealing. Zuber also studied the racemic complex and recovered 6.0% of the activity as the target material, 14% as unidentified activity, and 80% as Co^{2+} . These results are quite similar to those obtained for the optically pure form.

Costea and Dema (15) irradiated the optical and geometric isomers of several cobalt compounds. They irradiated solid D- $[\text{Co}(\text{en})_3](\text{NO}_3)_3$ and L- $[\text{Co}(\text{en})_3](\text{NO}_3)_3$ with thermal neutrons and extracted Co^{2+} from the dissolved compounds. They found that the percent activity not extracted as Co^{2+} from irradiated D- $[\text{Co}(\text{en})_3](\text{NO}_3)_3$ was 71.9%. The percent activity not extracted as Co^{2+} from L- $[\text{Co}(\text{en})_3](\text{NO}_3)_3$ was 73.6%. Although the values were nearly identical, Costea and Dema claimed that the difference in the values was real. It is difficult to reconcile such differences with generally accepted concepts of optical activity. The only possible explanation would lie in the chirality of the nuclear excited states interacting with the geometric chirality of the crystal lattice.

Saito et al. (16) irradiated the chloride, bromide, thiocyanate, nitrate and iodide salts of $[\text{Co}(\text{en})_3]^{3+}$ (unless otherwise noted, the compounds cited will be assumed to be racemic) at a flux of 3×10^{11}

$n/cm^2 \cdot sec$ for one hour and separated the radiochemical products. Storage prior to separation was in dry ice. Although the experimental procedures used in the separation were not described in detail, paper electrophoresis, ion exchange, precipitation and recrystallization techniques were used. In all cases, several radiochemical species containing cobalt were separated. In the case of the nitrate salt, 12.2% of the activity was present as $[Co(en)_3]^{3+}$, 6.0% was present as $[Co(en)_2a_2]^{3+}$; 7.0% was present as $[Co(en)_2aX]^{2+}$; and 1.4% was present as $[Co(en)_2X_2]^+$. In the paper Saito gave no details concerning the identity of the ligand designated "a." However, in previous papers (17,18) "a" designated a neutral ligand, possibly NH_3 or H_2O . The symbol "X" designated an anionic ligand. Depending on the separation methods used, the radiochemical distribution of these products may reflect solution equilibria and not be indicative of the situation in the solid state. In addition to the products mentioned, 69.4% of the activity was due to Co^{2+} , 1.8% and 1.4% were described as unidentified neutral and anionic species, respectively. For compounds of the type $[Co(en)_3]X_3$, $[Co(NH_3)_6]X_3$, $[Co(NH_3)_5(H_2O)]X_3$, where $X=NO_2^-$, NCS^- , NO_3^- , F^- , Cl^- , Br^- , I^- , Saito *et al.* (17) plotted retention as a function of the frequency of the first electronic absorption band of $[Co(NH_3)_5X]^{2+}$. They found that the percent activity as target complex decreased as a curved monotonic function of frequency. They also plotted S, defined in Equation (17), as a function of frequency and found a monotonic increasing relationship.

$$S = \frac{\text{Sum of percentages of } ^{60}\text{Co-labeled complexes containing more anionic ligands than the target}}{\text{Sum of percentages of all } ^{60}\text{Co-labeled complexes}} \quad (17)$$

The authors concluded that the ligand groups (NH_3 , ethylenediamine, or H_2O molecules) whose bonds to cobalt were more or less ruptured as a result of recoil and the counter anion competed with each other in the subsequent reaction. In these processes various ^{60}Co labeled complexes were formed through the reaction of recoil atoms with neighboring entities according to their concentrations and the stability of their complexes with cobalt.

De Maine and Kay (19) studied the chemical effects of radiative neutron capture on various cobalt-amine complexes. They concluded for $[\text{Co}(\text{en})_3]\text{Cl}_3 \cdot 3\text{H}_2\text{O}$ that less than 1% of the total activity was present in a form different from Co^{2+} or target material. The separation method used was electrophoresis with acetate buffers. They did not investigate the nitrate salt of tris(ethylenediamine)cobalt(III). However, in studying $[\text{Co}(\text{NH}_3)_6](\text{NO}_3)_3$ and the analogous chloride salt, they found that as much as 26.4% of the activity resided in a form which was speculated to be $[\text{Co}(\text{NH}_3)_5(\text{NO}_2)]^{2+}$, $[\text{Co}(\text{NH}_3)_5(\text{H}_2\text{O})]^{3+}$, or $[\text{Co}(\text{NH}_3)_5(\text{C}_2\text{H}_3\text{O}_2)]^{2+}$. It is interesting to note that in their studies the percent activity not extracted as Co^{2+} for the ethylenediamine salt was 0.1% when the material received a low neutron dose and was 85.6% when the material received a higher dose. Irradiation temperature and storage temperature seemed to affect radiochemical yields also.

Williams et al. (20) checked Zuber's results by irradiating $[\text{Co}(\text{en})_3](\text{NO}_3)_3$ for five minutes at a flux of 1.1×10^{13} n/cm²·sec. Radiochemical Co^{2+} was extracted with 8-hydroxyquinoline in chloroform; retention of activity as parent was determined by repeated

recrystallization to constant specific activity. They reported an initial retention of 10%. No mention was made of other radiochemical species, nor were discrepancies between the recrystallization and extraction results reported.

Yasukawa (21) irradiated several salts of $[\text{Co}(\text{en})_3]^{3+}$ and reported an initial "total retention" of 53% for the nitrate salt. The irradiations were carried out at ambient temperatures for one hour at a flux of 3×10^{11} neutrons/cm²·sec. No mention was made of activity being present in forms other than Co^{2+} or target material. However, from the experiments described, it is difficult to tell whether a complete investigation of such a possibility was made. Chloroform extraction of the oxine complex was performed to separate Co^{2+} from target material, but whether ion exchange analysis (22) was performed to determine other products in the case of the $[\text{Co}(\text{en})_3]^{3+}$ could not be determined from the described experiments.

Dimotakis and coworkers in two articles (14,23) studied the recoil reaction of tris(ethylenediamine)cobalt(III) nitrate. They reported initial total retentions of 65% and 61% in which the total integrated neutron fluxes were 4.1×10^{14} and 9.1×10^{15} n/cm², respectively. The methods used to separate Co^{2+} activity were $\text{Co}(\text{OH})_2$ precipitation and ion exchange. The authors concluded from a review of the prior literature that initial retention or "total retention" increased as the total integrated neutron flux increased. They attributed this increase to an increase in the dose of concomitant gamma rays and fast neutrons. These gamma rays and fast neutrons could cause radiation induced annealing and

an increase in the relative radiochemical yield of $[\text{Co}(\text{en})_3]^{3+}$. Subsequent experiments in the literature indicated that this may not have been the case. Since most workers have not separated or identified radiochemical species other than $[\text{Co}(\text{en})_3]^{3+}$ or Co^{2+} , one cannot readily surmise which activities were reported in the Co^{2+} fraction and which are reported as retention. Therefore, correlation between the data of different workers is frequently difficult. In two later papers, (24,25) Dimotakis reported results concerning studies of the Szilard-Chalmers process in $[\text{Co}(\text{en})_3](\text{NO}_3)_3$. When an integrated flux of 1.67×10^{16} neutrons/cm² was employed, the initial "total retention" was found to be 66%. In two experiments where the samples were held at liquid nitrogen temperatures during irradiation and prior to separation, initial "total retentions" were found to be 20.7% and 14.6%. The neutron flux was not reported for these two experiments. It is clear that the irradiation temperature was an important factor which affected initial radiochemical yields.

Lazzarini and Fantola-Lazzarini have contributed a great deal to the study of Szilard-Chalmers recoil in transition metal complexes. They found that $^{60\text{m}}\text{Co}$ and $^{60\text{g}}\text{Co}$, formed by the (n, γ) reaction in Co(III) complexes irradiated in the solid state, behave differently in their Szilard-Chalmers recoil (26). Such differences in behavior were termed the isomer effect. For $[\text{Co}(\text{en})_3](\text{NO}_3)_3$, "total retentions", determined from solvent extraction of Co^{2+} , were 27% and 21.9% for the "m" and "g" isomers, respectively. They found that the isomer effect varied little as a function of the counter anion. In later articles (27-29) Lazzarini

and Fantola-Lazzarini studied the isomer effect further. They found that the rest of the crystal structure outside the first coordination sphere of Co(III) had only a second order influence in the isomer effect despite a difference in absolute "total retention" values. The role of cis-trans geometric isomers in the isomer effect was small. They proposed that the magnitude of the isomer effect was linearly depending on the splitting of the 3d-orbitals of the Co(III) by the ligand field. The isomer effect was considered to depend on the ability of the ligand to promote back-donation from the cobalt atom. The isomer effect was essentially an additive property of the ligands.

It must be concluded from the preceding discussion that the literature is not consistent concerning the products that are obtained in the Szilard-Chalmers recoil of cobalt in $[\text{Co}(\text{en})_3](\text{NO}_3)_3$ or in the percentage yields of radioactive target material. Separation methods used sometimes did not serve to uniquely isolate target material or other products. The effects of temperature, ambient gases, concomitant ionizing radiation and total integrated neutron flux are important factors in determining the initial retention. These many factors make comparisons of reported initial retentions difficult. The purpose of this research has been to separate and identify the various recoil products produced in the (n,γ) Szilard-Chalmers reaction of D- $[\text{Co}(\text{en})_3](\text{NO}_3)_3$. Irradiation under standard conditions with a minimum of thermal effects have provided comparison of data within the study so the effects of thermal annealing can have meaning.

C. Annealing of Products and Solid State Isotopic Exchange

Since concomitant gamma rays and fast neutrons may affect radiochemical distribution ratios, and thermal annealing during neutron irradiation may change such radiochemical distribution ratios, various workers have studied the effects of gamma pre-irradiation, gamma post-irradiation, ambient gases and post-irradiation annealing on the radiochemical yields of various products obtained in Szilard-Chalmers recoil. In an early article, Willard (30) stated that radiation effects were not important in determining the yields of recoil products. He based his opinion on experiments performed on organic liquids.

For organic complexes of cobalt, however, several workers have concluded that concomitant radiation effects were important combined with thermal annealing effects. Costea (31) found, in samples of $[\text{Co}(\text{NH}_3)_6](\text{NO}_3)_3$ irradiated with thermal neutrons, that "total retention" increased with time of irradiation, until it reached a saturation value, R_∞ less than 100%, characteristic of a certain γ dose rate. The greater the γ dose rate, the greater the value of R . In fact, R was found to be proportional to the logarithm of the γ dose rate within the range of γ dose rates studied. As a further experiment, samples irradiated in the reactor were subsequently submitted to irradiation from a ^{60}Co source. Samples which had been irradiated in the reactor at a higher dose rate than at the ^{60}Co source did not increase in retention, but samples irradiated in the reactor at a lower dose rate than at the ^{60}Co source showed a large increase in retention. At a given γ dose rate, retention became independent of irradiation time after a short period of time.

Costea suggested that a dynamic equilibrium existed during the annealing process. According to his proposal, although new radioatoms were continually being formed during irradiation the ratio between the number of interstitial radioatoms and the number of coordinated atoms remained constant, independent of the period of irradiation.

Yoshihara and Harbottle (32) found that irradiation time had no effect on the radiochemical product yield in the neutron irradiation of $[\text{Co}(\text{NH}_3)_6]\text{Br}_3$. In addition to Co^{2+} and target material, they found a radiochemical product identified as $[\text{}^{60}\text{Co}(\text{NH}_3)_5\text{Br}]^{2+}$. It was found that ^{82}Br and ^{80}Br formed by neutron capture was incorporated into the $[\text{Co}(\text{NH}_3)_5\text{Br}]^{2+}$ fraction. Pre-activation gamma irradiation and post-activation gamma annealing decreased the yield of radio-bromine in $[\text{Co}(\text{NH}_3)_5\text{Br}]^{2+}$ ion.

Stucky and Kiser (33) examined the Szilard-Chalmers process for a series of cobalt(III) complexes. They found that a combination of gamma irradiation and room temperature thermal effects produced increases in retention of activity in $[\text{Co}(\text{NH}_3)_6](\text{NO}_3)_3$. From their studies they concluded that radiation damage was the influencing factor in the determination of initial retention.

Zuber (13) reported that retention in neutron irradiated $[\text{Co}(\text{en})_3](\text{NO}_3)_3$ increased on exposure to 1.6 MR of ^{60}Co gamma rays. The "total retention" increased from 30% to 47% upon this exposure. He concluded, however, that concomitant gamma annealing had little effect on his initial yields since the dose received during neutron bombardment was only 1 KR.

The preceding studies considered only the effects of gamma irradiation at the tracer level in neutron irradiated compounds. In general, macroscopic effects were ignored or were minimal. Witiak (34) studied the gross effects of gamma and X-rays on a series tris-(ethylenediamine) cobalt(III) salts. He found that the compounds racemized and decomposed to Co^{2+} as a logarithmic function of total X-ray or gamma dose. He found that the stability of $[\text{Co}(\text{en})_3]\text{X}_3$ salts was a function of the anion. The stability to decomposition decreased in the order $\text{Cl}^- > \text{NO}_3^- > \text{Br}^- > \text{I}^-$. Witiak also studied the solid state thermal racemization of these compounds. He found that the compounds racemized by a first order process and that the activation energies were approximately equal for the halide salts. However, the nitrate salt was racemized much more slowly with an activation energy three times that of the halide salts. Further, the nitrate salt did not racemize appreciably until about 210°C . No gross thermal decomposition was observed by Witiak in his studies.

Thermal effects are important in the determination of the radiochemical distributions in neutron irradiated cobalt salts. It has been observed in almost all cobalt(III)-amine salts studied, that following Szilard-Chalmers recoil, retention in the target compound increased at the expense of Co^{2+} . Zuber (13) was the first to observe this effect for tris-(ethylenediamine)cobalt(III) nitrate. Upon thermal treatment at 60° , 80° , and 100°C , retention increased in the neutron irradiated compound from about 6% to 70%. Radiocobalt(II) decreased a corresponding amount. The percentage of radiocobalt as $\text{L}-[\text{Co}(\text{en})_3]^{3+}$ changed very little and there was little change in the percent of unknown activity.

Zuber found that by plotting $\log(R_\infty - R)$ (where R is either "total retention" or $[\text{Co(en)}_3]^{3+}$ retention) as a function of time he could resolve his annealing curves into two straight lines. He concluded that the thermal annealing consisted of two first order processes. At 80°C the rate constant for the slower process was observed to be $1.25 \times 10^{-6} \text{ sec}^{-1}$ and the rate constant for the faster process was $2.61 \times 10^{-5} \text{ sec}^{-1}$. The activation energies were 25 kcal/mole (105 kJ/mole) and 20 kcal/mole (84 kJ/mole) for the slower and faster processes, respectively.

Williams *et al.* (20) extended Zuber's annealing kinetic studies and found that retention did not reach a true temperature-dependent plateau upon extended annealing of neutron irradiated $[\text{Co(en)}_3](\text{NO}_3)_3$. They found that the retention of samples annealed at room temperature or at 60°C and then annealed at 100°C reached the same value as that of a sample annealed at 100°C throughout. They concluded that competing annealing reactions did not occur in this system and that the retention of all irradiated samples would reach the same plateau value upon extended annealing, regardless of the annealing temperature. They also found that although plots of $\log(R_\infty - R)$ vs. time (where R is retention) could be resolved into two components, the intercepts of these components varied with the annealing temperature. They were unable to reconcile these intercept variations with the absence of temperature-dependent plateaus and concluded that the annealing reaction could not be readily described in terms of two first order reactions.

De Maine and Kay (19) studied thermal annealing effects in a series of neutron irradiated cobalt(III) amine complexes. For $[\text{Co}(\text{NH}_3)_6]\text{Cl}_3$

after irradiation for 7 hours with a flux of 2×10^{12} n/cm²·sec, the initial retention was 76.0%. After the sample was heated at 137°C for three hours, its retention had increased to 94.5%. When $[\text{Co}(\text{NH}_3)_6](\text{NO}_3)_3$ was irradiated for 8 hours the initial retention was only 27.8%. When the irradiated sample was held at 137°C for three hours, its retention had increased to only 31.4%. The effect of both irradiation time and thermal annealing was studied in $[\text{Co}(\text{en})_3]\text{Cl}_3$. When this compound was irradiated for 0.5 hours at 2×10^{12} n/cm²·sec, the initial retention was only 0.87%. The retention increased to 18.4% upon heating of the samples for 3 hours at 137°. If the $[\text{Co}(\text{en})_3]\text{Cl}_3$ was irradiated for 7 hours at 2×10^{12} n/cm²·sec, the initial retention was 84.3%. Following thermal annealing for 0.5 hours, the retention increased to 90.5%. It was observed that there were permanent or reversible color changes at 170° in the solid salts studied and markedly less ⁶⁰Co as parent compound in all cases.

Costea et al. (35) studied the competition between thermal annealing and decomposition in $[\text{Co}(\text{en})_3](\text{NO}_3)_3$, $[\text{Co}(\text{NH}_3)_6](\text{NO}_3)_3$, and $[\text{Co}(\text{NH}_3)_6](\text{CrO}_4)_3$. They heated samples of neutron irradiated $[\text{Co}(\text{en})_3](\text{NO}_3)_3$ for similar periods of time. Between 85°C and 160°C they found that "total retention" was larger following heating at higher temperatures than it was following heating at lower temperatures. However, between 160°C and 190°C "total retention" was smaller following heating at higher temperatures than it was following heating at lower temperatures. They interpreted these results to mean that between 85°C and 160°C the annealing rate (the rate of conversion of radiochemical cobalt(II) to

radiochemical $[\text{Co}(\text{en})_3]^{3+}$ increased with increasing temperature, but in the $160^\circ\text{C} - 190^\circ\text{C}$ range the decomposition rate exceeded the annealing rate. The decomposition was manifest in the conversion of radio $[\text{Co}(\text{en})_3]^{3+}$ to radio-cobalt(II). The experimental result observed was rather surprising, since gross decomposition did not occur until 233°C . Costea et al. proposed the recombination - decomposition theory to explain their results. They said that thermal decomposition began with lower rates even at temperatures below the spontaneous decomposition point. Alternatively, after irradiation the compound became more sensitive toward decomposition. If the former theory is considered, it may explain Witiak's racemization results in terms other than intramolecular nonbond breaking mechanisms.

Perhaps the most support for the recombination or decomposition theory was presented by Dimotakis and Yavas (24) and Dimotakis and Papadopoulos (25) when they reported results for the linear tempering annealing and isothermal annealing of $[\text{Co}(\text{en})_3](\text{NO}_3)_3$. Although most plots of retention as functions of time for isothermal annealing showed a steeply rising portion followed by an apparent plateau, they observed oscillations or waves in their annealing curves. For isothermal or linear tempering annealing curves of retention as functions of time there appeared maxima and minima in the "total retention." Annealing curves were not monotonic. In a family of isotherms at different temperatures the corresponding maxima and minima shifted to shorter times at higher temperatures. Dimotakis considered this oscillating behavior to be a general property of damaged lattices. The magnitude of the amplitude of such waves

increased with decreasing annealing temperatures and needed to be more pronounced if the irradiations were performed at low temperatures (-196°C).

It is difficult to attribute the maxima and minima to experimental error since 9 determinations were performed to position each point in the curve. It must be pointed out, however, that no radioactive products other than Co^{2+} or target $[\text{Co}(\text{en})_3]^{3+}$ were detected and this feature may have contributed to error. Dimotakis and coworkers have observed waves in annealing Szilard-Chalmers recoil products in many other compounds such as ^{60}Co in $[\text{Co}(\text{en})_2\text{X}_2](\text{NO}_3)$, ($\text{X} = \text{Cl}^-$, Br^-) (36), ^{58}Cr in $\text{CrO}_4 =$ salts (23,37), and ^{116}In in $\text{Na In}(\text{EDTA})$ (38). They observed oscillation in the diffraction patterns for annealing $[\text{Co}(\text{en})_3](\text{NO}_3)_3$ which had been irradiated with neutrons. Although most other workers have not observed such wave behavior, Costea et al. (35) observed waves in the annealing curves of both the solid and liquid state for several inorganic compounds. Anderson et al. (39) observed oscillation in the thermal annealing curves of radiolytic fragments of HBrO_3 . The steep maxima and deep minima reported by Dimotakis were attributed to competitive processes, some leading to recombination and some to microdecomposition.

Yasukawa (21,22) also studied thermal annealing effects in $[\text{Co}(\text{en})_3]\text{X}_3$ and $[\text{Co}(\text{NH}_3)_6]\text{X}_3$ where $\text{X} = \text{Cl}^-$, Br^- , I^- , NO_3^- . Annealing curves similar to Zuber's were obtained. Apparent activation energies increased in the order $\text{Cl}^- > \text{Br}^- > \text{I}^- > \text{NO}_3^-$. The outer anions affected recombination processes rather than the primary processes. He found that recombination rates were greater for $[\text{Co}(\text{en})_3]\text{X}_3$ complexes than for

$[\text{Co}(\text{NH}_3)_6]\text{X}_3$ complexes even though $[\text{Co}(\text{en})_3]^{3+}$ is more stable than $[\text{Co}(\text{NH}_3)_6]^{3+}$. He claimed that if diffusion were the rate determining process, the opposite would be the case. But if electron transfer were important (i.e., $[\text{Co}(\text{en})_3]^{3+} + e^- = [\text{Co}(\text{en})_3]^{2+}$), $[\text{Co}(\text{en})_3]^{3+}$ compounds should anneal faster since the rate of electron exchange in the aqueous ethylenediamine system was faster than in the ammine system (40). It was further observed by Yasukawa that addition of ethylenediamine or ammonia to the salts during annealing accelerated the recombination. The stereospecificity of the recombination was not studied. However, his results may support the theory that diffusion of ligand molecules is important in such recombination reactions.

Nath et al. (41) have proposed the isotopic exchange model to explain thermal annealing of recoil damage in cobalt complexes. In this model, the recoil atom was said to stabilize primarily as simple Co^{2+} . The multicomponent exponential annealing curves observed were explained by the release of electrons from variable depth traps formed and populated by fragmentation, by the effect of Auger electrons in the recoil track, and by the effect of extraneous radiation during reactor irradiation in the bulk. The electrons, lifted from traps or from the valence band to the conduction band, were captured by the recoil species (radio-cobalt(II), to give Co^+ in an excited state which exchanged instantaneously with neighboring chelated molecules. The observed result was an increase in retention upon thermal treatment. In this process, the rate determining step (the release of electrons from donors) would be reflected in the kinetics of thermal annealing. Alternatively, trapped

holes could be released and the holes could interact with radio-cobalt(II) to give Co^{3+} , followed by exchange. According to Nath et al., doping Co^{3+} complexes with radio- Co^{2+} produced annealing similar to that following Szilard-Chalmers recoil. In their experiments solutions of high specific activity $^{60}\text{Co}^{2+}$ or carrier free $^{58}\text{Co}^{2+}$ were added to solutions of $\text{Co}(\text{acetylacetonate})_3$, $\text{Na}[\text{CoEDTA}] \cdot 4\text{H}_2\text{O}$, or $\text{Co}[\text{dipyridyl}]_3(\text{ClO}_4)_3 \cdot 3\text{H}_2\text{O}$, and the complex salts were crystallized to contain radio- Co^{2+} . Upon heating, radio-cobalt was incorporated into the Co(III) complexes. The effects of radiation annealing and the effects of ambient air and vacuum upon the incorporation rates were studied. They found that oxygen suppressed the rate of annealing, and that ionizing radiation enhanced the rate.

When activated $\text{Co}(\text{acetylacetonate})_3$ was isothermally annealed in air, the rate of annealing was markedly slower than when it was annealed in vacuum (42). The absorbed oxygen molecules acted as deep electron traps and suppressed annealing. If the O_2 was displaced by vacuum or N_2 , annealing could proceed no further.

Shankar et al. have further extended the isotopic exchange theories of Szilard-Chalmers annealing by identifying two types of electron traps (43). The first type of trap was caused by radiation and Auger electron effects; the second was caused by naturally occurring defects in the crystal lattice. When samples of tris-(acetylacetonato)cobalt(III) were heated and then bombarded with thermal neutrons, the fast components of the post-irradiation annealing curves were eliminated. It was postulated that the shallow, naturally occurring traps were destroyed by

pre-irradiation annealing. The deeper irradiation induced traps were responsible for the slow components of the post-irradiation annealing curves.

Khorana (44) irradiated $^{57}\text{Co}^{2+}$ -doped tris-(dipyridyl)cobalt(III) perchlorate with thermal neutrons. He showed that the kinetics of thermal annealing of recoil ^{60}Co in the doped irradiated complex were identical to the kinetics of isotopic exchange of ^{57}Co .

Aalbers and LeMay (45) studied radiocobalt exchange in $^{60}\text{Co}^{2+}$ -doped $[\text{Co}(\text{pn})_2\text{Cl}_2]^+$ (pn = 1,2 diaminopropane) salts. The solid doped complex was subjected to various thermal treatments. The radiochemical identity of ^{60}Co was determined. They found that radiocobalt was incorporated into the complex form at 100°C . Furthermore, radiocobalt was incorporated into $[\text{Co}(\text{pn})_3]^{3+}$. When the trans isomer was heated, no activity was found as the cis isomer. If the cis isomer was heated, it isomerized to the trans form and radiocobalt was found in both isomeric forms. Only a small quantity of macroscopic $[\text{Co}(\text{pn})_3]^{3+}$ was produced, but a large relative amount of radiocobalt was found in the $[\text{Co}(\text{pn})_3]^{3+}$ form. This observation suggested that the incorporation of ^{60}Co into the $[\text{Co}(\text{pn})_3]^{3+}$ form occurred predominantly during the formation of this ion rather than subsequent to the formation of this ion.

Lazzarini and Fantola-Lazzarini (46) have investigated the thermal annealing of atoms which suffered Szilard-Chalmers recoil in double complexes like cis and trans- $[\text{Co}(\text{en})_2(\text{NO}_2)_2][\text{CoEDTA}] \cdot n\text{H}_2\text{O}$. They found that the isothermal annealing curves of ^{60}Co recoil species at cationic and anionic sites showed a step-like pattern. The retentions at cationic

sites were found to be linearly correlated with those at anionic sites. Since oxygen can serve as an electron trap, the isotopic exchange model would predict that the absolute annealing rates at cationic and anionic sites would be influenced by the concentration of oxygen impurity in the crystal. The ratio of annealing rates, however, would be independent of impurity concentration. Lazzarini and Fantola-Lazzarini found that the annealing probability ratio at cationic and anionic sites was dependent on the concentration of oxygen impurities. To explain this apparent contradiction to the isotopic exchange model, it was proposed that the recoil atom underwent a random walk in the recoil zone prior to making the fatal jump to a normal lattice position. Thus, since impurities influenced the diffusion process in a region around impurity centers, it may be that the impurity centers favored certain diffusion pathways more than others.

Lazzarini and Fantola-Lazzarini (47) have also studied the solid state isotopic exchange reaction between cationic and anionic Co atoms in $[\text{Co}(\text{H}_2\text{O})_6][\text{CoEDTA}]_2 \cdot 4\text{H}_2\text{O}$. Heating the $[\text{}^{60}\text{Co}(\text{H}_2\text{O})_6]^{2+}$ labeled complex caused no migration of activity from $[\text{Co}(\text{H}_2\text{O})_6]^{2+}$ to $[\text{CoEDTA}]^+$ prior to the dehydration temperature. Following dehydration, 10% of the activity was found in the anion. Gamma irradiation followed by isochronal annealing transferred ${}^{60}\text{Co}$ into the anion to the extent of 55% where 67% was the theoretical maximum exchange at isotopic equilibrium.

The influence of radiation shows the production of radiation defects to be important in exchange reactions. It will be the purpose of the

research described in this thesis to correlate radiochemical product distribution and the annealing behavior of each of the radiochemical products to the isotopic exchange theory.

II. EXPERIMENTAL

A. Materials

Water used in this study was tap deionized distilled water. Potassium tris(oxalato)cobaltate(III), which had been prepared by Witiak (48), was recrystallized with an ethanol-water mixture and dried at room temperature under vacuum. Standard cobalt(II) solutions (48) were used to test the Beer's law behavior of extracted cobalt(II). All other compounds used in this study were reagent grade and used without further purification.

Ion exchange resins used in this study were Dowex resins. For anion exchange Dowex 1-X8 strongly basic, quaternary ammonium styrene type resin, 50-100 mesh was used. This resin was originally obtained in the chloride form. The nominal capacity was 3.2 meq/dry gram. A large quantity of the resin was slurried with methanol, aspirated dry and rinsed with concentrated HCl. The resin in a large tube was backwashed with concentrated HCl containing 1 ml 0.5 M NaBrO₃ per 1000 ml acid. After the resin was allowed to stand in the acid solution for 30 minutes, the acid was drained and the resin was washed with distilled water. The resin was then treated with concentrated ammonia, allowed to stand for 30 minutes, drained and washed with water. It was stored in 6M HCl until used. Cation exchange resin, Dowex 50WX8, 50-100 mesh in the H⁺ form with 5 meq/g capacity, was conditioned according to the following procedure. The resin was washed with water and 4.0M HCl until the test for iron with thiocyanate was negative. The resin was washed with water

and treated with 0.5% NaOH containing 40 ml, 20% H₂O₂ per 1000 ml aqueous solution. The mixture was allowed to stand overnight. The resin was washed with water, then with 4.0 M HCl again, and finally stored in water until used. Anion exchange columns were prepared by adding a slurry of the resin to a glass tube fitted with a coarse sintered glass frit above a stopcock at the bottom. Columns were initially 10 mm in diameter and 13 cm in height. Exchange columns in the chloride form were washed with water prior to use. Columns of anion exchange resins in the SCN⁻ form were prepared by washing with water and then with 5% NH₄ SCN solution. Cation exchange columns were prepared by adding a slurry of the resin to similar glass tubes. Resin in the H⁺ form was washed with water prior to use. To prepare the resin in the Na⁺ form, the columns were washed with saturated NaCl solution until the washings were neutral and then with water until no Cl⁻ ion could be detected with dimercury(I) perchlorate.

B. Equipment

All visible absorption spectra and measurements were recorded with a Cary-14 spectrophotometer or a JASCO UV-ORD/5 spectropolarimeter. Either 1.0 or 5.0 cm cells with fused quartz windows were used.

Optical rotatory dispersion and circular dichroism spectra were recorded with the JASCO instrument. Wavelengths were calibrated with a diodymium glass and CD curves were calibrated with standard solutions of d-10-camphor sulfonic acid. The path length of the cells was 1.000 cm.

The gamma photons of ⁶⁰Co decay were detected with a well type NaI

scintillation spectrometer. A solution (10 ml.) in a polyethylene vial was placed over the scintillation crystal in a lucite holder arranged to provide a reproducible geometry. A Radiation Instruments Development Laboratory 400 channel multichannel analyzer was used to accumulate the pulses in various energy channels. The windows and gain settings were such that counts were recorded from 0-2 MeV. Counts from channels 200-299 (1.0 - 1.5 MeV) were printed by a Friden adding machine and summed so that the twin ^{60}Co gamma peaks were counted. A ^{137}Cs (0.25 μCi) source was used to determine that the resolution was 14.2%. A standard ^{60}Co (0.09 μCi) source was used to determine that the counting efficiency was 7.8%.

Thermal annealing studies were performed using a TECAM sand bath. Temperatures were maintained with a mercury contact thermostat connected to a Precision Scientific Company temperature controller. Temperatures were maintained to $\pm 0.5^\circ\text{C}$ and monitored with a chromel-alumel thermocouple attached to a Sargent model MR recorder. Lower temperature (40°C) annealing experiments were performed in a water bath equipped with a thermostated Braum thermomix (II) heater-circulator. Solution kinetic studies were performed using the water bath.

The Ames Laboratory Research Reactor (ALRR) was used for all thermal neutron irradiations.

A Research Specialties Company Automatic Fraction Collector with a photoelectric time-drop counter was used to collect fractions for the determination of elution curves.

C. Preparations

1. D-Tris(ethylenediamine)cobalt(III) chloride d-tartrate pentahydrate

The compound $D-[Co(en)_3](d-tart)Cl \cdot 5H_2O$ was prepared and resolved in the following manner in a typical synthesis (49). To a 500 ml filter flask was added 20.4 ml 88% ethylenediamine, diluted with 50 ml water. Concentrated HCl was added. The solution was cooled to $0^\circ C$, and a solution of $CoSO_4 \cdot 7H_2O$ (28.1 g) in 50 ml water was added. Then charcoal (4.0 g) was added, and air (which had been filtered) was passed through the solution over night. The pH of the solution was monitored and found to be neutral. The charcoal was filtered off and washed with water. Barium d-tartrate was prepared by mixing saturated solutions of d-tartaric acid (15 g) and $BaCl_2 \cdot 2H_2O$ (24.4 g) at $90^\circ C$ for 0.5 hours. The resulting solution was cooled and neutralized with ethylenediamine until slightly basic. As the amine was added a white precipitate of barium-d-tartrate formed. The resulting precipitate was filtered and used in its entirety. The barium-d-tartrate was added to the solution and barium sulfate immediately precipitated. The mixture was heated on the steam bath with good mechanical stirring for 40 minutes. The $BaSO_4$ was filtered and washed with warm water, and the resulting solution was evaporated to 60 ml on the steam bath with a stream of air. The crystallization was allowed to proceed as the solution stood for a period of 48 hours. The solution was cooled in ice and the desired crystals of $D-[Co(en)_3](d-tart)Cl \cdot 5H_2O$ were separated by filtration on a medium frit glass filter. The crystals were washed with about 100 ml ice-cold 40%

ethanol-water. They were recrystallized by dissolution in 30 ml hot water. When the solution was cooled in ice, the crystals were collected on a medium-frit filter. The recrystallized product was washed with 40% ethanol-water and then with absolute ethanol. The product was dried in air for 48-56 hours and analyzed spectrophotometrically and polarimetrically on the JASCO Spectropolarimeter. Yield: 17.6 g, Theoretical: (based on $1/2 \text{ CoSo}_4 \cdot 7\text{H}_2\text{O}$) 25.7; 69%.

2. D-Tris(ethylenediamine)cobalt(III) bromide dihydrate

D- $[\text{Co}(\text{en})_3] \text{ Br}_3 \cdot 2\text{H}_2\text{O}$ was prepared from $[\text{D-Co}(\text{en})_3](\underline{\text{d-tart}})\text{Cl} \cdot 5\text{H}_2\text{O}$ (54). To $[\text{D-Co}(\text{en})_3](\underline{\text{d-tart}})\text{Cl} \cdot 5\text{H}_2\text{O}$ (5.0 g) which had been ground to a fine powder in a mortar was added 10.0 ml warm concentrated HBr. A slurry of the powdered compound in a deep orange solution resulted. After the mixture stood overnight, deep orange needles resulted. The crystals were collected on a medium frit filter and recrystallized twice with hot water (about 15.0 ml). The recrystallized product was allowed to air dry for 48-56 hours and analyzed in the same manner as the tartrate salt. Yield: 3.2 g, Theoretical: 5.0g, 64%.

3. D-Tris(ethylenediamine)cobalt(III) nitrate

The D- or L-isomers of $[\text{Co}(\text{en})_3](\text{NO}_3)_3$ were prepared from the D- or L-isomers of $[\text{Co}(\text{en})_3] \text{ Br}_3 \cdot 2\text{H}_2\text{O}$, respectively (50). In a typical synthesis, 40 ml of a solution of hot AgNO_3 (12.0 g) was added to a solution of D- $[\text{Co}(\text{en})_3] \text{ Br}_3 \cdot 2\text{H}_2\text{O}$ (12.0 g) in 100 ml of water. AgBr immediately precipitated. The silver halide was removed by filtration, and the filtrate was allowed to evaporate for a time on a steam bath under

a stream of air. The solution was cooled to room temperature and then in ice. The desired product $D\text{-}[\text{Co}(\text{en})_3](\text{NO}_3)_3$ was collected on a medium frit filter, recrystallized with water and dried for one week in the air. Yield: 6.9 g, Theoretical: 9.9 g; 70%.

4. Trans-dichlorobis(ethylenediamine)cobalt(III) chloride

Bailar's method for the preparation of trans- $[\text{Co}(\text{en})_2\text{Cl}_2]\text{Cl}$ was used (51). To a solution of 160 g cobalt(II) chloride in 500 ml of water was added 600 g of 10% ethylenediamine in water. A vigorous stream of filtered air was passed through the solution for 12 hours. Concentrated hydrochloric acid was added and the solution was evaporated on a steam bath until a crust formed on the surface. The solution was allowed to cool overnight and the bright green crystals of the hydrochloride salt were filtered on a medium glass frit. The crystals were filtered and washed with alcohol and ether and dried at 110°C . The hydrogen chloride was lost and the crystals of $[\text{Co}(\text{en})_2\text{Cl}_2]\text{Cl}$ were recovered as a dull green powder.

5. Cis-aminechlorobis(ethylenediamine)cobalt(III) chloride

$[\text{Co}(\text{en})_2(\text{NH}_3)\text{Cl}]\text{Cl}_2$ was prepared according to the method of Werner (52). To 20.0 g $[\text{t-Co}(\text{en})_2\text{Cl}_2]\text{Cl}$ was added 20 ml aqueous ammonia. The mixture was triturated. The resulting red compound was filtered and recrystallized in ethanol-water, yield: 4.8 g (24%).

6. Cis-dinitrobis(ethylenediamine)cobalt(III) iodide

To 1.0 g $[\text{t-Co}(\text{en})_2\text{Cl}_2]\text{Cl}$ was added 10.0 ml water. The green

suspension was heated on the steam bath for 5 minutes to produce a purple solution of the cis product. Ten ml NaNO_2 (.67M) solution was added and after 20 minutes the solution turned orange. Ten ml NaI (.34M) was added and the solution was allowed to cool to room temperature and then in ice. The resulting crystals were collected on a medium frit and recrystallized three times.

7. Resolution of tris(oxalato)cobaltate(III) ion

The tris(oxalato)cobaltate(III) ion was resolved according to the method of Witiak (48). To a solution of racemic $\text{K}_3[\text{Co}(\text{C}_2\text{O}_4)_3]$ (2g) dissolved in a minimum amount of cold water was added a solution of $[\text{D-Co}(\text{en})_3](\text{NO}_3)_3$ (1 g) dissolved in water. The resulting mixture was shaken for 15 seconds and a dull green precipitate of $[\text{D-Co}(\text{en})_3][\text{D-Co}(\text{C}_2\text{O}_4)_3]$ was formed. The precipitate was removed by filtration. The resulting filtrate which contained the $[\text{L-Co}(\text{C}_2\text{O}_4)_3]^{3-}$ anion was immediately added to ice cold absolute ethanol. The resulting crystals of $\text{K}_3[\text{L-Co}(\text{C}_2\text{O}_4)_3]$ formed in the alcohol were filtered and washed with absolute ethanol and air dried.

D. Analysis

1. Cobalt(II)

Cobalt(II) (present in aqueous solution as $[\text{Co}(\text{H}_2\text{O})_6]^{2+}$ ion) was analyzed spectrophotometrically. The solution to be analyzed (5 ml) was added to a 25 ml volumetric flask. To the flask was added 5 ml ammonium thiocyanate (5%) solution and a drop of concentrated hydrochloric acid.

Acetone was added to the mark, the solution was mixed, and the absorbance due to the $[\text{Co}(\text{NCS})_4]^{2-}$ ion at 622 nm in a 1 cm cell was determined. It had been determined previously from standard solutions of Co(II) that the $[\text{Co}(\text{NCS})_4]^{2-}$ ion follows Beer's law from 0.04 to 0.24 g/l in the original solution with a molar absorptivity, $\epsilon_{620} = 397.8 \text{ l-mole}^{-1}\text{-cm}^{-1}$. The concentration of Co^{2+} was determined from the calibration curve and the absorbance of the solution.

2. Spectrophotometric determination and characterization of cobalt(III) compounds

Concentration of solutions containing various cobalt(III) complexes were determined by measuring the absorbance of light at absorption maxima. The cobalt(III) complexes were characterized by their visible spectra. Beer's law curves were constructed by measuring the absorbance of solutions containing various amounts of the solid complex. Absorption maxima, molar absorptivities and range of Beer's law concentrations are listed in Table 2. From the molar absorptivities and the absorbance of the various solutions the concentration of the complex ions were determined.

3. Optical rotatory dispersion measurements

The optical purity of the $\text{D-}[\text{Co}(\text{en})_3]^{3+}$ and $\text{D-}[\text{Co}(\text{C}_2\text{O}_4)_3]^{3-}$ ions were determined by the measurements of their specific rotations at extrema in their optical rotatory dispersion curves. Concentrations of the ions were determined by spectrophotometric measurements or by dissolving weighed amounts of the pure salts in known volumes of water.

Table 2. Spectrophotometric analysis of Co(III) containing ions

Ion Absorption Maxima (nm)	Molar Absorptivities, ϵ (l-moles ⁻¹ cm ⁻¹)	Range of Beer's Law (Moles/ liter)
[Co(en) ₃] ³⁺ 460(340) ^a	91.5	1.0 - 200 x 10 ⁻³
[Co(C ₂ O ₄) ₃] ³⁻ 602(420)	153	6.5 - 13.1 x 10 ⁻³
[Co(en) ₂ (NO ₂) ₂] ⁺ 433	187	0.2 - 2.6 x 10 ⁻³
[Co(en) ₂ (NH ₃)Cl] ⁺² 520(360)	70.6	1.0 - 12.0 x 10 ⁻³

^aAbsorption maxima in parentheses were not used for analysis.

The specific rotations $[\alpha]_{\lambda}$ were determined from Equation (18) where α is the degrees rotation at wavelength, λ , l is the path length in decimeters, and c is the concentration in g per 100 ml.

$$[\alpha]_{\lambda} = (100 \alpha)/lc \quad (18)$$

The specific rotation for the two ions as well as the wavelength of optical rotatory dispersion extrema are listed in Table 3.

Table 3. Specific rotation of $[\text{Co}(\text{en})_3]^{3+}$ and $[\text{Co}(\text{C}_2\text{O}_4)_3]^{3-}$ ions

Compound	Wavelength (nm)	Specific Rotation (deg-ml-g ⁻¹ dm ⁻¹)
$[\text{D-Co}(\text{en})_3] (\text{NO}_3)_3$	520 (460)	+575
$\text{K}_2[\text{L-Co}(\text{C}_2\text{O}_4)_3]$	660	-1044

E. Irradiation Conditions

In early experiments 50 mg samples of $\text{D-}[\text{Co}(\text{en})_3] (\text{NO}_3)_3$ were irradiated in polyethylene vials in the R-3 position of the ALRR. The thermal neutron flux was 3.0×10^{13} n/cm²·sec. Irradiation times were from 20 to 40 minutes. Samples were stored at room temperature for 3 to 5 days prior to dissolution and analysis. It was found that considerable room temperature annealing occurred in 5 days. Therefore, in

later experiments samples were irradiated in the R-8 position of the reactor for 10 minutes with a thermal neutron flux of 1.0×10^{13} n/cm². sec. Immediately following irradiation, the samples were cooled in dry ice. The samples were stored at dry-ice temperature for 24 hours prior to dissolution and analysis.

F. Radiochemical Measurements

The gamma ray spectrum due to the decay of ⁶⁰Co is shown in Figure 2. The area under the twin gamma peaks were used to determine the activity of the sample. All samples were counted for sufficient time that the total number of counts was greater than 5000. The activities were determined as counts per minute (cpm) above background.

The relative activity, R(Y), in a given chemical form (percent) is defined by the following equation:

$$R(Y) = \frac{A(Y)}{A(T)} \times 100\% . \quad (19)$$

In Equation (19) A(Y) is the activity (cpm) in chemical form Y, and A(T) is the total activity in the sample from which Y was separated. Retention is R(Y) for the target, [Co(en)₃]³⁺ ion. In the case of recrystallization experiments, the molar specific activity, SA_M(Y), was determined from the activity in a solution of the recrystallized salt and the molar concentration of the ion of interest in that solution.

$$SA_M(Y) = \frac{A(Y)}{\text{moles Y}} \quad (20)$$

The relative activity of species Y was determined from the specific

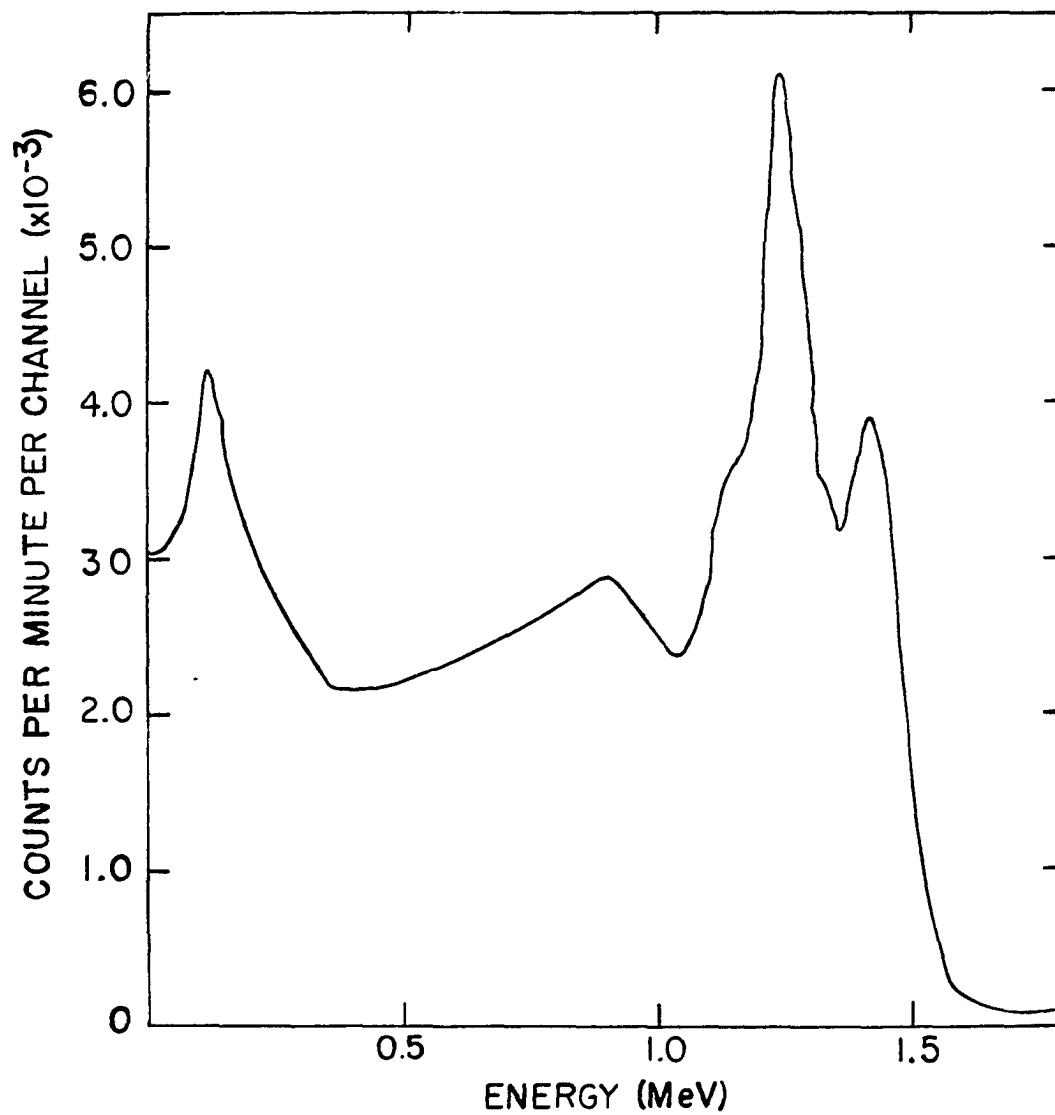


Figure 2. Gamma ray spectrum of ^{60}Co

activity of Y and a knowledge of the number of moles of the ion Y added as carrier and present in the sample originally.

$$R(Y) = \frac{SA_M(Y) \times M_O(Y)}{A(T)} \quad (21)$$

In Equation (21), $M_O(Y)$ is the number of moles of Y in the sample prior to recrystallization. In the case of activities separated by ion exchange methods, $R(Y)$ was corrected for the dilution caused by the eluting agent. For example, 10-ml of a solution containing the radioactive form was sorbed onto a column followed by elution of the form so that the total activity of interest was contained in a volume of 50 ml after leaving the column. A 10 ml portion of this 50 ml was counted. The dilution factor was $50 \div 10$ since 10 ml of the original solution and 10 ml of the diluted, eluted fraction were counted. For such a case, the relative activity of Y was determined from Equation (22).

$$R(Y) = \frac{\text{(Activity (cpm) in 10 ml eluate) } \times 5}{\text{total activity}} \quad (22)$$

G. Separations

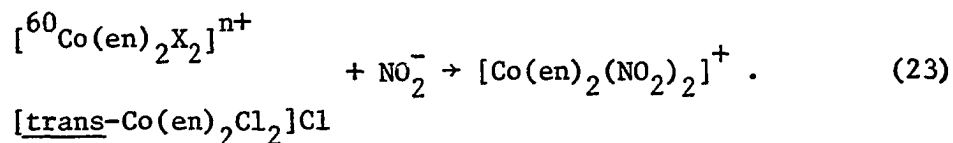
1. Recrystallization to constant specific activity

The D- and L- $[\text{Co}(\text{en})_3]^{3+}$ ion was recrystallized to constant specific activity in two ways. A solution containing racemic carrier and Co^{2+} carrier (10 ml) was added to 1.0 g racemic $[\text{Co}(\text{en})_3] (\text{NO}_3)_3$. The mixture was heated on the water bath until dissolution occurred. Absolute

ethanol was added until the solution became cloudy. A few drops of water were added to dissolve the suspension. The resulting solution was cooled to room temperature and then in ice. Crystals were recovered by filtration on a medium frit. A portion of the crystals was dissolved in water and the molar specific activity of the solution was determined. The recrystallization was repeated several times for the remainder of the crystals. It was found that three recrystallizations were sufficient to reach constant specific activity. A second method was used to crystallize the total $[\text{Co}(\text{en})_3]^{3+}$ ion activity. To a warm solution containing the irradiated salt and known amount of racemic carrier was added a stoichiometric amount of NaI. The salt $[\text{Co}(\text{en})_3]\text{I}_3 \cdot \text{H}_2\text{O}$ precipitated upon cooling. The salt was recrystallized from water to constant specific activity.

Activity present in the form $[\text{Co}(\text{en})_2\text{X}_2]^{n+}$ was isolated and identified by converting the complex ion to a form identical with that to which a carrier ion was converted. In the formulation, $[\text{Co}(\text{en})_2\text{X}_2]^{n+}$, X is some relatively labile ligand which is subject to displacement. In an aqueous chloride solution, X probably is H_2O or Cl^- . The $[\text{Co}(\text{en})_2\text{X}_2]^{n+}$ species contains cobalt(III); thus the charge $n+$ is determined by the ligand X. Trans- $[\text{Co}(\text{en})_2\text{Cl}_2]\text{Cl}$ (1.0 g) was added to a 10 ml solution of the irradiated salt. A 2.0 molar ratio of NaNO_2 was added to the mixture which was subsequently heated on the steam bath to 70°C for 30 minutes. Sodium iodide was added, the solution was allowed to cool, and yellow crystals of cis- $[\text{Co}(\text{en})_2(\text{NO}_2)_2]\text{I}$ formed. The $[\text{Co}(\text{en})_2(\text{NO}_2)_2]\text{I}$ crystals were recrystallized three times to constant

specific activity. In this process trans- $[\text{Co}(\text{en})_2\text{Cl}_2]^{n+}$ was converted to cis- $[\text{Co}(\text{en})_2(\text{NO}_2)_2]^+$ ion and the $[\text{}^{60}\text{Co}(\text{en})_2\text{X}_2]^{n+}$ was expected to be converted to the same species, i.e.:



For determining the $[\text{Co}(\text{en})_2\text{NH}_3\text{X}]^{n+}$ activity, the compound $[\text{Co}(\text{en})_2\text{NH}_3\text{Cl}]\text{Cl}_2$ was recrystallized in the presence of the dissolved irradiated salt. No added chloride was present and only sufficient heating was used to dissolve the irradiated compound. The crystals were recrystallized three times from ethanol-water. The specific activity of the compound was then determined. In this procedure the X ion was replaced by Cl^- and the radioactive recoil product was in the same chemical form as the carrier.

2. Ion exchange separations

Ion exchange chromatography was used to separate activity as Co^{2+} from the other activities produced. Cation exchange chromatography was used initially for such separations. Solution "A" (10 ml), containing Co^{2+} carrier, racemic $[\text{Co}(\text{en})_3]^{3+}$ carrier, and the irradiated salt, was added to the cation exchange column in the H^+ form. The column was eluted with 5% NH_4SCN solution to 50 ml. The Co^{+2} ion was eluted through the column quantitatively as a thiocyanato anionic complex, and the cationic species containing Co(III) were retained. The Co^{2+}

activity was determined by counting the solution eluted through the columns. Alternatively, an anion exchange column in the SCN^- form was used to separate Co^{2+} . To 10 ml solution "A" was added 10 ml NH_4SCN , 5% solution. This solution was added to the top of the anion exchange column and eluted to 50 ml with NH_4SCN solution. A blue band containing the $[\text{Co}(\text{NCS})_4]^{2-}$ developed at the top of the column and the cationic species were eluted through. The percent activity as species other than Co^{2+} were determined by counting the eluted solution and the percent activity as Co^{2+} was determined by subtracting the cationic activity from the total activity of the irradiated salt.

Separation of the various recoil species by recrystallization to constant specific activity is time consuming, tedious, and inconvenient for the analysis of many samples. Therefore, a method which utilized ion exchange chromatography was investigated. Although several experimental conditions were tried with a cation exchange column and elution with various concentrations of HCl , only the results of two of the elution experiments will be reported here. In the first experiment, 10 ml of solution "A" was sorbed onto a cation exchange column in the H^+ form. Fractions (10 ml) were collected in polyethylene vials, counted, and analyzed for Co^{2+} . The first 100 ml was eluted with distilled water. Only 0.5% of the total activity was eluted. With 100 ml 0.5 M HCl virtually no activity was eluted. The column was eluted with 1.0 M HCl and Co^{2+} was eluted in a broad symmetric band over a range of 20 fractions. Specific $\text{Co}(\text{II})$ activities were constant over this range. Therefore, no apparent contamination of the Co^{2+} activity had

occurred. The column was then eluted with 2.0 N HCl and 17% activity was eluted. Finally, the column was eluted with 10 N HCl but the specific activity of $[\text{Co}(\text{en})_3]^{3+}$ for each of the fractions decreased indicating that the $[\text{Co}(\text{en})_3]^{3+}$ eluted was contaminated with some other radioactive species. A second HCl elution experiment was performed in which 0.04 g trans- $[\text{Co}(\text{en})_2\text{Cl}_2]\text{Cl}$ and 0.04 g $[\text{Co}(\text{en})_2(\text{NH}_3)\text{Cl}]\text{Cl}_2$ were dissolved in 2.0 N HCl. Solution "A" (10 ml) was added and the mixture heated on the hot water bath for 90 minutes. The mixture was allowed to cool for 2 hours, then added to the cation exchange column. The column was eluted with 1.5 N HCl and 5 ml fractions were collected for 50 samples. A large band was eluted containing 50% of the total activity corresponding to Co^{2+} and $[\text{Co}(\text{en})_2\text{X}_2]$ species. A broad band was eluted at 3.0 N HCl for 100 samples. This band corresponded to the $[\text{Co}(\text{en})_2(\text{NH}_3\text{Cl})]$ species and accounted for 19% of the total activity. Further elution with 5.0 N HCl resulted in the elution of the $[\text{Co}(\text{en})_3]^{3+}$ activity for 40 samples with 27% of the total activity. Unfortunately, 10% of the activity could not be accounted for. The elution curve is shown in Figure 3.

The chloride separations are complicated by the action of several competing equilibria. For the $[\text{Co}(\text{en})_2\text{X}_2]^{n+}$ species the following equilibria must be considered (53).

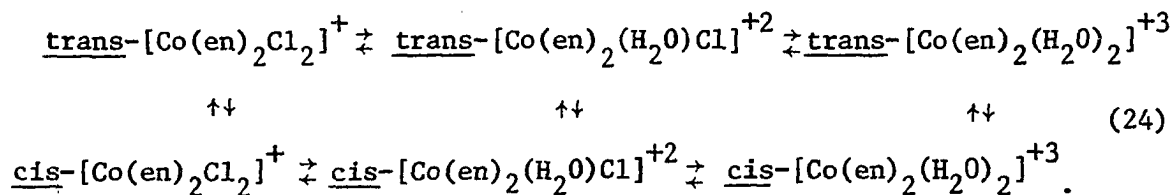
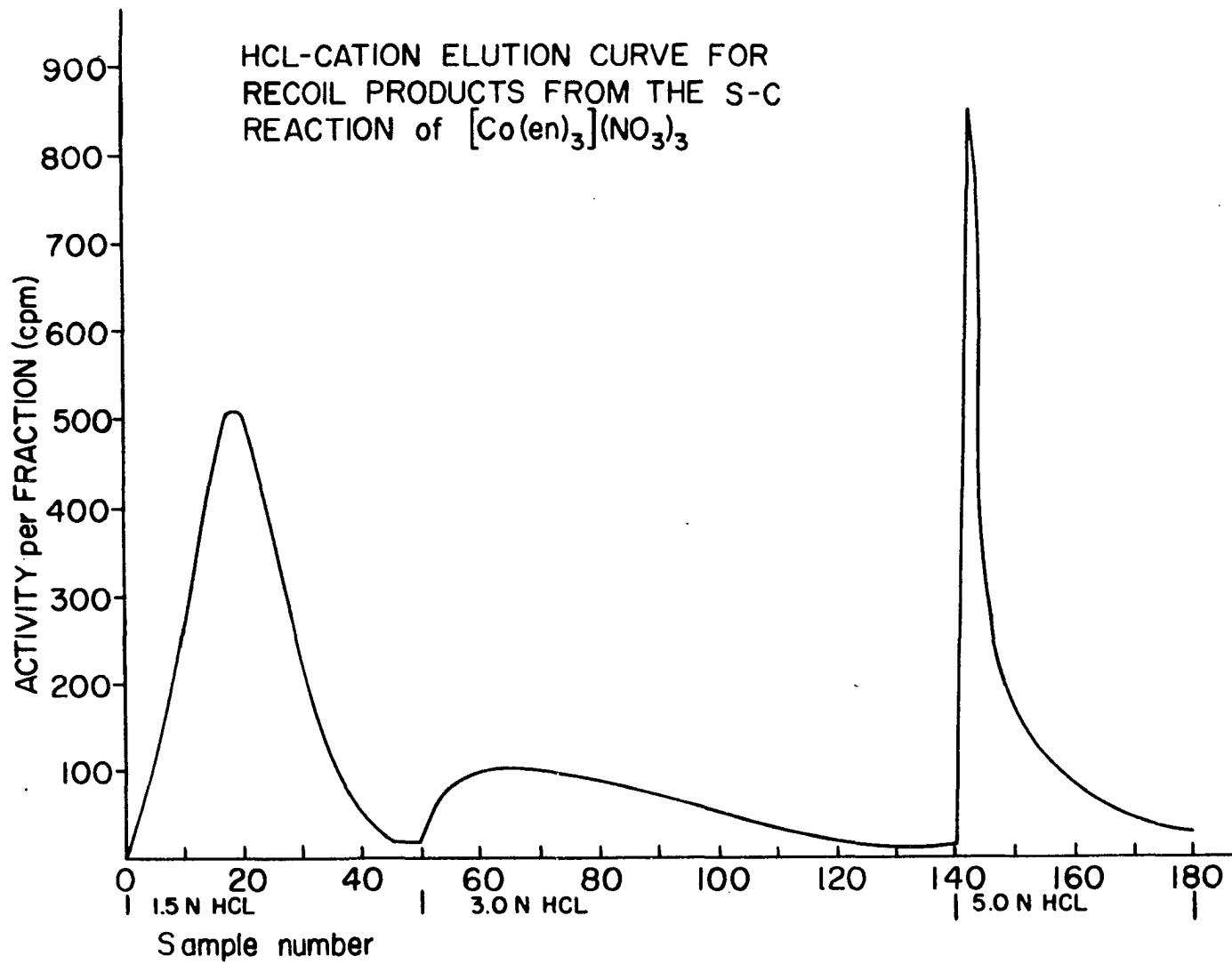
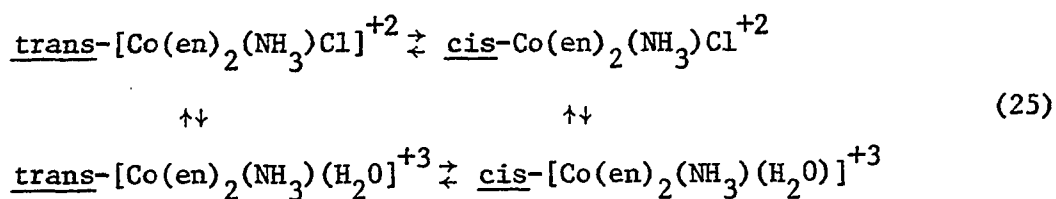


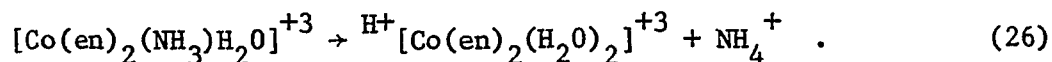
Figure 3. HCL-cation elution curve for recoil products from the S-C reaction of $[\text{Co}(\text{en})_3](\text{NO}_3)_3$



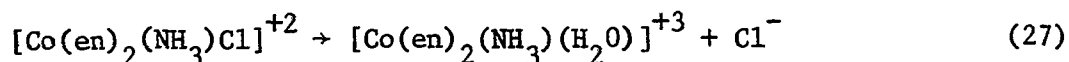
The following equilibria must be considered for the $[\text{Co}(\text{en})_2(\text{NH}_3)\text{X}]^{\text{m}+}$ species.



The following reaction can occur at temperatures above 80°C (54)

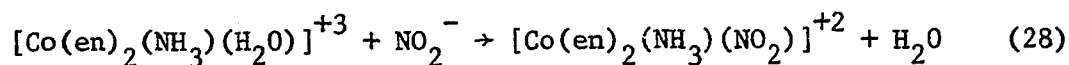


Unfortunately, Le Chatelier's principle cannot be utilized effectively in these reactions because the rates are slow. Pseudo first order rate constants are on the order of 10^{-5} sec^{-1} (53). Equilibrium constants, for example, for:

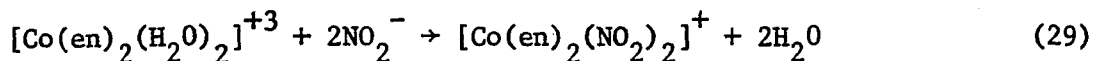


are of the order of 0.8 M (53). The rate of approach to equilibrium is too slow to establish the equilibrium and too fast to ignore it.

A separation scheme has been developed which takes advantage of the fact that for the reactions



and



the equilibrium constant is large (53) ca. 10^{10} M^{-1} for reaction (28). A flow chart for this separation scheme is shown in Figure 4. Solution "A" (10 ml) was mixed with 10 ml, 5% ml, 5% NH_4SCN solution. The mixture was added to an anion exchange column in the SCN^- form with 5% NH_4SCN solution in the aqueous phase. The column was eluted to 50 ml with water. Ten ml were reserved for counting. Co^{2+} was removed in this manner. The remaining 40 ml was added to an anion column in the Cl^- form and eluted with water to 50 ml; 10 ml was reserved for counting. The Cl^- anion column removed possibly interfering SCN^- ions. To the remaining 40 ml was added 0.05 g NaNO_2 , 0.02 g $[\text{Co}(\text{en})_2(\text{NH}_3)\text{Cl}]\text{Cl}_2$ and 0.02 g $[\text{trans-Co}(\text{en})_2\text{Cl}_2]\text{Cl}$. The mixture was heated on the steam bath for 30 min at 80°C . The solution was added to a cation exchange resin in the Na^+ form and eluted to 200 ml with NaNO_2 . Ten ml were counted. In the heating $[\text{Co}(\text{en})_2\text{X}_2]^{n+}$ was converted to $[\text{Co}(\text{en})_2(\text{NO}_2)_2]^+$; $[\text{Co}(\text{en})_2(\text{NH}_3)\text{X}]^{m+}$ was converted to $[\text{Co}(\text{en})_2(\text{NH}_3)(\text{NO}_2)]^{+2}$. $[\text{Co}(\text{en})_2(\text{NO}_2)_2]^+$ was eluted with 1M NaNO_2 . The column was then eluted with 3.5 M NaNO_2 to 200 ml to elute $[\text{Co}(\text{en})_2(\text{NH}_3)\text{NO}_2]^{+2}$. After washing with water, the column was eluted with 8 N HCl to 50 ml. The column was allowed to rest for 10 hours and then was eluted with 8N HCl to a total of 200 ml to remove the $[\text{Co}(\text{en})_3]^{3+}$ activity. The relative amount of each species was determined. The Co^{2+} activity was eluted from the anion column with 15% K_2CO_3 (100 ml) (not quantitatively). The activity of Co^{2+} was

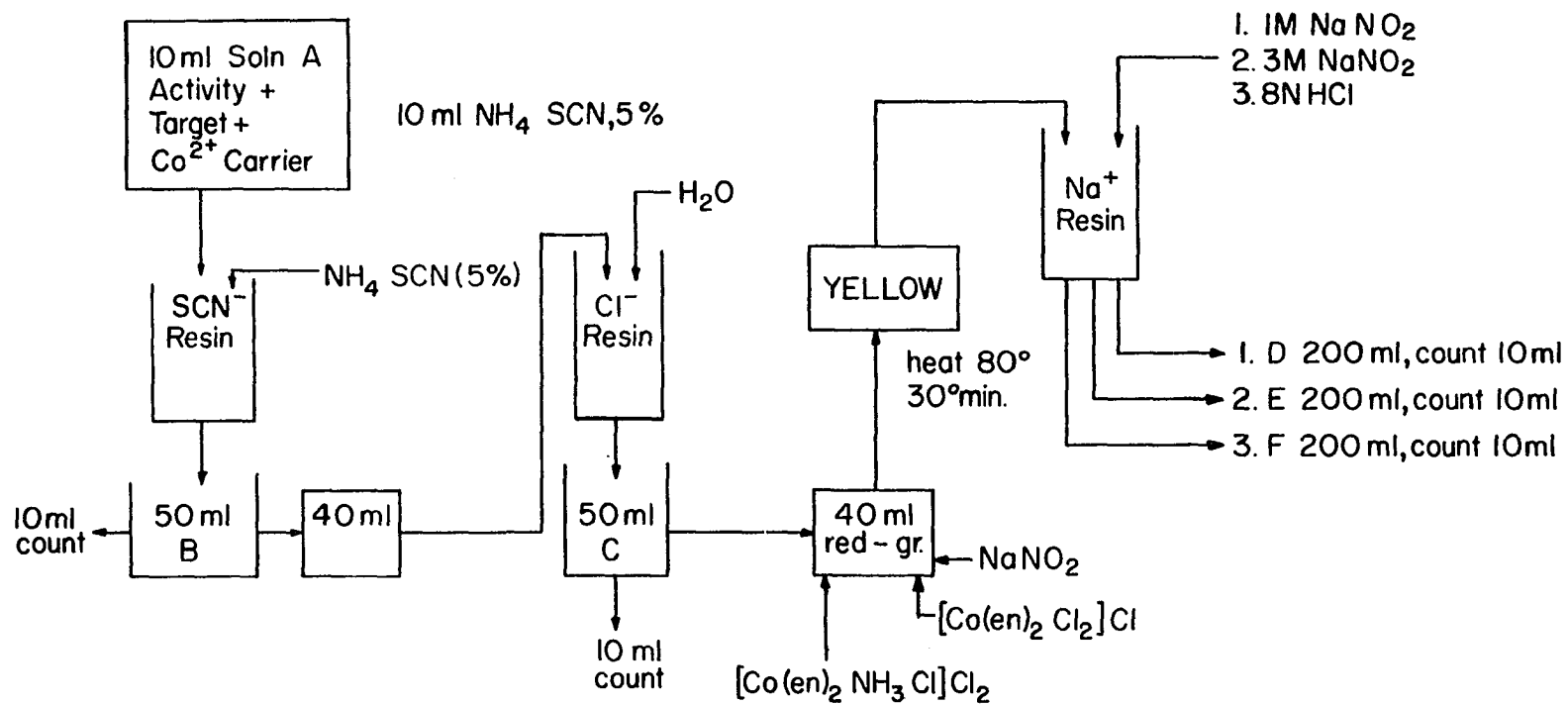


Figure 4. Ion exchange scheme for the separation of radiochemical species produced in the Szilard-Chalmers process in D-[Co(en)₃(NO₃)₃]

determined from the formula

$$A(\text{Co}^{2+}) = \frac{\text{moles Co}^{2+} \text{ in}}{\text{moles Co}^{2+} \text{ out}} A(\text{Co}^{2+}) \text{ measured).} \quad (30)$$

The amount of Co^{2+} was measured spectrophotometrically as the $\text{Co}(\text{NCS})_4^{2-}$ complex in acetone. The results of such a method were identical to the value taken by the difference in the activity added to the SCN^- anion column and that eluted from the anion column. Of each of the fractions collected, (A,B,C,D,E,F), 10 ml aliquots were counted. The counting rate for each fraction was used to determine the percent activity present in each chemical form. The relative activities of the various radiochemical species were determined from Equations (31-34), where A,B,C,D,E,F represent the counting rates for individual fractions.

$$R(\text{Co}^{2+}) = (1 - 5B/A) \times 100\% \quad (31)$$

$$R([\text{Co}(\text{en})_2\text{X}_2]^{n+}) = (20 D/4C) \times 5B/A \times 100\% \quad (32)$$

$$R([\text{Co}(\text{en})_2(\text{NH}_3\text{X})^{m+}) = (20E/4C) \times (5B/A) \times 100\% \quad (33)$$

$$R([\text{Co}(\text{en})_3]^{3+}) = (20 F/4C) \times (5B/A) \times 100\% \quad (34)$$

The uncertainties in radiochemical yields, determined by the ion exchange technique, were estimated by performing four analyses on the same well-aged solution. Results of four analyses are shown in Table 4. Standard deviations were calculated and used as the basis for the estimation of the uncertainty in radiochemical yields for the analysis of other samples. In some samples, uncertainties were based on the deviation of

Table 4. Four radiochemical analyses of the same solution of irradiated D-[Co(en)₃](NO₃)₃^a

Analysis (n)	Radiochemical Yields R(Y) (%)			
	Co ²⁺	[Co(en) ₂ X ₂] ⁿ⁺	[Co(en) ₂ (NH ₃) _X] ^{m+}	D- or L-[Co(en) ₃] ³⁺
1	34.0	14.4	15.8	36.0
2	36.5	15.5	12.7	35.4
3	36.9	13.9	14.2	35.0
4	38.3	13.6	14.1	34.0
Mean ^b $\overline{R(Y)}$	36.4	14.4	14.2	35.1
Standard Deviation(σ) ^c	1.8	0.8	1.3	.9

^aSample irradiated 40 min, 3×10^{13} n-cm⁻²-sec⁻¹, ambient temperature; stored 3 days room temperature, dissolved in carrier solution; solution aged 25 days at room temperature.

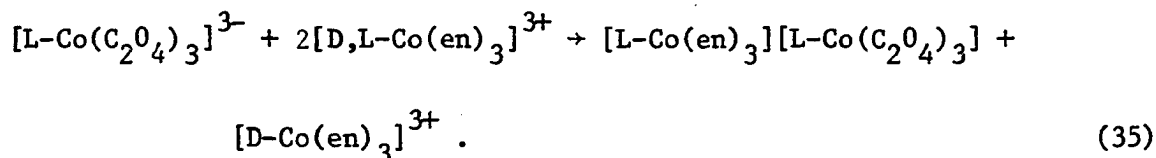
$${}^b \overline{R(Y)} = \left(\sum_{n=0}^4 R(Y)_n \right) / 4.$$

$${}^c \sigma(R) = \left(\sum_{n=0}^4 \frac{(\overline{R(Y)} - R(Y)_n)^2}{3} \right)^{1/2}.$$

duplicate analyses. In some cases, the sum of the radiochemical yields did not equal 100%. When the sum varied from 100% by an amount greater than the sum of the uncertainties, the uncertainties in the yields were increased to account for the incomplete recovery of activity.

3. Diastereomeric precipitation separation of the activities contained in the optical isomers of tris-(ethylenediamine) Cobalt(III) ion

Resolved $K_3[L-Co(C_2O_4)_3]$ has been used to provide a rapid separation of the isomers of $[Co(en)_3]^{3+}$. The following reactions took place:



If the required mole ratios were used to effect separation only 30% resolution was obtained. If the number of moles of the oxalato complex were doubled, optically pure $[D-Co(en)_3]^{3+}$ was obtained in a 40% yield. In a typical experiment, 1.0 g $L-K_3[Co(C_2O_4)_2]$ was dissolved in 30 ml. ice cold water and added to 1.0 g recrystallized $[Co(en)_3](NO_3)_3$ containing activity as D- and L- $[Co(en)_3]^{3+}$ ions. The solution was agitated for 15 sec. and filtered. The filtrate was found to contain optically pure D- $[Co(en)_3]^{3+}$ ion. $[\alpha]_{520} = 538.4^\circ C \text{ deg ml g}^{-1} \text{ dm}^{-1}$. The specific activity of D- $[Co(en)_3]^{3+}$ in the filtrate was determined by counting 10 ml of the filtrate and measuring the absorbance at 460 mm and the optical rotation of the solution at 520 nm.

H. Thermal Annealing

1. Isothermal annealing

Samples which had been irradiated and stored in dry ice for 24 hours were placed in stoppered glass test tubes. The test tubes were placed in the sand bath set at the desired temperature. One sample was not placed in the sand bath but was dissolved immediately after removal from dry ice. The samples in the sand bath were removed at timed intervals and dissolved in a solution containing Co^{2+} carrier and racemic $[\text{Co}(\text{en})_3]^{3+}$ ion. The solutions were allowed to age at room temperature for one month and then were analyzed for their radiochemical cobalt distributions with the ion exchange procedure described previously.

2. Isochronal annealing

For the isochronal annealing study, 12 samples of the irradiated salt were placed in the sand bath at 59°C . One sample was dissolved prior to thermal treatment. At 30 min. intervals samples were withdrawn and dissolved in carrier solution, and the temperature of the bath was increased by approximately 3°C . The final temperature was 114°C . Temperature was controlled to $\pm 0.5^\circ\text{C}$ and it took less than 7 minutes to change temperatures. After aging for two months the resulting solutions were analyzed for their radiochemical distribution.

I. Storage Conditions and Solution Aging

Dimotakis and Papadopoulos (25) observed that considerable thermal annealing occurred in neutron irradiated $[\text{Co}(\text{en})_3](\text{NO}_3)_3$ at room

temperature and below. In preliminary experiments in this study it was found that samples of $[\text{Co}(\text{en})_3](\text{NO}_3)_3$ which had been irradiated at ambient reactor temperatures and stored for 24 hours in dry ice exhibited room temperature annealing. The Co^{2+} radiochemical yield decreased from 67.7% immediately following removal from dry ice to 60.7% following aging at room temperature for 192 hours. The $[\text{Co}(\text{en})_3]^{3+}$ yield increased from 11.1% to 23.8% in the same period in the same samples. To minimize the effects of such room temperature annealing, samples should ideally be irradiated and stored at the lowest possible temperature. Since the ALRR does not have facilities available for low temperature irradiation, room temperature annealing effects were minimized by irradiation of solid samples for a short period of time (10 min) and the storage of them in dry ice following the irradiation prior to analysis or annealing at other temperatures.

When the radiochemical analyses of samples which had been irradiated, stored in dry ice, annealed at 40°C , and dissolved in carrier solution were repeated, some time later after standing in solution, it was observed that the percent activity as Co^{2+} had increased considerably between the time of the first analysis and that of the second. This was a rather surprising result since such a phenomenon had not been previously reported in the literature. The change could not be explained in terms of random or systematic experimental error, and it was concluded that there was a ^{60}Co containing species in solution which either exchanged with Co^{2+} in solution or which decomposed to Co^{2+} in the time between the first analysis and the reanalysis. Experiments (see Part B,

Results and Discussion Section) showed that this transient species was essentially all converted to Co^{2+} in one month at room temperature in solution. Therefore, to avoid the possibility of such species affecting the analysis, solutions were aged from one to two months prior to analysis. The apparent radiochemical yield of Co^{2+} , therefore, will include the fraction of activity present originally as transient species.

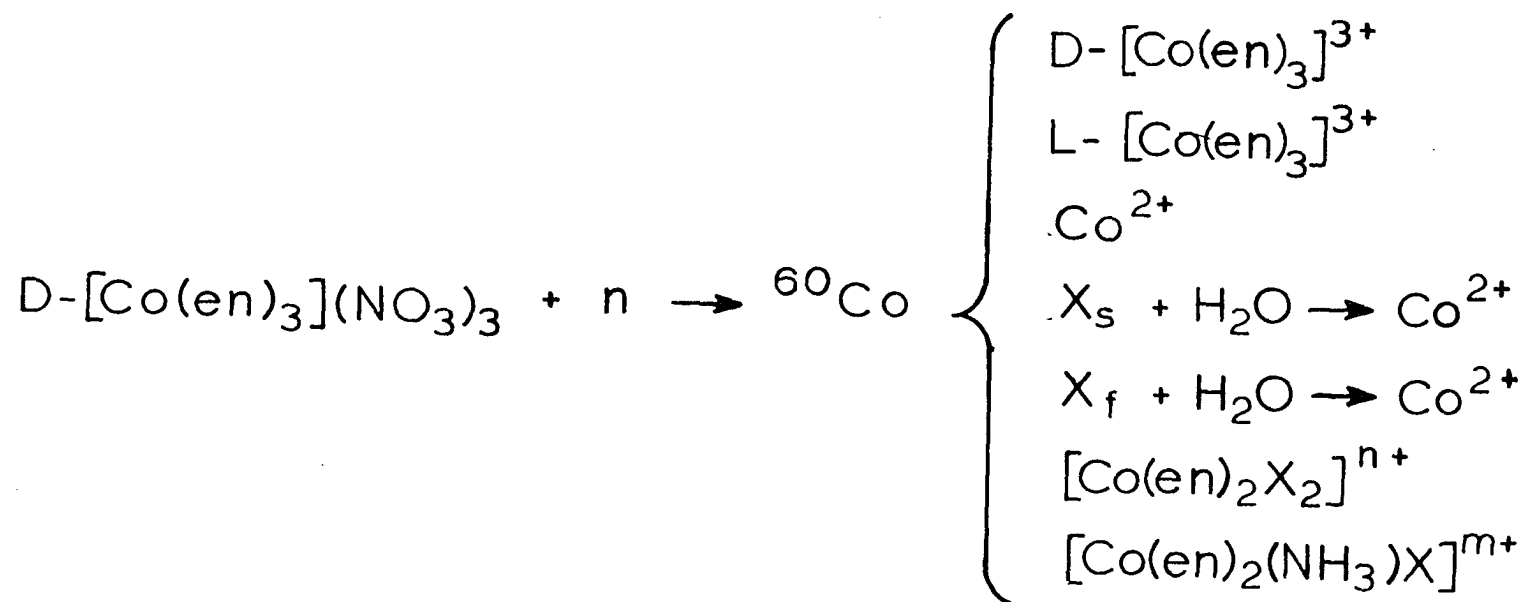
III. RESULTS AND DISCUSSION

A. Characterization of Radiochemical Species

Seven radiochemical species produced as a result of $^{59}\text{Co}(n,\gamma)^{60}\text{Co}$ recoil in $\text{D-}[\text{Co}(\text{en})_3](\text{NO}_3)_3$ have been at least partially characterized. The production of these species is illustrated in Figure 5. The initial yields (before thermal annealing) of these species depended on the irradiation and storage conditions and will be discussed under the discussion of each product. The $[\text{Co}(\text{en})_3]^{3+}$ ion was detected as both optical isomeric forms. However, no more than two percent of the total activity was ever present as the L-isomer. Most of the activity present as $[\text{Co}(\text{en})_3]^{3+}$ ion was, therefore, in the same isomeric form as the target material. The predominant product detected immediately following dissolution of the target was the $[\text{Co}(\text{H}_2\text{O})_6]^{2+}$ ion. Two unknown ^{60}Co containing species decomposed in solution to the $[\text{Co}(\text{H}_2\text{O})_6]^{2+}$ ion and will be discussed in Section B. The $[\text{Co}(\text{en})_2\text{X}_2]^{n+}$ and $[\text{Co}(\text{en})_2(\text{NH}_3)\text{X}]^{m+}$ ions contained ^{60}Co in the +3 oxidation state. These species are inert in water solution and do not exchange with Co^{2+} . The X ligands are most probably NO_3^- ions or water molecules which are added after dissolution, and which can be replaced by Cl^- or $-\text{NO}_2^-$ ligands for analysis. The charges on the complexes would be determined by the charge on the X ligand.

Initial yields of the two isomers of $[\text{Co}(\text{en})_3]^{3+}$ are shown in Table 5. Results from three different irradiation conditions and from Zuber's (13) experiment are shown. Retention as $\text{D-}[\text{Co}(\text{en})_3]^{3+}$ ion was probably

RECOIL PRODUCTS



67

Figure 5. Production of radiochemical species as a result of the neutron bombardment of D- $[\text{Co}(\text{en})_3](\text{NO}_3)_3$

Table 5. Initial radiochemical yields of $[\text{Co}(\text{en})_3]^{3+}$ ion from the neutron irradiation of solid $\text{D-}[\text{Co}(\text{en})_3](\text{NO}_3)_3$

Irradiation time (min)	Thermal neutron flux ($\text{n-cm}^{-2}\text{-sec}^{-1}$)	Storage Condition	Separation Procedure	Radiochemical Form Isolated	Percent Activity in Radiochemical Form Isolated
40	3.0×10^{13}	7 days room temp.	ion exchange	$\text{D- and L-}[\text{Co}(\text{en})_3]^{3+}$	35.1 ± 0.4
40	3.0×10^{13}	7 days room temp.	recrystallization as iodide salt in presence of racemic carrier	$\text{D- and L-}[\text{Co}(\text{en})_3]^{3+}$	36.5 ± 1.2
20	3.0×10^{13}	3 days room temp.	recrystallization as nitrate salt in presence of racemic carrier	$\text{D- and L-}[\text{Co}(\text{en})_3]^{3+}$	21.5 ± 1.0
20	3.0×10^{13}	3 days room temp.	diastereomeric precipitation	$\text{D-}[\text{Co}(\text{en})_3]^{3+}$	19.7 ± 1.0
20	3.0×10^{13}	3 days room temp.	diastereomeric precipitation	$\text{L-}[\text{Co}(\text{en})_3]^{3+}$	1.8 ± 1.0
10	1.0×10^{13}	24 hours dry ice	recrystallization as nitrate salt in presence of racemic carrier	$\text{D- and L-}[\text{Co}(\text{en})_3]^{3+}$	5.5 ± 1.0

Table 5. (continued)

Irradiation time (min)	Thermal neutron flux (n-cm ² -sec ⁻¹)	Storage Condition	Separation Procedure	Radiochemical Form Isolated	Percent Activity in Radiochemical Form Isolated
10	1.0 x 10 ¹³	24 hours dry ice	diastereomeric precipitation	D-[Co(en) ₃] ³⁺	4.4 ± 1.0
10	1.0 x 10 ¹³	24 hours dry ice	diastereomeric precipitation	L-[Co(en) ₃] ³⁺	1.1 ± 1.0
1440	1.0 x 10 ⁹	unknown, Zuber's result (Ref. 13)	recrystallization as bromide in presence of racemic carrier	D- and L-[Co(en) ₃] ³⁺	4.0 ± 0.6
1440	1.0 x 10 ⁹	unknown, Zuber's result (Ref. 13)	recrystallization as bromide in presence of optical carrier	D-[Co(en) ₃] ³⁺	4.5 ± 0.5
1440	1.0 x 10 ⁹	unknown, Zuber's result (Ref. 13)	recrystallization as bromide in presence of optical carrier	L-[Co(en) ₃] ³⁺	0.4 ± 0.2

not due to the ^{60}Co atom remaining in its original coordination sphere since the ^{60}Co recoil atom had more than enough energy to escape. Furthermore, Zuber's experiments (13) showed that following irradiation in solution, only $^{60}\text{Co}^{2+}$ could be detected. It can be seen from Table 5 that the radiochemical yield of $\text{D,L-}[\text{Co}(\text{en})_3]^{3+}$ and $\text{D-}[\text{Co}(\text{en})_3]^{3+}$ increased with increased neutron dose and with increased storage time at room temperature. The increase may be due to room temperature thermal annealing effects or to radiation annealing in the reactor. The radiochemical yield of $\text{L-}[\text{Co}(\text{en})_3]^{3+}$ increased only to a small extent (if at all) with increased thermal neutron dose and room temperature storage. Much of the initial retention of $\text{D-}[\text{Co}(\text{en})_3]^{3+}$ ion can be accounted for in terms of thermal or radiation induced annealing. It will be demonstrated in Section C that thermal annealing at least is stereospecific. Therefore, one would expect the yield of $\text{D-}[\text{Co}(\text{en})_3]^{3+}$ to be greater than the yield of $\text{L-}[\text{Co}(\text{en})_3]^{3+}$ under conditions which fail to completely suppress annealing. Note in Table 5 that the ion exchange method of separation gives essentially the same results as the recrystallization of racemate.

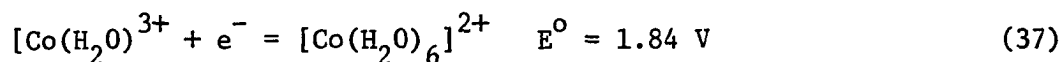
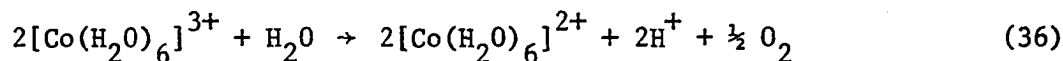
The Co^{2+} yield represents those recoil atoms which have not recombined with other molecules in the crystal lattice to form inert complexes. Initial Co^{2+} yields under various irradiation conditions are shown in Table 6. Under irradiation conditions which suppress thermal annealing, most of the activity produced was found in this Co^{2+} form. The Co^{2+} activity decreased under conditions where room temperature

Table 6. Initial radiochemical yields of Co^{2+} from the neutron irradiation of solid $\text{D}[\text{Co}(\text{en})_3](\text{NO}_3)_3$

Time of Irradiation (min)	Thermal Neutron Flux ($\text{n}/\text{cm}^2 \cdot \text{sec}$)	Storage	Yield (% activity as Co^{2+})
40	3.0×10^{13}	7 days room temp.	29.4 ± 0.9
20	3.0×10^{13}	3 days room temp.	36.4 ± 0.9
10	1.0×10^{13}	1 day dry ice	82.1 ± 0.9

annealing could occur. Furthermore, of the two samples stored at room temperature, the sample which received the larger neutron dose exhibited the lower yield of Co^{2+} . Radiation annealing may have played an important role in the decrease of Co^{2+} activity. The radioactive $[\text{Co}(\text{H}_2\text{O})_6]^{2+}$ detected in solution may not have been present as Co^{2+} ions trapped in the crystal lattice. Stucky and Kiser (33) claimed, as a result of their magnetic susceptibility studies on neutron irradiated $\text{Co}(\text{III})$ and $\text{Co}(\text{II})$ complexes, that recoil cobalt detected as Co^{2+} in solution was not present as simple Co^{2+} . In the case of $\text{Co}(\text{II})$ glycinate, magnetic susceptibility decreased following irradiation. In the case of $\text{Co}(\text{III})$ complexes the susceptibility increased following irradiation. Their conclusion was that such increase or decrease was due to the formation of some complex $\text{Co}(\text{II})$ species. On the other hand, Khorana (55) attributed these changes in magnetic susceptibility to bulk radiolysis in

the solid state as a result of concomitant gamma rays and fast neutrons. He maintained that recoil ^{60}Co stabilized as Co^{2+} ions in the solid state. Khorana claimed that Stucky's conclusions were in error since $[\text{Co}(\text{H}_2\text{O})_6]^{2+}$ is known to exchange with other $\text{Co}(\text{II})$ complexes in solution. There is still another possibility. Hexaquo cobalt(III) is known to oxidize in water (56) to $\text{Co}(\text{II})$ according to the reaction:



One would expect any $[\text{Co}(\text{H}_2\text{O})_6]^{3+}$ in solution to readily exchange with Co^{2+} carrier solution and appear as radiocobalt(II) in the analysis. The Co^{2+} yield therefore may have been the result of radioactivity present as some species which had not recombined with molecules in the crystal lattice to form species that were stable or inert in water solution.

By conversion of the activity present as the $[\text{Co}(\text{en})_2\text{X}_2]^{n+}$ ion to a chemical form which could be obtained as a solid compound, the activity present as $[\text{Co}(\text{en})_2\text{X}_2]^{n+}$ was deduced. Initial yields of $[\text{Co}(\text{en})_2\text{X}_2]^{n+}$ are tabulated in Table 7. The tabular results show that the effect of irradiation conditions was important, but that the various separation techniques used gave comparable results. Note that the yield increased with increased neutron dose. Increased bulk radiolysis by concomitant gamma radiation may have been responsible for such an effect. Thermal effects were probably not important since room temperature annealing did

Table 7. Initial radiochemical yield of $[\text{Co}(\text{en})_2\text{X}_2]^{n+}$ from the neutron irradiation of $\text{D-}[\text{Co}(\text{en})_3](\text{NO}_3)_3$

Irradiation time (min)	Flux ($\text{n- cm}^{-2}\text{-sec}^{-1}$)	Storage	Method	Yield
20	3.0×10^{13}	3 days room temp.	recrystallization ^a	17.0
40	3.0×10^{13}	1 day room temp.	recrystallization ^a	15.7
40	3.0×10^{13}	7 days room temp.	ion exchange ^b	14.4 ± 0.4
10	1.0×10^{13}	1 day dry ice	ion exchange ^b	9.3 ± 0.5

^aRecrystallization to constant specific activity from trans- $[\text{Co}(\text{en})_2\text{Cl}_2]\text{Cl}$ as cis- $[\text{Co}(\text{en})_2(\text{NO}_2)_2]\text{I}$.

^bIon exchange as $[\text{Co}(\text{en})_2(\text{NO}_2)_2]^+$.

not produce such an increase in the yield of this product. The radio-synthesis of $[\text{Co}(\text{en})_2\text{X}_2]^{n+}$ probably came about as the result of the disruption of the crystal lattice by the recoiling atom and recombination of the cobalt atom with two ethylenediamine molecules immediately following recoil. The stereochemistry of this species has not been determined and the ion may have been in the trans or the D- or L- cis forms. Since these isomers are readily transformed to one another in solution, the trans- $[\text{Co}(\text{en})_2\text{Cl}_2]\text{Cl}$, added as carrier and converted to the solid cis salt, would be expected to have carried all three isomers.

It should be pointed out that a $[\text{Co}(\text{en})_2\text{X}_2]^{n+}$ fraction has not been explicitly reported in the previous literature as a result of the Szilard-Chalmers process. However, Zuber (13) reported products which he could not identify. Also, Saito et al. (16) reported species which they identified as $[\text{Co}(\text{en})_2\text{a}_2]^3$, $[\text{Co}(\text{en})_2\text{Xa}]^2$, and $[\text{Co}(\text{en})_2\text{X}_2]^+$. The species which Saito et al. described may all have contributed to the activity which is identified here as $[\text{Co}(\text{en})_2\text{X}_2]^{n+}$. They did not clearly describe their analytical procedure, but it can be assumed that their species were separated by paper electrophoresis in aqueous solution. They reported that the a ligand was either water or ammonia and that the X ligand was an anion. It is clear that water could have been introduced in the dissolution process. Their X ligand could have combined with the complex following dissolution since an electrolyte is generally used in electrophoresis studies. The species described by Saito et al. could not be used to distinguish between processes which occurred as a result of recoil in the solid state and processes which occurred as a result of

the analytical method used. These species may all have contained activity which was due to $[\text{Co}(\text{en})_2\text{X}_2]^{n+}$ and $[\text{Co}(\text{en})_2(\text{NH}_3)\text{X}]^{m+}$. Furthermore, Saito's species did not distinguish between $[\text{Co}(\text{en})_2\text{X}_2]^{n+}$ and $[\text{Co}(\text{en})_2(\text{NH}_3)\text{X}]^{m+}$. Conversion to a solid compound and recrystallization to constant specific activity removed the ambiguity in this study since the X ligand which may have been added as a result of dissolution was replaced with the $-\text{NO}_2^-$ group.

The activity in the form $[\text{Co}(\text{en})_2(\text{NH}_3)\text{X}]^{m+}$ was isolated by coprecipitation with $[\text{Co}(\text{en})_2(\text{NH}_3)\text{Cl}]\text{Cl}_2$. Chloride ion was substituted for the X ion in solution, and the complex precipitated as the chloride salt with carrier. In the ion exchange procedure, NO_2^- ion was substituted for the X ligand to form the stable ion $[\text{Co}(\text{en})_2(\text{NH}_3)(\text{NO}_2)]^{2+}$. Again, the stereochemistry was not determined since isomerization between the cis and trans forms readily occurs in solution. The radiochemical yields of $[\text{Co}(\text{en})_2(\text{NH}_3)\text{X}]^{2+}$ are recorded in Table 8 for various irradiation conditions and separation techniques. The identity of the X ligand in the solid state was not known. However, it was readily replaced by H_2O , NO_2^- , or Cl^- ligands in solution.

The production of $[\text{Co}(\text{en})_2(\text{NH}_3)\text{X}]^{m+}$ has not been reported previously. This species may have been part of Zuber's (13) unknown activity and probably was part of the activity reported by Saito et al. as $[\text{Co}(\text{en})_2\text{aa}]^{3+}$ and $[\text{Co}(\text{en})_2\text{aX}]^{2+}$. It is important to point out that all the many authors other than Saito or Zuber have reported no radioactive products other than $[\text{Co}(\text{en})_3]^{3+}$ and Co^{2+} .

The complex $[\text{Co}(\text{en})_2(\text{NH}_3)\text{X}]^{m+}$ was formed in the solid state by the

Table 8. Radiochemical yields of $[\text{Co}(\text{en})_2(\text{NH}_3)\text{X}]^{\text{m}+}$ from the neutron irradiation of solid D- or L- $[\text{Co}(\text{en})_3](\text{NO}_3)_3$

Neutron flux ($\text{n-cm}^{-2}\text{-sec}^{-1}$)	Irradiation time (min)	Storage	Method	Yield %
3×10^{13}	20	room temp.	recrystallization ^a	17.0
3×10^{13}	20	room temp.	ion exchange	15.8
1×10^{13}	10	dry ice	ion exchange	4.5

^aRecrystallization to constant activity as $[\text{Co}(\text{en})_2(\text{NH}_3)\text{Cl}]\text{Cl}_2$.

combination of the recoiling cobalt atom with available ethylenediamine molecules and ammonia or NH_2 radicals present in the disrupted crystal lattice. The existence of this species is an indication of the breaking of C-N covalent bonds in ethylenediamine. The ultraviolet irradiation of aqueous solutions of the $[\text{Co}(\text{en})_3]^{3+}$ ion has been shown to yield Co^{2+} , ammonia and ethylenediamine (57). This behavior was indicative of C-N bond breaking so it is perhaps not surprising that similar decomposition occurred in the more energetic hot atom process.

B. Transient Species

The discovery that the Co^{2+} activity increased in solution was a surprising result. Prior to the discovery of this phenomenon, it was assumed that the following dissolution, the relative activities of the various species would not change. When solutions of solid irradiated $\text{D-}[\text{Co}(\text{en})_3](\text{NO}_3)_3$ were analyzed for radioactive Co^{2+} immediately following dissolution, the Co^{2+} activity was 15% lower than that in the same sample analyzed a month following dissolution. The conclusion was drawn from this observation that some cobalt activity was present either as a water unstable form or as a form exchangeable with Co^{2+} . Such transient forms have not been reported in the literature previously.

At room temperature the rate of conversion was not affected by the concentration of Co^{2+} carrier, nor was the rate diminished in the absence of Co^{2+} carrier. When the function $\log[\text{R}(\text{Co}^{2+})_\infty - \text{R}(\text{Co}^{2+})_t]$ was plotted as a function of time (where $\text{R}(\text{Co}^{2+})_t$ is the percent activity as Co^{2+} at time = t, $\text{R}(\text{Co}^{2+})_\infty$ is the percent activity as Co^{2+} after two months in

solution), the resulting curve could be resolved into two linear portions as shown in Figure 6. From this information, it was deduced that two radiochemical species, produced in the recoil process, decomposed to Co^{2+} in solution. These components have been designated by the symbols X_f and X_s to indicate the species which respectively react rapidly and slowly to produce Co^{2+} in solution.



Although the identities of X_s and X_f were not determined, it can be speculated that they may have been Co(III) complexes which did not contain sufficient numbers of ammine ligands to be stabilized in solution. It is tempting to speculate that the formulas for the two complexes in solution were $[\text{Co}(\text{en})(\text{H}_2\text{O})_4]^{3+}$ and $[\text{Co}(\text{en})(\text{NH}_3)(\text{H}_2\text{O})_3]^{3+}$ for X_f and X_s , respectively. A search of the literature yielded no information concerning complexes with exactly these formulations. However, there have been several reports of similar species in the literature. Bodek *et al.* (58) have reported reactions of complex ions with the formulas $[\text{Co}(\text{NH}_3)_2(\text{H}_2\text{O})_4]^{3+}$ and $[\text{Co}(\text{NH}_3)_3(\text{H}_2\text{O})_3]^{3+}$. Wilairate and Garner (59) have prepared the complex ion $[\text{Co}(\text{dien})(\text{H}_2\text{O})_3]^{3+}$. White *et al.* (60) have studied reactions of $[\text{Co}(\text{NH}_3)(\text{H}_2\text{O})_5]^{3+}$ and $[\text{Co}(\text{H}_2\text{O})_6]^{3+}$ in acid media. These compounds are rapidly reduced by water above pH 3.5 (58). Studies of the decomposition of these compounds in water have been performed in high concentrations of HClO_4 (0.1 - 6.0 M). For example, the

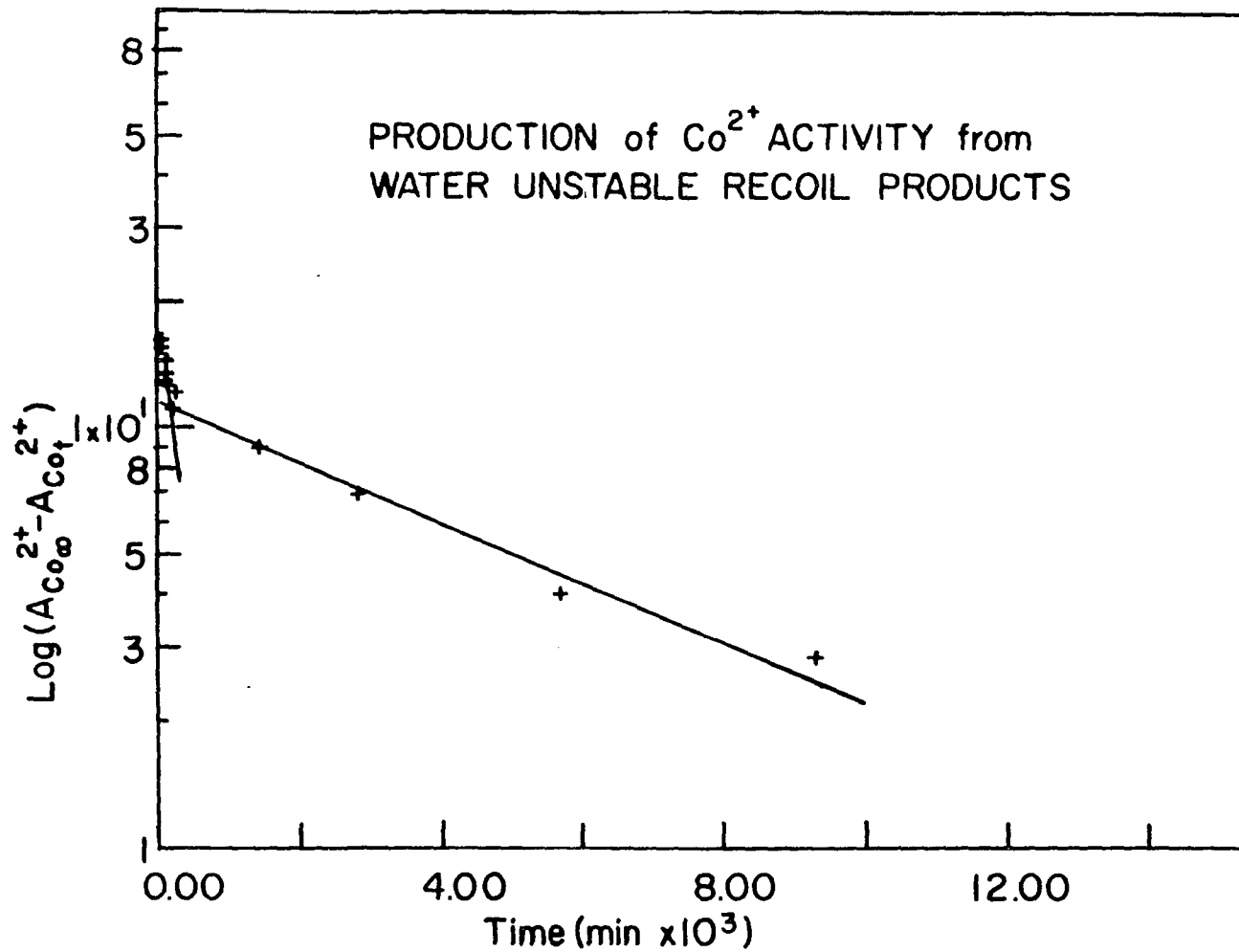


Figure 6. Production of Co^{2+} activity from water unstable recoil products

$[\text{Co}(\text{dien})(\text{H}_2\text{O})_3]^{3+}$ complex with three nitrogen donor atoms decomposed to Co^{2+} in 0.1 - 2.0 HClO_4 . The rate law for decomposition was $-\text{d}[\text{C}]/\text{dt} = (k_1 + k_2/[\text{H}^+])[\text{C}]$ where $[\text{C}]$ was the concentration of the complex. At 80.7°C the following rate constants were determined: $k_1 = 0.7 \times 10^{-7} \text{ sec}^{-1}$, $k_2 = 1.4 \times 10^{-7} \text{ M-sec}^{-1}$ (58). It would appear that any aquo-amine cobalt(III) complex would be rapidly reduced to Co^{2+} in neutral solution if it contained less than four nitrogen donor atoms. The available data, however, neither support nor rule out the identification of X_s or X_f as $[\text{Co}(\text{en})(\text{H}_2\text{O})_4]^{3+}$ or $[\text{Co}(\text{en})(\text{NH}_3)(\text{H}_2\text{O})_3]^{3+}$.

Since there was little chance that the activity of X_s and X_f could be trapped and recrystallized for positive identification, the kinetics of conversion to Co^{2+} were investigated at 30°C and 40°C . Activities of Co^{2+} as a function of time in solution at the two temperatures are listed in Table 9.

For a first order reaction, the rate of decomposition of the species X_s is described by Equation (40), where $[X_s]$ is the concentration of X_s at time t and $[X_0]$ is the initial concentration of X_s , and k_s is the rate constant.

$$-\frac{\text{d}[X_s]}{\text{dt}} = k_s [X_s] \quad (40)$$

Equation (40) can be rearranged to yield Equation (41).

$$\frac{\text{d}[X_s]}{[X_s]} = -k_s \text{ dt} \quad (41)$$

Table 9. Production of $^{60}\text{Co}^{2+}$ from transient species in solution following dissolution of irradiated, dry-ice stored solid $\text{D}[\text{Co}(\text{en})_3](\text{NO}_3)_3$

<u>30°C Expt. 1</u>		<u>30°C Expt. 2</u>		<u>40°C Expt. 1</u>		<u>40°C Expt. 2</u>	
time (min)	R(Co^{2+}) (%)	time (min)	R(Co^{2+}) (%)	time (min)	R(Co^{2+}) (%)	time (min)	R(Co^{2+}) (%)
8.9	61.3	11.8	63.9	21.4	63.8	16.6	61.2
18.7	61.1	130.5	66.7	30.4	64.4	48.5	63.0
30.7	61.3	528.3	68.5	40.7	64.9	78.2	64.3
40.9	61.8	1406.4	71.0	53.6	67.4	116.9	66.0
50.2	63.9	1990.5	71.5	61.6	66.5	203.2	67.5
59.6	64.5	2805.1	71.2	71.8	65.8	1159.7	71.9
70.8	62.9	3500.9	71.9	110.5	68.9	1554.4	72.3
123.2	64.8	4171.5	72.6	140.1	69.3	2685.3	74.9
150.4	66.3	4917.6	73.4	193.5	69.9	3308.4	75.0
203.7	65.2	5682.3	73.5	1150.2	73.4	4124.4	76.3
1399.2	68.3	6373.0	74.2	5488.6	74.6	4764.9	75.4
2791.9	70.4	7436.3	74.5	4.0×10^4	80.9	5522.6	75.8
5665.3	73.3	10672.3	73.7			7045.6	77.4
9258.2	74.5	2.0×10^4	77.1			9047.8	76.2
1.6×10^4	76.8	2.0×10^4	77.1			4.0×10^4	80.8
1.6×10^4	77.6	2.0×10^4	77.2			4.0×10^4	80.9
1.6×10^4	77.3	2.0×10^4	77.1			4.0×10^4	81.1

Equation (41) can be integrated to yield Equation (42).

$$\ln \frac{[X_s]}{[X_o]} = -k_s t \quad (42)$$

After 1000 min, essentially all of the X_f species will have been converted to Co^{2+} . The concentration of X_s is proportional to the activity of X_s . The activity of X_s is proportional to the final activity of Co^{2+} , A_∞ , minus the activity of Co^{2+} , A_t , at time t greater than 1000 min. Let A_o be the activity of Co^{2+} when the sample was originally dissolved assuming that no X_f species was present. Equation (43) then holds.

$$\frac{(A_\infty - A_t)}{(A_\infty - A_o)} = \frac{[X_s]}{[X_o]} \quad (43)$$

Substitution in Equation (42) yields Equation (44).

$$\ln \frac{(A_\infty - A_t)}{(A_\infty - A_o)} = -k_s t \quad (44)$$

$$2.303 \log_{10} (A_\infty - A_t) = -k_s t + \ln(A_\infty - A_o) \quad (45)$$

The function $\log_{10}(A_\infty - A_t)$ was plotted as a function of time. A least squares program was used to determine the slope of the line for times greater than 1000 min. The rate constant was determined from the slope of the line.

$$k_s = -2.303 \cdot \text{slope} \quad (46)$$

From a knowledge of the rate constants for the slow reaction, the

activities of Co^{2+} at shorter times were corrected for the effect of the slow reaction. A plot of $\log (A_{f,\infty} - A_{f,t})$ as a function of time for times less than 1000 min. yielded a straight line from which could be deduced the rate constant for the decomposition of X_f .

By comparing rate constants, k_1 and k_2 , at two temperatures, T_1 and T_2 , the Arrhenius activation energies for the two processes were calculated from Equation (47).

$$E_a = \frac{2.303RT_1T_2}{T_2 - T_1} \log \frac{k_2}{k_1} \quad (47)$$

The enthalpy of activation ΔH^\ddagger was determined from Equation (48),

$$H^\ddagger = E_a - RT \quad (48)$$

The entropy of activation was determined from Equation (49) where N is Avogadro's number; h is Planck's constant.

$$S^\ddagger = R \ln k_1 - \ln \frac{RT}{Nh} + \frac{\Delta H^\ddagger}{RT} \quad (49)$$

A summary of the rate constants and the activation parameters derived for the two processes is presented in Table 10. Note large differences in rate constants for the two processes. For example, at 30°C k_f equals $1.4 \times 10^{-4} \text{ sec}^{-1}$; k_s equals $2.6 \times 10^{-6} \text{ sec}^{-1}$. The large difference in rates permitted the separation of the two processes and the convenient evaluation of the individual rate constants. The small differences in rates for a given process at the two temperatures is a consequence of the large negative entropy changes and the relatively small activation

Table 10. Rate constants and activation parameters for the production of Co^{2+} in solution from transient species

Reaction	$k(30^\circ\text{C}) (\text{sec}^{-1})$	$k(40^\circ\text{C}) (\text{sec}^{-1})$	$E_a (\text{kJ-M}^{-1})$	$\Delta H^\ddagger (\text{kJ-M}^{-1})$	$\Delta S^\ddagger (\text{J-M}^{-1}\text{-K}^{-1})$
$X_f \rightarrow [\text{Co}(\text{H}_2\text{O})_6]^{2+}$	$1.4 \pm 0.4 \times 10^{-4}$	$1.5 \pm 0.2 \times 10^{-4}$	6 ± 23	4 ± 23	-310 ± 75
$X_s \rightarrow [\text{Co}(\text{H}_2\text{O})_6]^{2+}$	$2.6 \pm 0.3 \times 10^{-6}$	$3.8 \pm 0.4 \times 10^{-6}$	30.5 ± 10.8	27.9 ± 10.8	-260 ± 34

energies. These features indicated that the conversion of X_s or X_f to Co^{2+} were ones which mostly involved ordering about the activated complex.

C. Solid-State Thermal Annealing

As a result of heating solid samples of the irradiated complex salts, the radiochemical distribution changed as a function of time and the temperature of heating. The results of the analysis of samples heated at 40°, 80°, 100°, 120°, 160°C are listed in Tables 11-15, respectively. Samples annealed at 100° and 160°C were analyzed for radiochemical cobalt(II) only. Radiochemical yields of samples which had undergone isochronal annealing are listed as a function of temperature in Table 16. It should be pointed out that considerable changes in the radiochemical distribution occurred at room temperature. For example, the radiochemical yield of Co^{2+} in one sample decreased from 67.7% immediately following removal from dry ice to 60.7% following storage of the sample at room temperature for 193 hours.

The percent activity recovered as Co^{2+} is plotted as a function of time in Figure 7. Isothermal annealing curves for data collected at 80°, 100°, and 160° were calculated from the analysis of samples which were analyzed immediately following dissolution. The 120° and 40° curves were estimated by subtracting the estimated yield of X_s and X_f species from the Co^{2+} yield of aged samples (see Table 15). These estimated yields were calculated from analysis of initial and final samples prior to and following solution aging for one month. The Co^{2+} activity decreased considerably at all five temperatures. At 40°C the decrease

Table 11. Radiochemical yields of various radiochemical species in neutron irradiated D-[Co(en)₃](NO₃)₃ following isothermal annealing at 40°C. (Samples aged 1.5 months in solution prior to analysis)^a

Time (min)	Co ²⁺	Radiochemical Yield (%) Determined by the Ion Exchange Method				Sum of Components Determined
		[Co(en) ₂ X ₂] ⁿ⁺	[Co(en) ₂ (NH ₃)X] ^{m+}	D- and L-[Co(en) ₃] ³⁺		
no heating	79.2 ^{a,b}	4.8	4.7	10.1	98.8	
31.8	76.9	10.6	3.3	7.7	98.5	
51.1	76.2	8.5	3.4	9.6	97.7	
70.6	73.8	7.7	5.0	10.0	96.5	
90.1	74.3	6.5	4.8	12.7	98.3	
111.5	75.4	7.1	5.3	10.6	98.4	
139.8	74.7	9.1	6.1	10.2	100.1	
170.7	73.4	9.2	6.0	11.8	100.4	
201.0	71.3	8.5	8.6	11.5	99.9	
231.2	75.2	9.3	4.9	11.4	100.8	
270.5	73.4	9.4	5.2	14.1	102.1	
311.0	71.5	11.0	4.9	12.6	100.0	
1458.0	64.2	4.8	5.9	24.6	99.5	
4346.0	51.8	3.9	6.6	34.5	96.8	

^aSamples stored in dry ice prior to heating; irradiation time, 10 min; flux, 1×10^{13} n/cm² sec.

^bCo²⁺ includes X_s and X_f fractions.

Table 12. Radiochemical yields of various radiochemical species in neutron irradiated D-[Co(en)₃](NO₃)₃ following isothermal annealing at 80°C. (Samples not aged in solution prior to analysis)^a

Time (min)	Radiochemical Yield (%)				D- and L- [Co(en) ₃] ³⁺	Sum of Components Determined
	Co ²⁺	[Co(en) ₂ X ₂] ⁿ⁺	[Co(en) ₂ (NH ₃)X] ^{m+}			
No heating	67.7	15.6	5.6		11.1	100.3
378.0	38.0	9.7	12.6		39.6	99.9
6000.0	26.7	8.7	10.5		52.3	98.2
15840.0	24.0	9.6	13.7		52.7	100.0

^aSamples stored in dry ice prior to heating; irradiation time, 10 min; flux, 1×10^{13} n/cm² sec.

Table 13. Radiochemical yields of various radiochemical species in neutron irradiated D-[Co(en)₃](NO₃)₃ following isothermal annealing at 120°C. (Samples aged in solution prior to analysis)^a

Time (min)	Radiochemical Yield (%)				Sum of Components determined
	Co ²⁺	[Co(en) ₂ X ₂] ⁿ⁺	[Co(en) ₂ NH ₃)X] ^{m+}	[Co(en) ₃] ³⁺	
0	79.8 ^b	9.4	4.2	9.3	102.7
18.3	24.7	6.8	11.7	54.7	97.9
31.8	19.8	3.5	11.9	71.4	106.6
48.3	15.7	3.6	6.6	85.2	111.1
59.9	18.9	6.9	7.6	69.3	102.7
178.4	14.0	2.8	9.1	70.9	96.8
343.6	13.3	1.5	7.1	81.6	103.5
380.3	8.2	2.9	5.3	81.7	98.1
487.8	11.0	1.7	5.6	82.2	100.5
1102.2	8.2	1.6	6.3	83.7	99.8
1419.2	12.3	0.0	3.3	83.7	99.3
1889.9	7.4	1.4	3.9	82.9	95.6
2609.5	6.8	6.9	6.8	78.3	98.8
3270.2	8.9	0.2	2.3	87.3	98.7
4436.3	9.3	1.1	10.2	75.8	96.4
10173.2	8.0	0.7	5.5	87.4	101.6

^aStored in dry ice prior to heating; irradiation time, 10 min; flux, 1×10^{13} n/cm² sec.

^bCo²⁺ includes X_f and X_s fractions.

Table 14. Radiochemical yields of Co^{2+} in neutron irradiated $[\text{Co}(\text{en})_3](\text{NO}_3)_3$ following isothermal annealing at 100° and 160°C . (Separations performed immediately following dissolution)

100°C			160°C		
Time (min)	Radiochemical Yield (%)		Time (min)	Radiochemical Yield (%)	
	Co^{2+}	$[100-R(\text{Co}^{2+})]$		Co^{2+}	$[100-R(\text{Co}^{2+})]$
0	$67.2 \pm 0.5^{a,b}$	32.8	0	1.9 ± 0.6	28.1
30.1	30.1 ± 0.1	69.9	26.7	3.0 ± 0.3	97.0
210.3	23.0 ± 0.3	76.0	48.0	2.9 ± 0.6	97.1
483.3	23.5 ± 0.3	76.5	110.3	4.0 ± 0.7	96.0
1062.4	19.9 ± 0.5	80.1	277.2	4.6 ± 1.3	95.4
1715.3	16.5 ± 3.6	83.5	450.5	3.7 ± 2.1	96.3
2735.0	14.0 ± 0.5	86.0	760.7	1.4 ± 0.5	98.6
5770.0	11.9 ± 1.4	88.1	1548.2	5.0 ± 0.1	95.0
9622.0	12.5 ± 1.0	87.5	3296.6	6.3 ± 0.9	93.7

^a Mean value from duplicate analyses.

^b Samples stored in dry ice prior to heating; irradiation time, 10 min; flux, 1×10^{13} n/cm² sec.

Table 15. Estimated radiochemical yields of Co^{2+} following thermal annealing of neutron irradiated $\text{D-}[\text{Co}(\text{en})_3](\text{NO}_3)_3^{\text{a}}$

40°C		120°C	
Time (min)	Co^{2+} Yield (%)	Time (min)	Co^{2+} Yield (%)
0	64.2	0	64.75
31.8	61.9	18.3	24.7
51.1	61.2	31.8	19.8
70.6	58.8	48.3	15.7
90.1	59.3	59.9	18.9
111.5	60.4	178.4	14.0
139.8	59.3	343.6	13.3
170.7	58.4	380.3	8.2
202.0	56.3	487.8	11.0
231.2	60.2	1102.2	8.2
270.5	58.4	1419.2	12.3
311.0	56.5	1889.3	7.4
1458.0	49.2	2609.5	6.8
4345.7	36.8	3270.2	8.9
		4436.3	9.3
		10173.2	8.0

^aCalculated by subtracting the estimated yield of water unstable species to the result from ages solutions. See Tables 11 and 13.

Table 16. Isochronal annealing results (samples aged 2 months in solution prior to analysis)^{a,b}

Temperature (°C)	Radiochemical Yield (%)				Sum of Components determined
	Co ²⁺	[Co(en) ₂ X ₂] ⁿ⁺	[Co(en) ₂ (NH ₃)X] ^{m+}	D- and L- [Co(en) ₃] ³⁺	
Initial	81.8 ^c	6.3	4.5	5.5	98.1
58.7	79.9	7.8	4.1	8.5	100.3
63.2	75.8	3.5	3.5	15.0	97.8
68.2	74.7	4.4	3.9	15.4	98.4
72.2	72.1	5.3	3.3	13.9	94.6
76.5	60.1	4.4	7.6	27.3	99.4
81.2	49.5	9.3	6.5	34.9	100.2
86.5	51.9	3.3	4.4	34.9	94.5
90.8	44.9	4.7	9.6	40.5	99.7
95.8	36.2	4.8	12.0	48.3	101.3
102.5	38.5	5.8	11.7	43.4	94.4
108.0	33.8	4.8	8.6	50.0	97.2
114.0	25.5	6.0	11.1	56.1	98.7

^aSamples stored in dry ice prior to heating; irradiation time, 10 min; flux 1×10^{13} n/cm² sec.

^bAll samples were placed in the sand bath at 58.7°C. At half hour intervals the temperature of the bath was increased by approximately 3°C and one sample was removed for analysis. The time required for each temperature increase was less than 5 min. During each isochronal pulse the temperature varied by less than 0.5°C.

^cCo²⁺ includes X_f and X_s fractions.

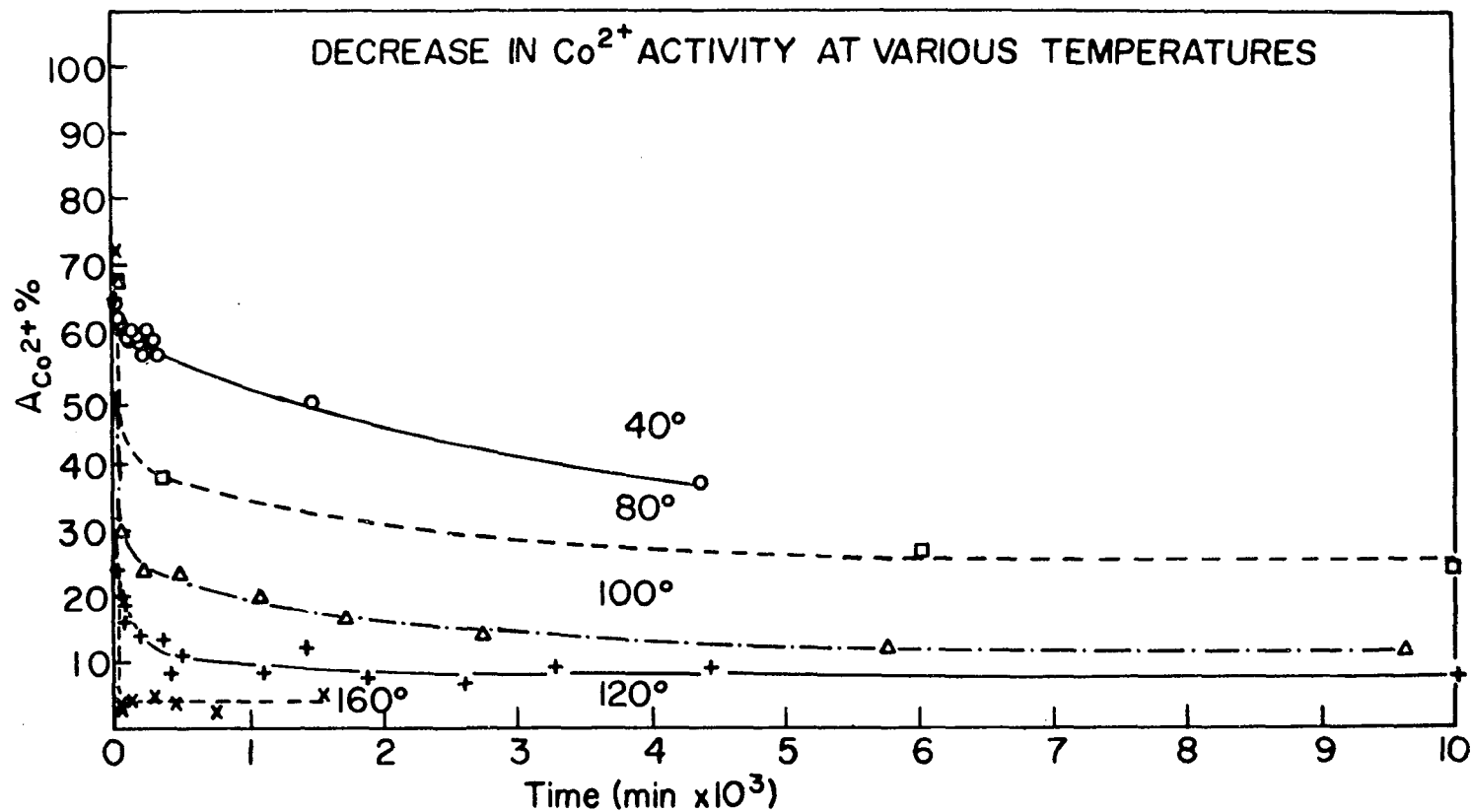


Figure 7. Decrease in Co^{2+} activity as a function of time at various temperatures in solid neutron irradiated D-tris-(ethylenediamine)cobalt(III)₂nitrate. Samples were irradiated with a thermal flux of $1.0 \times 10^{13} \text{ n-cm}^{-2}\text{-sec}^{-1}$ for the 10 min and stored in dry ice for 1 day prior to thermal treatment

seemed to slow upon extended annealing. A limit had not been reached at 4400 min. At 80° the decrease was initially rapid, but the yield of Co^{2+} reached an apparent plateau value of ca. 30% after 6000 min. At 100° there was a rapid decrease to 30%, followed by a slow decrease to an apparent plateau value of ca. 15%. At 120° there was a rapid decrease to ca. fifteen percent followed by a slower decrease and after 500 min. a plateau value of ca. 10% was reached. At 160° the relative activity of Co^{2+} decreased from 72% to 4% within 30 min. After 30 min. no further effect was observed.

The retention of percent activity as D- and L- $[\text{Co}(\text{en})_3]^{3+}$ is plotted as function of time at various temperatures in Figure 8. Radiochemical $[\text{Co}(\text{en})_3]^{3+}$ was being produced at the expense of Co^{2+} . The rate of production of $[\text{Co}(\text{en})_3]^{3+}$ was equal to the rate of disappearance of Co^{2+} . At 40° the retention as D- and L- $[\text{Co}(\text{en})_3]^{3+}$ had not approached a limit in 4400 min. At 80° there was a rapid increase in the retention followed by a plateau after 6000 min. At 120° there was a very rapid initial increase in retention. After 300 min. an apparent plateau of ca. 82% was reached.

Thermal annealing had a small but erratic effect on the radiochemical yield of $[\text{Co}(\text{en})_2\text{X}_2]^{n+}$ below 120°C. At 40°C (Table 10) the yield increased from 4.8% for the sample which was not annealed to 10.6% following just 31.8 min. of annealing at 40°C. The yield remained rather constant ($8.8 \pm 1.4\%$) for 30 min., but upon extended annealing for 1458 and 4346 min. decreased to 4.8 and 3.9%, respectively. It may be equally valid, however, to deduce from the data that the radiochemical yield

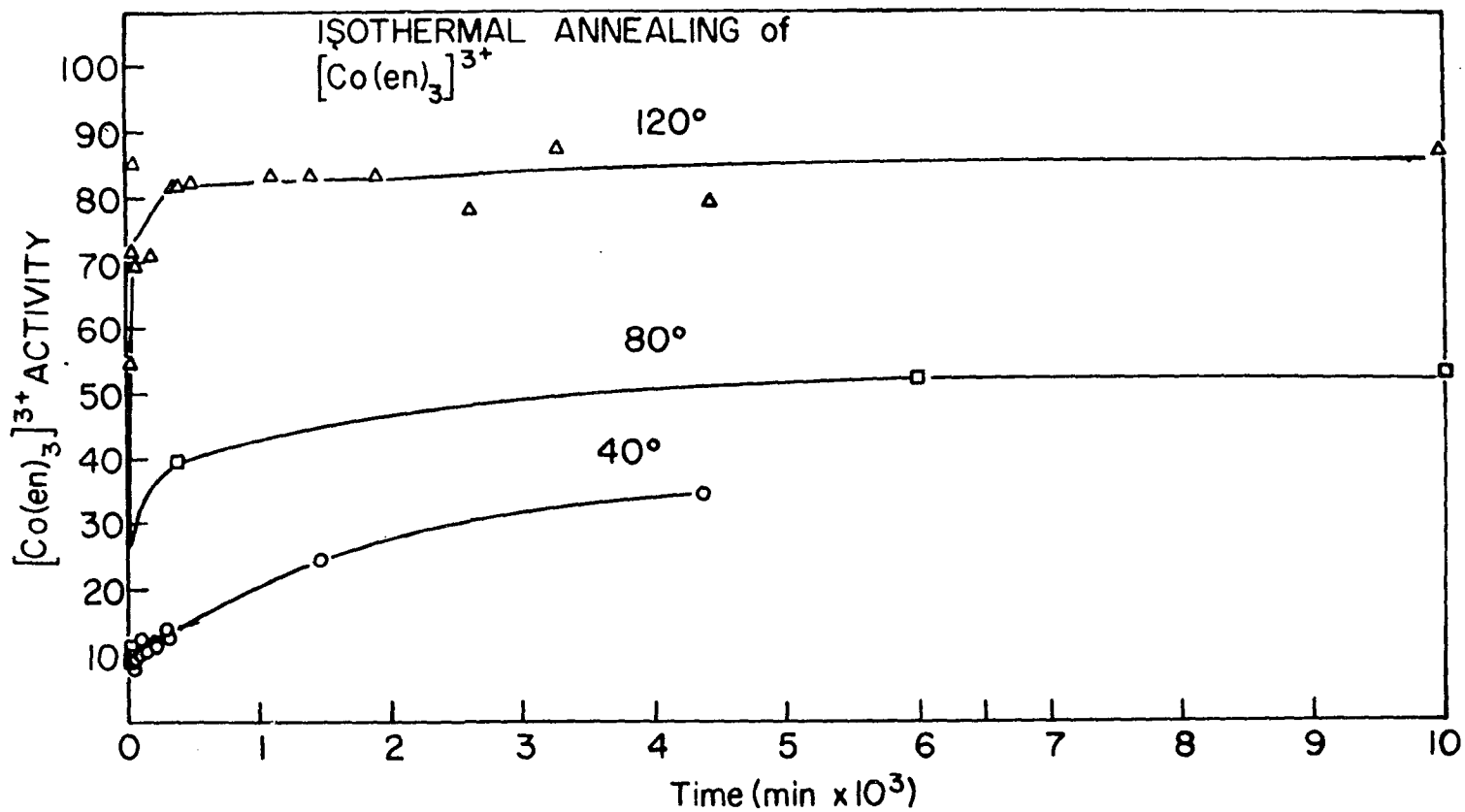


Figure 8. The radiochemical yield of D- and L- $[\text{Co}(\text{en})_3]^{3+}$ as a function of time at various temperatures in solid D-tris-(ethylenediamine)cobalt(III) nitrate. Samples were irradiated with a thermal flux of 1.0×10^{13} $\text{n-cm}^{-2}\text{-sec}^{-1}$ for 10 min and stored in dry ice for one day prior to thermal treatment

remained constant with time of heating, and the fluctuations were due to experimental error. The mean value of the yields would be $7.9 \pm 2.2\%$. The Pierce-Chauvenet (61) criterion would not require the rejection of any of the points. However, the uncertainty of $\pm 2.2\%$ of the total activity is much greater than the uncertainty obtained from an independent analysis (see Section II-G). This rise in the uncertainty may have occurred because separate solid samples were analyzed for each point. At 80°C the yield of the initial point was high (15.6%) but later points had rather constant values of $9.3 \pm 0.6\%$ upon extended annealing. If we again assume the constancy of the $[\text{Co}(\text{en})_2\text{X}_2]^{n+}$ yields for all four points in Table 12, the mean would be $10.9 \pm 3.2\%$. Again the value of the uncertainty is much larger than that expected from the independent analysis. However, Chauvenet's criterion does not require the rejection of the no-heating point.

At 120°C the activity of $[\text{Co}(\text{en})_2\text{X}_2]^{n+}$ decreased with time as shown in Figure 9. After 178.4 min., essentially all of the activity as $[\text{Co}(\text{en})_2\text{X}_2]^{n+}$ had been converted to some other form. After 178.4 min. the mean value for $R([\text{Co}(\text{en})_2\text{X}_2]^{n+})$ was $1.4 \pm 0.9\%$. The point at 2609.5 min. could be rejected based on Chauvenet's criterion (63) for points after 178.4 min. Upon isochronal annealing, the yield of $[\text{Co}(\text{en})_2\text{X}_2]^{n+}$ did not change in any uniform manner with increased temperature. The mean yield was $5.4 \pm 1.7\%$.

Heating had a small but erratic effect on the radiochemical yield of the $[\text{Co}(\text{en})_2(\text{NH}_3)\text{X}]^{m+}$ species. No discernible trend could be detected from the 40°C data. However, the yields measured ranged between 3.3%

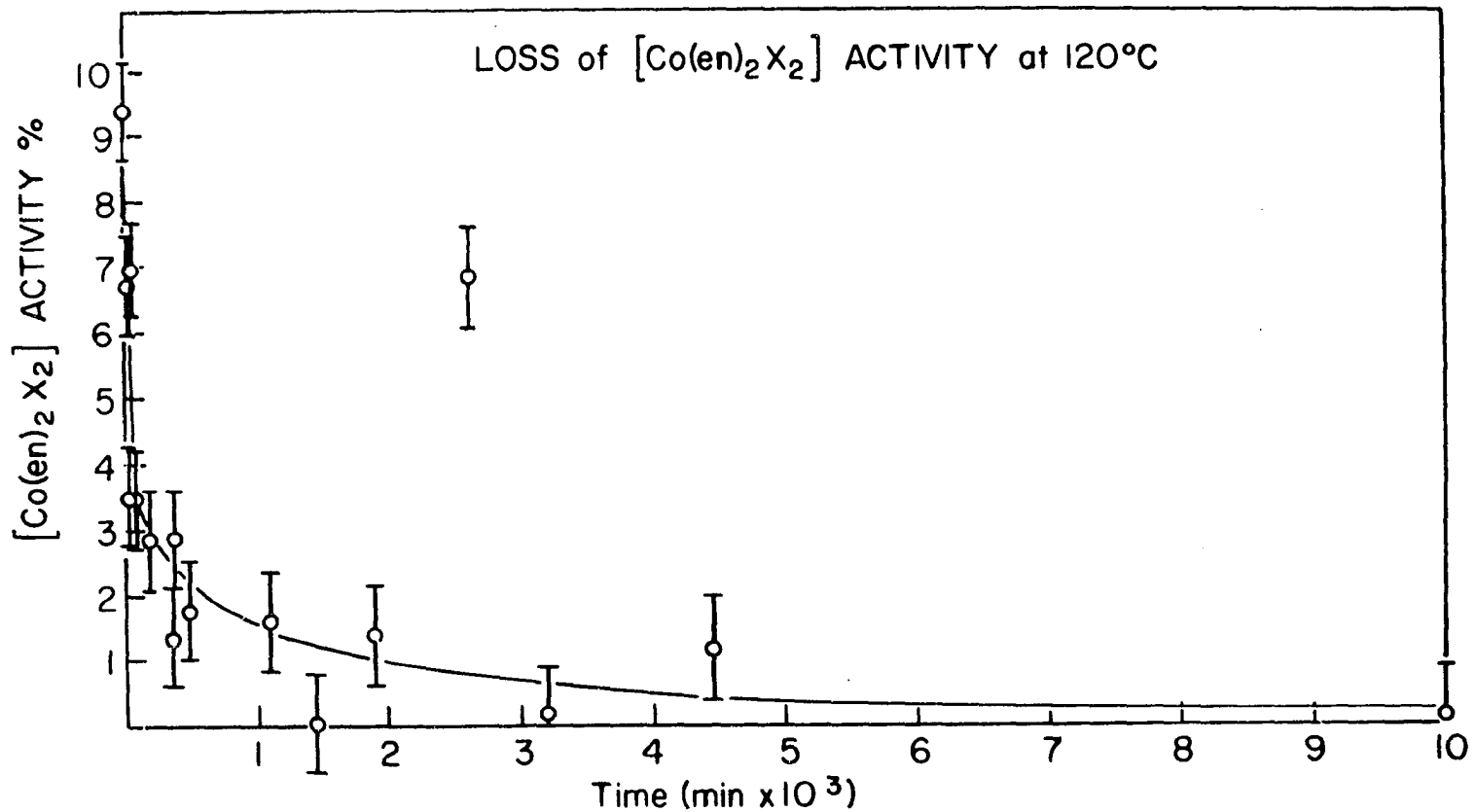


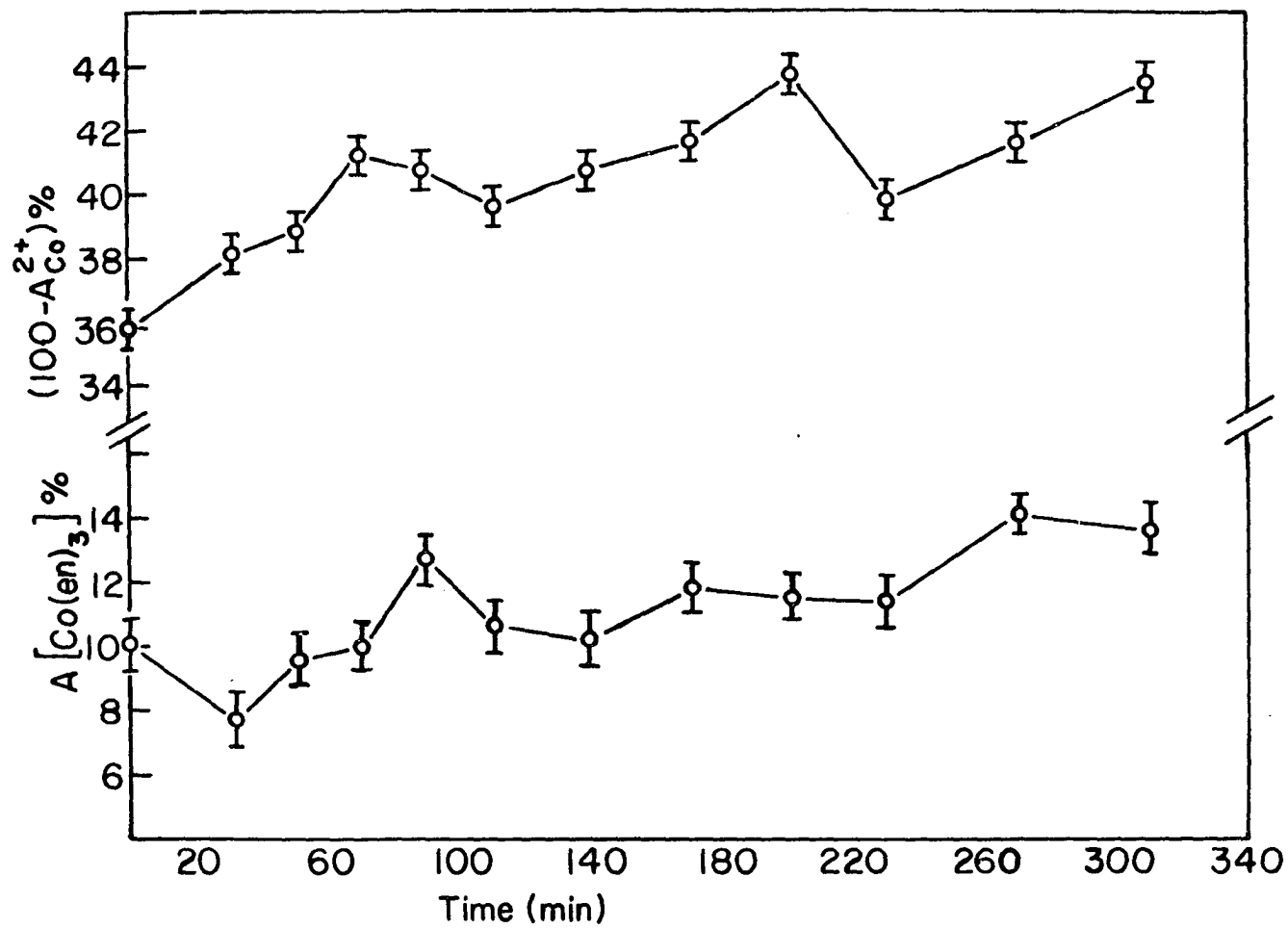
Figure 9. Loss of $[\text{Co(en)}_2\text{X}_2]^{n+}$ activity with time of heating at 120°C in solid neutron irradiated D-tris-(ethylenediamine)cobalt(III) nitrate. Samples were irradiated with a thermal flux of $1.0 \times 10^{13} \text{ n-cm}^{-2}\text{-sec}^{-1}$ for 10 min and stored in dry ice for one day prior to thermal treatment

and 8.6%. The mean value was $5.3 \pm 1.3\%$. At 80°C the yield of this species was initially low (5.6%) but increased rapidly to a plateau value of $12.3 \pm 1.6\%$. The data in Table 12 indicate that the $[\text{Co}(\text{en})_2(\text{NH}_3)\text{X}]^{\text{m}+}$ yield did not vary in a regular fashion with time at 120°C . In the isochronal annealing, the yield seemed to increase erratically from a value of 4.5% to 11.1%.

The oscillation in annealing curves reported by Dimotakis et al. (24,25) was deemed worthy of investigation. They had observed that for isothermal annealing the increase in retention was not monotonic with time, and that the annealing curves had peaks and valleys which were at least 10% of the total activity at 38°C . The 40°C annealing curve of neutron irradiated $\text{D}-[\text{Co}(\text{en})_3](\text{NO}_3)_3$ determined in the present work is shown in Figure 10. These results are inconclusive concerning the existence of oscillations, since the magnitude of the largest deviation from a smooth curve was only twice the standard deviation of the determination, Table 4, and in no case greater than 2% of the total activity. However, it must be admitted that the conditions of Dimotakis et al. were not duplicated exactly since the irradiations were performed at reactor temperatures after which the samples were stored in dry ice. The samples which Dimotakis studied were irradiated and stored at liquid nitrogen temperature, but such a facility was not available at the ALRR. On the other hand, Dimotakis was not aware of the X_f and X_s products. If he determined the ^{60}Co present as Co^{2+} at varying times after irradiation, and dissolution, he would have recorded different amounts of X_f and X_s with his samples.

Figure 10. Short term isothermal annealing of neutron irradiated D-tris(ethylenediamine) cobalt(III) nitrate at 40°C. Samples were irradiated with a thermal flux of $1.0 \times 10^{13} \text{ n-cm}^{-2}\text{-sec}^{-1}$ for 10 min and stored in dry ice for one day prior to thermal treatment

Short Term Thermal Annealing at 40°C



The isochronal annealing curve for the production of $[\text{Co}(\text{en})_3]^{3+}$ is shown in Figure 11. The Co^{2+} curve is a mirror image of this. The radiochemical yield of $[\text{Co}(\text{en})_3]^{3+}$ increased with a typical step-like behavior.

According to Lazzarini and Fantola-Lazzarini (46), isochronal annealing curves give good indications of processes involved in thermal annealing since such curves yield multi-step patterns which are a consequence of different types of annealing. If there were several types of defects present which made available energy for isotopic exchange, according to the isotopic exchange model, the activation energy for exchange becomes available upon the annealing of the various defects. Each of the steps in the isochronal annealing curve reflect the annealing of each type of defect. Electrons are made available to the conduction band which then provides the energy for exchange. The rate determining step is the release of electrons or holes and the exchange reaction occurs rapidly after the annealing of defects. The activation energy for the annealing process can be determined from an analysis of the isochronal and isothermal annealing curves using the method of Meehan and Brinkman (62). This method was later modified by Damask and Dienes (63). In this method, the recovery of certain physical properties in solids during thermal annealing is assumed to obey a rate equation of the form

$$dp/dt = F(p, q_1, q_2, \dots) e^{-E/KT} \quad (50)$$

where p represents the property measured and the q 's represent variables which are independent of time, t and temperature, T . In the case of our

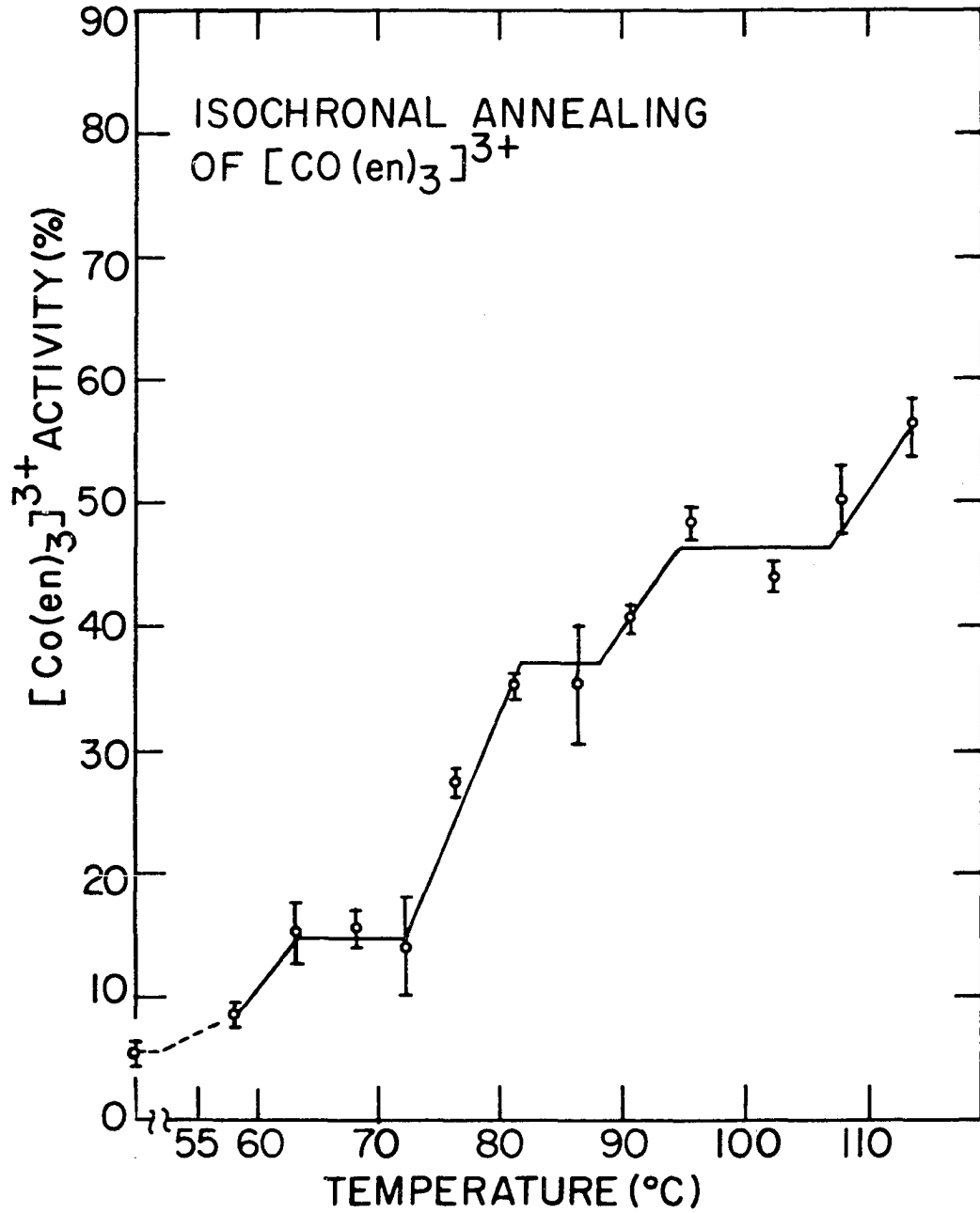


Figure 11. Isochronal annealing of solid neutron irradiated D-tris(ethylenediamine)cobalt(III) nitrate. Samples were irradiated with a thermal flux of $1.0 \times 10^{13} \text{ n-cm}^{-2}\text{-sec}^{-1}$ for 10 min and stored in dry ice prior to thermal treatment

analysis p would be $R([\text{Co(en)}_3]^{3+})$. For a given recovery state, (all of the property change which is associated with a given unique activation energy) it is generally believed that a particular kind of lattice imperfection is thermally excited and thereby induced to undergo a change such as migration to a position of lower energy, where its contribution to the measured property is altered. The activation energy E , then represents the energy difference between the height of an energy barrier which must be overcome and the initial energy of the imperfection. Then the Boltzmann factor $e^{-E/kT}$, represents the temperature dependence of the probability per unit time that the imperfection overcomes the barrier. The density of such imperfections in their initial state is denoted by n . The more basic rate equation should then be:

$$dn/dt = f(n, q_1, q_2, \dots) e^{-E/kT} \quad (51)$$

In order that Equation (51) follow from Equation (50) it is necessary to assume that the relationship between p and n is a small single-valued monotonically increasing or decreasing function, independent of t , T and the q 's. That is,

$$p = g(n) \quad (52)$$

The q 's which depend on the previous history of the specimen involve the spatial distribution of the sink to which the imperfection must migrate. They can be constant or a function of n for specimens having identical histories.

In general, Equation (50) can be integrated as follows:

$$\lambda(p, q_1, q_2 \dots) \equiv \int_{p_0}^p \frac{dp}{F(p, q_1, q_2 \dots)} = \int_0^t e^{-E/kT} dt \equiv \theta \quad (53)$$

where θ is designated as the temperature-compensated time. For identical specimens (same history prior to annealing treatment), the q 's need not be considered; then for such specimens,

$$p = p(\theta) . \quad (54)$$

Consider now two specimens with identical history. The first specimen is to be annealed at a series of successively higher temperatures for equal time intervals (temperature pulse, i); the temperature intervals need not necessarily be equal. This would be isochronal annealing. A property, p , is measured at the end of each such temperature pulse. If the temperature coefficient of p is negligible or accurately known, measurements can be made at the temperature of each pulse. If not, after each pulse the specimen can be quenched to a standard base temperature at which the recovery is negligible, for the purpose of making measurements. During each pulse the temperature must be maintained constant. Let T_i denote the temperature of the specimen during the i th pulse, p_i the measured value of p after the i th pulse, θ_i the corresponding value of θ according to Equation (53) and t_i the total elapsed time at the end of the i th pulse. For a given pulse:

$$\Delta\theta_i = \theta_i - \theta_{i-1} ; \quad (55)$$

$$\Delta\theta_i = \Delta t_i e^{-E/kT_i} . \quad (56)$$

If the recovery is characterized by a single activation energy E , according to Equation (51), then:

$$\Delta t_i = C \text{ (a constant);} \quad (57)$$

$$\ln \Delta \theta_i = C' - E/kT_i: \quad (58)$$

$$C' = \ln C. \quad (59)$$

Consider the second specimen annealed at a single temperature (isothermal annealing) and the recovery of a property p measured as a function of annealing time. Let T_a denote the temperature of isothermal annealing and τ_i the annealing time at which p attains a value of p_i . According to Equation (54), the values of θ_i and θ_{i-1} corresponding to the values of p_i and p_{i-1} in an isothermal annealing curve will be the same as for the isochronal annealing curve. From Equation (53) applied to isothermal annealing,

$$\tau = \theta_i e^{E/kT_a}, \quad (60)$$

$$\Delta \tau_i = \tau_i - \tau_{i-1} = (\theta_i - \theta_{i-1}) e^{E/kT_a} = \Delta \theta_i e^{E/kT_a}. \quad (61)$$

$$\ln \Delta \tau_i = n \Delta \theta_i + C'' \quad (62)$$

where

$$C'' = E/kT_a.$$

Upon substitution of $\ln \Delta \theta_i$ from Equation (58), $\Delta \theta_i$ can be eliminated in Equation (62) to give:

$$\ln \Delta \tau_i = C''' - E/kT_i \quad (63)$$

where $C''' = C' + C''$. From the p vs. τ curve, one can determine τ_i corresponding to each p_i (also τ_{i-1} and p_{i-1}). Thus, $\Delta\tau_i$ for each successive pulse corresponding to the appropriate T_i , can therefore be determined. A plot of $\ln \Delta\tau_i$ vs. $1/T_i$ should yield a straight line for each portion associated with a unique activation energy. From Equation (63), the slope of each straight line portion would be equal to $-E/k$. If the recovery associated with annealing in a given temperature interval has more than a single activation energy, the $\ln \Delta\tau$ vs. $1/T_i$ plot will exhibit straight line segments in each interval of which a single activation energy is effective but the plot will curve in regions of overlapping energy.

Since p , the property measured, is $R([\text{Co(en)}_3]^{3+})$ for the system under consideration in this work, by comparing the times and temperatures in the isothermal and isochronal annealing curves for different values of $R([\text{Co(en)}_3]^{3+})_i$ and $R([\text{Co(en)}_3]^{3+})_{i-1}$, one can determine the activation energy for the various steps. Damask and Dienes (63) have combined Equations (56) and (61) and derived the following equation for the evaluation of activation energies for the various steps:

$$\ln \frac{\Delta\tau_i}{\Delta t_i} = \frac{E}{k} \left(\frac{1}{T_a} - \frac{1}{T_i} \right) \quad (64)$$

or

$$E = k \left(\frac{T_i T_a}{T_i - T_a} \right) \ln \left(\frac{\Delta\tau_i}{\Delta t_i} \right) \quad (65)$$

A tabulation of calculated activation energies for each step is

shown in Table 17. Activation energies were determined for the three observed steps. Within each step the activation energy is considered constant. Activation energies of 100 kJ/mol, 95 kJ/mol for the first two steps agree well with those calculated by Zuber (13) from resolved isothermal annealing curves only. Zuber calculated an activation energy of 25 ± 5 kcal/mol (105 ± 25 kJ/mol) for the slow component of his resolved isothermal annealing curves and 20 ± 5 kcal/mol (84 ± 25 kJ/mol) for the fast component of his resolved isothermal annealing curves. It is rather unusual that such similar activation energies should be observed for two processes which occur at two different temperatures. It must be concluded from this that the entropies of activation for the two processes must be quite different. A third kinetic component with an activation energy of 270 kJ/mol was not observed by Zuber from his isothermal curves.

Immediately following the irradiation, little or no $L-[Co(en)_3]^{3+}$ containing ^{60}Co was detected. Following thermal treatment, the amount of activity present in this isomer increased very little as shown in Table 18. On the other hand, the retention or percent activity as $D-[Co(en)_3]^{3+}$ increased from 4% to 56% of the total activity. It is clear that the annealing reaction was stereospecific.

D. Conclusions and Significance of Results for the Various Recoil and Thermal Annealing Models

In conclusion, the important features of the Szilard-Chalmers process in $D-[Co(en)_3](NO_3)_3$ can be summarized as follows. 1) At least seven

Table 17. Calculated activation energies from isothermal and isochronal annealing curves of D- and L-[Co(en)₃]³⁺ from neutron irradiated D-[Co(en)₃](NO₃)₃

Step	R _i (%)	R _{i-1} (%)	Isochronal Temp (K)	Isothermal Temp (K)	Isothermal Time (min)	E _a kJ/mol
1	14.5	8.5	336	313	400	98.5
2	27.3	14.5	350	313	1550	96.5
2	34.9	27.3	354	313	2350	97.8
3	40.5	34.9	364	353	500	272.1
3	46.4	40.5	369	353	1500	260.0

Table 18. Stereospecificity of $[\text{Co}(\text{en})_3]^{3+}$ annealing in neutron irradiated $\text{D-}[\text{Co}(\text{en})_3](\text{NO}_3)_3$

Condition	Radiochemical Yield (%)		
	Total $[\text{Co}(\text{en})_3]^{3+}$	$[\text{D-Co}(\text{en})_3]^{3+}$	$[\text{L-Co}(\text{en})_3]^{3+}$
Prior to Annealing	$5.5 \pm 1.0^{\text{a}}$	4.4 ± 1.0	1.1 ± 1.0
	$4.9 \pm 0.6^{\text{b}}$	4.5 ± 0.5	0.4 ± 0.2
Following Annealing	$57.5 \pm 2.5^{\text{c}}$	55.7 ± 2.5	1.8 ± 2.5
	$58.0 \pm 1.7^{\text{d}}$	55.4 ± 1.7	2.6 ± 0.2

^aCurrent result

^bZuber's result (Reference 13)

^cCurrent results following isochronal annealing to 114°C.

^dZuber's result (Reference 13) following isothermal annealing at 80°C for 34 hours.

radiochemical species were produced as a result of the recoil event. These were detected in solution as D-[Co(en)₃]³⁺, L-[Co(en)₃]³⁺, Co²⁺, [Co(en)₂X₂]ⁿ⁺, [Co(en)₂(NH₃)X]^{m+}, X_s, and X_f. 2) The X_s and X_f species are unstable in aqueous solutions and are transformed to Co²⁺. 3) The X_s, X_f, [Co(en)₂X₂]ⁿ⁺ and [Co(en)₂(NH₃)X]^{m+} components were detected and at least partially characterized for the first time, although hints of the latter two products were suggested by Zuber (13) and by Saito *et al.* (16). 4) Although there were apparent changes in the relative activities of the [Co(en)₂X₂]ⁿ⁺ and [Co(en)₂(NH₃)X]^{m+} species upon thermal annealing, the changes were not of great significance below 120°, and the percent yields of each never reached values greater than 17% of the total activity. 5) Upon thermal annealing, the percent activity as [Co(en)₃]³⁺ increased at the expense of Co²⁺ activity with time and temperature of annealing. The annealing curves which were constructed could not be satisfactorily resolved into simple first order components, but were indicative of at least three independent annealing processes with activation energies of 100, 95 and 270 kJ/mol, respectively. 6) The annealing process was stereospecific. When D-[Co(en)₃](NO₃)₃ was irradiated and annealed, virtually all of the activity as [Co(en)₃]³⁺ appeared as the D isomer.

There have been five models applied to describe the recoil event:

- 1) the elastic collision or billiard ball model, 2) the elastic-inelastic collision model, 3) the epithermal reaction model, 4) the random fragmentation model or brushheap, and 5) the hot zone model.
- Three models have been proposed to explain the annealing process:

1) the ligand diffusion model, 2) the competition microscopic decomposition-recombination model, 3) the solid-state isotopic exchange model. In order to explain the results of the experiments described in this work in terms of these models, it would be desirable to separate the effects of radiation and thermal annealing from the effects due to recoil alone. It has been shown that the thermal annealing processes occurred at room temperature. Dimotakis and Yavas (24) showed that the annealing occurred well below room temperature. Concomitant ionizing radiation also would contribute to the observed effect. Dissolution in water may have destroyed some of the radiochemical products formed in the solid state. Finally, the method of analysis may have affected the yields observed. Therefore, the initial apparent yields of radiochemical products may not have been indicative of the radiochemical products produced completely in the solid state as a result of the recoil reaction alone. Although changes in the apparent yields of radiochemical products as a result of annealing no doubt showed that changes were occurring to the radiochemical distribution in the solid, systematic errors in the analysis, dissolution, or heating procedure may have contributed to the results so that inferences from the data do not completely describe the solid state reaction. It should be kept in mind that the recoil models describe only the recoil event and not subsequent events, and that the thermal annealing models describe only changes which occur in the solid state long after the recoil event and prior to dissolution.

The elastic collision model would predict the production of only two

radiochemical species as a result of the recoil event, interstitial cobalt (detected as Co^{2+} in solution), and $\text{D}[\text{Co}(\text{en})_3]^{3+}$. The $\text{D}[\text{Co}(\text{en})_3]^{3+}$ yield should be much lower than the Co^{2+} yield. The radiochemical $[\text{Co}(\text{en})_3]^{3+}$ would be produced by head-on collisions of the recoil atom with ^{59}Co . The inactive ^{59}Co would be displaced from the coordination sphere by the recoil atom and continue with the kinetic energy of the recoil atom. In a volume occupied primarily by lighter atoms the probability of such a collision would be quite low. If the head-on collision did not occur the recoil atom would be slowed by elastic collisions with other atoms. Such elastic collisions would preclude the breaking of chemical bonds, since the breaking of bonds would require energy and the collision would not be elastic. The appearance of radiochemical products other than Co^{2+} and $[\text{Co}(\text{en})_3]^{3+}$ would cast doubt on the ability of the billiard ball model to describe the recoil process. However, it might be argued that the other products were produced as a result of radiation effects or thermal annealing effects and not as a result of recoil.

The inelastic-elastic collision model would provide an explanation for the variety of radiochemical products observed. In an inelastic collision, energy could be transferred to an atom and a net breakage of bonds could occur. However, the inelastic-elastic collision model is simply an extension of the billiard-ball model and does not predict what products would be formed or their distribution.

A more precise description of the recoil process is provided by the epithermal reaction model. Applied to recoil in the $\text{D}[\text{Co}(\text{en})_3](\text{NO}_3)_3$

system, the epithermal reaction theory would predict that the recoil atom was slowed to velocities such that the kinetic energy was in the "epithermal region." In the epithermal region the recoil atom forms an excited intermediate complex with ligands in the bulk of the solid. This complex could decompose by several reaction paths to form the precursor to the species detected in solution, $[\text{Co}(\text{en})_3]^{3+}$, $[\text{Co}(\text{en})_2\text{X}_2]^{n+}$, $[\text{Co}(\text{en})_2(\text{NH}_3)\text{X}]^{m+}$, X_s , X_f , and Co^{2+} . Each path would be characterized by a definite probability which would be independent of the composition of the system. The theory predicts the production of several products. However, to explain the rather large initial yield of Co^{2+} it would have to be said that the probability of the complex decomposing to Co^{2+} would be quite high. It is not clear that the model would predict the formation of $[\text{Co}(\text{en})_2(\text{NH}_3)\text{X}]^{m+}$ since the breaking of the C-N bond would require the bond breaking to occur after the excited intermediate complex was formed.

The random-fragmentation or brush heap model offered a broad base by which the results of the recoil experiments could be explained. In this model, the recoil atom randomly breaks bonds as it travels through the crystal lattice. The random breaking of bonds would explain the large number of radiochemical products found. The radicals formed could then recombine with the recoil atom to form a large number of products. The recoil cobalt atoms which were not finally near the site of bond breaking could not recombine and would be detected as Co^{2+} in solution. This model would nicely explain the production of $[\text{Co}(\text{en})_2(\text{NH}_3)\text{X}]^{m+}$. If radicals which could combine with ^{60}Co were formed, however, those which did not

combine might be expected to combine with Co upon thermal annealing since their mobility would be increased at higher temperatures. Such was not the case, since a significant increase in the yields of $[\text{Co}(\text{en})_2\text{X}_2]^{\text{m}+}$ and $[\text{Co}(\text{en})_2(\text{NH}_3)\text{X}]^{\text{m}+}$ was not observed upon thermal annealing. The random fragmentation model provides the best explanation for the results obtained in the present work.

The hot zone model would explain why the predominate initial product observed was Co^{2+} . Since the hot zone model would predict that there would be a very low concentration of free radicals available for recombination, the initial yields of $[\text{Co}(\text{en})_2\text{X}_2]^{\text{n}+}$, $[\text{Co}(\text{en})_2(\text{NH}_3)\text{X}]^{\text{m}+}$, X_s and X_f should be quite low. However, in the hot zone there should be ample opportunity for the formation of $[\text{Co}(\text{en})_3]^{3+}$, the thermodynamically favorable species. The low initial yield of $[\text{Co}(\text{en})_3]^{3+}$, might be explained, by assuming that the hot zone cooled too fast for significant recombination, and that upon thermal annealing reaction within the former hot-zone could occur at a slower rate. The stereospecificity of the annealing process, however, would cast doubt on the formation of such a hot zone melt which would presumably be a random array of the organic ligands and recoil atom. A template effect, however, might be involved which would require the cooled hot zone to possess a certain order. If this order favored the formation of the D isomer over the L isomer, perhaps the stereospecificity could be explained.

The thermal annealing process has been described in terms of three models: 1) the ligand diffusion model, 2) the microscopic competition decomposition-recombination model, 3) the solid state isotopic exchange

model.

In the ligand diffusion model, ligands (ethylenediamine molecules or fragments generated from the recoil event) diffused in the crystal lattice so that they could interact with the recoil ^{60}Co atom. In this process the ligands may have formed stable chemical species with the cobalt atom which would be detected finally in solution. The rate of recombination upon thermal annealing would be determined by the rate of ligand diffusion. Although the ligand diffusion model would explain the increase in retention observed, it would not adequately explain the rest of the observed data. For the model to explain the three different activation processes observed it would have to be assumed that there were at least three different diffusion modes available to the system. One would expect fragments of ethylenediamine to diffuse so that there would be a significant increase in the yields of $[\text{Co}(\text{en})_2\text{NH}_3\text{X}]^{\text{m}+}$ upon annealing. Such an increase was not observed. One would expect diffusion to be a nonstereospecific process, but annealing to $[\text{Co}(\text{en})_3]^{3+}$ ion was in fact stereospecific. Therefore, it must be concluded that the ligand diffusion model is inadequate.

The microscopic competition decomposition-recombination model proposed by Costea (31) and Dimotakis and Papadopoulos (25) was found to be useful in describing the apparent decrease in retention found by annealing irradiated $[\text{Co}(\text{en})_3](\text{NO}_3)_3$ at a temperature greater than 180°C . In this model, two competing series of reactions occur. One series leads to retention, the other leads to decomposition. At certain temperatures and times one process dominates the other, leading to oscillations in the

degrees of retention observed. Perhaps this is the only model which can account for the observation of oscillation in the time-retention curves reported by Dimotakis. However, this model does not seem in agreement with much of the data presented here. The oscillation observed by Dimotakis could not be reproduced. If decomposition were an important process, during thermal annealing, we might expect an increase in the radiochemical yield of $[\text{Co}(\text{en})_2\text{X}_2]^{n+}$, a possible intermediate species between Co^{2+} and $[\text{Co}(\text{en})_3]^{3+}$. No significant increase was observed. If decomposition were occurring, we might expect a scrambling of the ligands and recombination in a nonstereospecific manner. However, the annealing process was observed to be stereospecific.

The third or solid state isotopic exchange model is another way in which to rationalize the experimental results. In this model the radioactive ^{60}Co exchanges with inactive ^{59}Co atoms in the $[\text{Co}(\text{en})_3]^{3+}$ ion in the bulk. Such a process would be expected to require the breaking and reforming of Co-N coordinate bonds and would be expected to have a high activation energy. The energy for such a process would be provided by the annealing of radiation induced or naturally occurring trapped electron defects in the crystal lattice. The rate determining step would be determined by the rate of annealing of such defects and not by the exchange process itself. The step-like behavior of the isochronal annealing curves, according to Lazzarini and Fantola-Lazzarini (47), is indicative of such annealing of defects, leading to observed isotopic exchanges. The activation energies derived were calculated

based on the annealing of defects and indicate that there are at least three types of defects which anneal. Since the annealing process would be explained in terms of isotopic exchange between Co^{2+} and bulk $[\text{Co}(\text{en})_3]^{3+}$, we would expect that the yields of other species such as $[\text{Co}(\text{en})_2\text{X}_2]^{n+}$ and $[\text{Co}(\text{en})_2\text{NH}_3\text{X}]^{m+}$ should not be affected. Finally, the stereospecificity of the annealing reaction would be explained in that $^{60}\text{Co}^{2+}$ replaces Co^{3+} in the D- $[\text{Co}(\text{en})_3]^{3+}$ ion in the bulk. The isotopic exchange model does not readily account for the oscillation of the type reported by Dimotakis. The model is also limited because it cannot explain what is happening at the molecular level between atoms and molecules.

IV. APPLICATION, IMPLICATION, AND SUGGESTION FOR FUTURE WORK

The application of the Szilard-Chalmers process to the production of high specific activity radioisotopes has already been demonstrated by Matsura (64). Another possible application of the recoil and thermal annealing process might be in the synthesis of radioactive labeled compounds which would be difficult to prepare by other methods.

This research has demonstrated that an identification of recoil products is important in the interpretation of experimental results. Failure to recognize the production of species other than target material and Co^{2+} has led to misinterpretation of results by other workers. The use of combined isochronal and isothermal annealing curves in the determination of activation energies of thermal annealing of recoil products has been demonstrated for a multicomponent annealing curve. Recrystallization and ion-exchange techniques have been shown to be feasible in the separation of systems which contain the same radioisotope in several chemical forms. The results have been interpreted in terms of several proposed models of recoil and thermal annealing. The random fragmentation model of recoil and the isotopic exchange model seem to explain the data better than the other models considered.

This research has brought to light several areas of investigation which might be pursued in the investigation of recoil and thermal annealing phenomena. The isolation and identification of the X_s and X_f species would be quite valuable. Perhaps this identification could be accomplished by the dissolution of the irradiated solid in nonaqueous or high perchloric acid media such that the species would not decompose. Other

species which may have decomposed to Co^{2+} in water might be identified in another solvent. If the isolation of X_s and X_f could not be accomplished, a study of the decomposition in buffered media would be useful so that their rates of conversion as a function of pH could be determined. The isotopic exchange in cobalt double complexes observed by Lazzarini and Fantola-Lazzarini in $[\text{Co}(\text{H}_2\text{O}_6)\text{Co}(\text{EDTA})]$ (47) and observed in some preliminary investigations in $[\text{Co}(\text{en})_3](\text{NCS})_4(\text{NO}_3)$ appear to be useful systems in the investigation of thermal annealing in the absence of recoil effects. The study of such exchange reactions in cobalt double complexes if they are general phenomena would support the isotopic exchange model in the interpretation of thermal annealing in irradiated complexes.

V. REFERENCES CITED

1. W. V. Prestwich, T. J. Kennet and L. B. Hughes, Nuclear Physics, 88, 548 (1966).
2. C. M. Lederer, J. M. Hollander and I. Perlman, "Table of Isotopes," 6th ed., John Wiley and Sons, Inc., New York, N.Y., 1967, pp. 21, 194.
3. G. Friedlander, J. W. Kennedy and J. M. Miller, "Nuclear and Radiochemistry," 2nd ed., John Wiley and Sons, Inc., New York, N.Y., 1964.
4. W. F. Libby, J. Amer. Chem. Soc., 69, 2523 (1947).
5. L. Szilard and T. A. Chalmers, Nature, 134, 462 (1934).
6. G. Harbottle and N. Sutin, Adv. Inorg. Chem. Radiochem., 1, 267 (1959).
7. G. Harbottle, Ann. Rev. Nucl. Sci., 15, 89 (1965).
8. L. Friedman and W. F. Libby, J. Chem. Phys., 17, 647 (1949).
9. J. M. Miller and R. W. Dodson, J. Chem. Phys., 18, 865 (1950).
10. J. E. Willard, Ann. Rev. Nucl. Sci., 3, 193 (1953).
11. G. Harbottle and N. Sutin, J. Phys. Chem., 62, 1344 (1958).
12. P. Süe and G. Kayas, J. Chim. Phys., 45, 188 (1948).
13. A. V. Zuber, Ph.D. Thesis, Columbia University, New York, N.Y., 1954.
14. P. N. Dimotakis, A. G. Maddock and B. Vassos, Radiochim. Acta, 8, 38 (1967).
15. T. Costea and I. Dema, Nature, 189, 478 (1961).
16. N. Saito, T. Tominago and H. Sano, Bull. Chem. Soc. Japan, 38, 1407 (1965).
17. N. Saito, T. Tominago and H. Sano, Bull. Chem. Soc. Japan, 35, 365 (1962).
18. H. Saito, T. Tominago and H. Sano, Bull. Chem. Soc. Japan, 33, 1621 (1960).
19. M. M. de Maine and J. G. Kay, Radiochim. Acta, 4, 149 (1965).

20. L. L. Williams, N. Sutin, J. M. Miller, J. Inorg. Nucl. Chem., 19, 175 (1961).
21. T. Yasukawa, J. Inorg. Nucl. Chem., 29, 605 (1967).
22. T. Yasukawa, J. Inorg. Nucl. Chem., 28, 17 (1966).
23. P. N. Dimotakis, J. Inorg. Nucl. Chem., 30, 29 (1968).
24. P. N. Dimotakis and G. Yavas, J. Inorg. Nucl. Chem., 32, 1065 (1970).
25. P. N. Dimotakis and B. P. Papadopoulos, J. Inorg. Nucl. Chem., 32, 1071 (1970).
26. E. Lazzarini and A. L. Fantola-Lazzarini, J. Inorg. Nucl. Chem., 29, 895 (1967).
27. E. Lazzarini, J. Inorg. Nucl. Chem., 29, 7 (1967).
28. E. Lazzarini, J. Inorg. Nucl. Chem., 29, 855 (1967).
29. E. Lazzarini and A. L. Fantola-Lazzarini, J. Inorg. Nucl. Chem., 31, 1947 (1969).
30. J. E. Willard, Am. Rev. Nucl. Sci., 3, 193 (1953).
31. T. Costea, J. Inorg. Nucl. Chem., 17, 20 (1961).
32. K. Yoshihara and G. Harbottle, Radiochim. Acta, 12, 68 (1963).
33. G. L. Stucky and R. W. Kiser, Radiochim. Acta, 11, 5 (1969).
34. D. Witiak, Ph.D. thesis, Iowa State University, Ames, Iowa, 1972.
35. J. Costea, I. Negoescu, P. Vasudev, D. R. Wiles, Can. J. Chem., 44, 885 (1966).
36. P. N. Dimotakis and A. G. Maddock, J. Inorg. Nucl. Chem., 26, 1503 (1964).
37. P. N. Dimotakis and M. I. Stamouli, Z. Phys. Chem. Neue Folge, 55, 197 (1967).
38. C. D. Demetroulas and P. N. Dimotakis, J. Inorg. Nucl. Chem., 28, 2756 (1966).
39. T. Anderson, H. E. L. Madsen, K. Oleson, Trans Faraday Soc., 62, 2409 (1966).

40. W. B. Lewis, C. P. Coryell and J. W. Irving, J. Chem. Soc. Suppl., 1949, 386 (1949).
41. A. Nath, S. Khorana, P. K. Mathur and S. Sarup, Indian J. Chem., 4, 51 (1966).
42. A. Nath, K. Annajika and V. G. Thomas, Indian J. Chem., 2, 331 (1964).
43. J. Shankar, A. Nath and V. G. Thomas, J. Inorg. Nucl. Chem., 30, 1361 (1968).
44. S. Khorana, J. Inorg. Nucl. Chem., 30, 2595 (1968).
45. D. L. Aalbers and H. E. LeMay, Jr., Inorg. Chem., 13, 940 (1974).
46. E. Lazzarini and A. L. Fantola-Lazzarini, J. Inorg. Nucl. Chem., 34, 817 (1972).
47. E. Lazzarini and A. L. Fantola-Lazzarini, J. Inorg. Nucl. Chem., 36, 3073 (1974).
48. D. Witiak, M. S. Thesis, Iowa State University, Ames, Iowa, 1969.
49. J. A. Broomhead, F. P. Dwyer and J. W. Holgrath, Inorg. Syn., 6, 183 (1960).
50. A. Werner, Ber., 45, 121 (1912).
51. J. C. Bailar, Inorg. Syn., 2, 222 (1956).
52. A. Werner, Ber., 44, 1890 (1911).
53. F. Barolo and R. G. Pearson, "Mechanisms of Inorganic Reactions," 2nd ed., John Wiley and Sons, Inc., New York, N.Y., 1967, pp. 124-346.
54. A. M. Newton and T. W. Swaddle, Can. J. Chem., 53, 2751 (1974).
55. S. Khorana, Radiochim. Acta, 11, 222 (1969).
56. F. A. Cotton and G. Wilkinson, "Advanced Inorganic Chemistry," 2nd ed., John Wiley and Sons, Inc., New York, N.Y., 1966, p. 864.
57. V. Balzani, L. Moggi, F. Scandola and V. Carassity, Inorg. Chimica Acta Rev., 1, 7 (1967).
58. I. Bodek, G. Davies and J. H. Ferguson, Inorg. Chem., 14, 1708 (1975).

59. P. Wilairate and C. S. Garner, J. Inorg. Nucl. Chem., 31, 1833 (1971).
60. J. D. White, J. C. Sullivan, H. Taube, J. Amer. Chem. Soc., 92, 4735 (1970).
61. H. J. Svec and N. C. Peterson, "Physical Chemistry Experiments," Revised ed., Iowa State University, Ames, Iowa, 1974, p. 13.
62. C. J. Meechan and J. A. Brinkman, Phys. Rev., 103, 1193 (1956).
63. A. C. Damask and G. J. Dienes, "Point Defects in Metals," Gordon and Breach, New York, 1963, pp. 145-161.
64. T. Matura, J. Inorg. Nucl. Chem., 27, 2669 (1965).

VI. ACKNOWLEDGMENTS

I would like to thank the staff at the Ames Laboratory Research Reactor and the health physics staff for their help in performing the radiation and handling of the radioisotopes. I would like to thank the members of Radiochemistry Group II for the many discussions and suggestions concerning this research and Dr. D. S. Martin for his guidance in the performance of this research and in the preparation of this dissertation. Finally, I would like to thank my wife, Martha, for her moral support and her help in preparing initial drafts of the dissertation.